# SOIL HEATING
## USING SUBSURFACE PIPES:

## A DECADE OF RESEARCH RESULTS AT OSU/OARDC

D. L. ELWELL
M. Y. HAMDY
W. L. ROLLER
A. E. AHMED
H. N. SHAPIRO
J. J. PARKER
S. E. JOHNSON

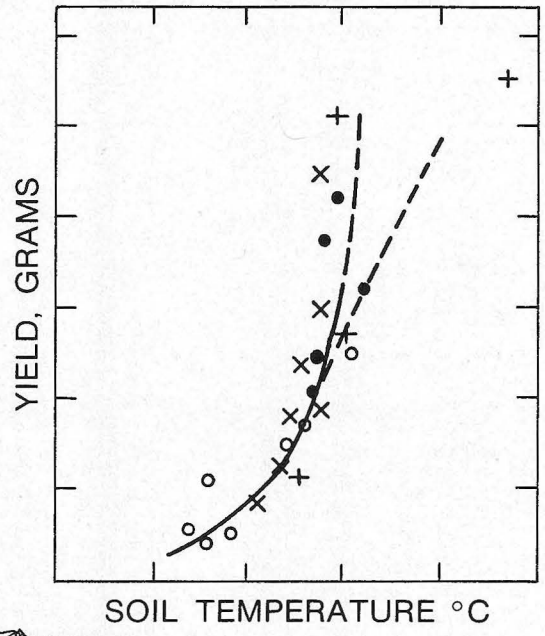


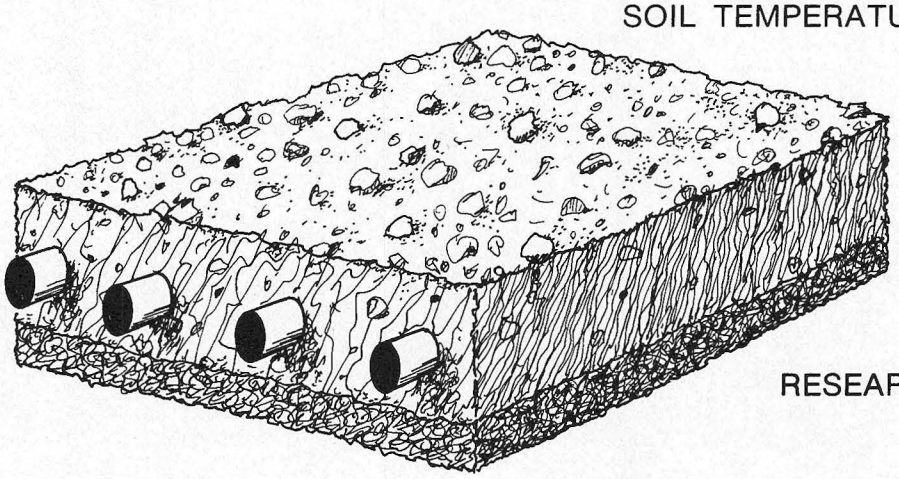

RESEARCH BULLETIN 1175
APRIL 1985

**The Ohio State University**
**Ohio Agricultural Research and Development Center**
**Wooster, Ohio**

## CONTENTS

**** ***** ****



## ACKNOWLEDGMENTS


In the first soil heating studies, important assistance was received from Dr. Michael Moran of the Department of Mechanical Engineering. During the latter part of this work, when energy studies were being conducted in conjunction with plant growth, considerable assistance was received from the Departments of Horticulture and Plant Pathology. In particular, the authors would like to acknowledge the assistance of Dr. William Bauerle, Dr. Randall Rowe, and Elsa Mora. In addition, the technical assistance of Mike Sciarini, Norman Hostetler, Paul Grimwood, and Dean Swisher is greatly appreciated.





AGDEX 717-731 4-85-2.5M

# Soil Heating Using Subsurface Pipes:
## A Decade of Research Results at OSU/OARDC

D. L. ELWELL, M. Y. HAMDY, W. L. ROLLER,
A. E. AHMED, H. N. SHAPIRO, J. J. PARKER, and S. E. JOHNSON[1]

## INTRODUCTION

Soil heating is an important, modern technique in high production, controlled-environment (greenhouse) agriculture. In this technique, warm water is circulated through the soil medium, usually in plastic pipes, in order to maintain the plant root zone temperature above some critical level and to transfer heat to the air above the soil. These effects can provide a considerable economic benefit for the grower who uses a soil heating system. In a cold climate, the warm soil provides an improved environment for plant growth and, in the light of present high energy costs, can result in considerable savings in greenhouse heating cost.

Very large quantities of low temperature, reject or waste heat are potentially available today as a by-product of various industrial processes. In particular, steam-driven, electric power generating plants dissipate twice as much energy through the condenser cooling water as is delivered to the electric power grid. In most cases, however, the rejected thermal energy is contained in large quantities of relatively low temperature water and is unsuitable for further use in industrial processes. On the other hand, this can constitute a suitable resource for soil heating and, in some cases, will have associated with it ancillary benefits (such as $CO_2$ production) which are of value to greenhouse production.

Heat transfer in any soil medium is a complex process which is strongly influenced by the amount of moisture present. Because of this, the low temperature of the reject heat resource is actually a benefit to the process. At higher temperatures, the soil near the heat source would become dry and would then conduct heat poorly. However, moist soil can conduct large amounts of low temperature heat and can thereby contribute significantly to the overall energy balance of the greenhouse aerial environment. In addition, warm soil can both enhance plant growth and reduce minimum air temperature requirements for good production. In these ways, and particularly when combined with effective energy conservation techniques, the use of large amounts of industrial reject heat can be beneficial for greenhouse production.

Scientists at The Ohio State University and Ohio Agricultural Research and Development Center (OSU/OARDC) have been working on obtaining a detailed understanding of soil warming processes for a decade. This work has included theoretical studies, computer simulations, laboratory experiments, and practical greenhouse operations. In the process, 16 scientific publications have been produced. This bulletin brings together this considerable wealth of information, along with related results obtained by other researchers, and sets forth a comprehensive view of this work.

## HISTORY

The earliest work at OSU/OARDC was undertaken to determine the feasibility of using power plant waste heat in a system which would provide soil warming for agricultural purposes and also meet a significant portion of a power plant's cooling requirement (47, 48). To do this, an initial model was derived for simultaneous heat and moisture transfer in a porous medium with variable properties, and this model was solved on an IBM digital computer in order to predict temperature and moisture profiles in the vicinity of a buried pipe system. From these profiles, and using soil property data available from the literature (21, 24, 29), heat and moisture transfer rates were determined. This initial study indicated that the basic agricultural requirements of elevated and uniform temperature and moisture in the plant root-zone could be met without any undue restraint on system design. However, it was also determined that the combined objective of meeting *both* agricultural requirements and power plant cooling needs imposed severe requirements on system design in terms of excessively long soil heat pipe runs. Therefore, all subsequent work in this area has been directed toward using low temperature heat for soil heating only for its agricultural benefits.

In order to verify the predictions of the initial computer study, and also in order to develop *in situ* methods of moisture determination, a laboratory scale study of heat and moisture transport in silt loam soil was undertaken (28). In this work, temperature and moisture gradients were generated in a 0.2 m thick, heavily insulated, slab of soil using electrically simulated heating pipes. A

[1]Senior Researcher, Professor, and Professor and Chairman, Dept. of Agricultural Engineering, The Ohio State University (OSU); Associate Professor of Agricultural Engineering, Alexandria University, Egypt (former Graduate Student, Dept. of Agricultural Engineering, OSU); Associate Professor of Mechanical Engineering, Iowa State University, Ames (former Graduate Student, Dept. of Mechanical Engineering, OSU); Director of Engineering and Quality Control, Kuss Corp., Findlay, Ohio (former Graduate Student, Dept. of Agricultural Engineering, OSU); and Advanced Engineer, Owens-Corning Fiberglass, Granville, Ohio (former Graduate Student, Dept. of Mechanical Engineering, OSU).

gamma ray attenuation apparatus was used to determine relative changes in moisture content in the soil while it remained in the experimental container. The results indicated some drying in the vicinity of the heating pipes at the highest temperatures (40° C), and in general were in agreement with the earlier computer predictions.

Parker (38) and Parker *et al.* (39) subsequently incorporated the soil heating model into a model of transient greenhouse heating which included plant growth and environment effects (50). This study used actual weather data for Wooster, Ohio, and indicated, without experimental confirmation, that the proposed system would be capable of meeting 18% and 36% of the greenhouse heat load when waste water temperatures were 25 and 35° C, respectively. Under the same circumstances, the model also indicated that the soil surface would be warmed by 2 to 4° C above its unheated condition. Thus, the basic results of this computer study showed that a buried pipe soil heating system could probably be of considerable value in greenhouse operations.

This indicated potential for soil heating in greenhouses made it important to take the work out of the laboratory and put it into a practical situation where a detailed examination of actual operation could take place. To some extent, the first part of this need was met with the inclusion of Shapiro's (47) basic soil heating design into the Sherco waste heat demonstration greenhouse (5). However, while this project was a very successful demonstration of waste heat utilization, its overall scope precluded a detailed examination of the heating contributions obtained in and through the soil. Therefore, under funding from the Electric Power Research Institute, a series of detailed experiments was initiated in 1977 in small scale greenhouse plots.

These plots, 2.9 x 3.0 m, contained three diverse but representative greenhouse soils: Wooster silt loam, a peat-vermiculite mixture, and sand. They were studied over the winters from the fall of 1977 to the spring of 1980, both with and without soil heating. During the first of these winters, no plants were grown in the soil and great care was exercised in obtaining accurate heat and moisture distribution/transport information. These initial results were published in Elwell *et al.* (15). In the subsequent two winters, lettuce was grown in the soil plots and the heat and moisture studies were continued. Three additional publications resulted directly from this research (16, 42, 43). In addition to and in parallel with this phase of the experimental studies, the computer simulation model of heat and moisture transfer in the soil was improved and expanded in scope (1, 2).

Finally, beginning late in 1981, a full-scale soil heating system was built into one bay of the research greenhouse. This system was operated in conjunction with an energy conserving, nighttime insulation scheme, and along with bag culture tomato production, during the winter of 1982-83. Further data on the operation of this system are being collected at the present time. Presently available publications on the results of this work are Elwell *et al.* (17, 18, 19, 20).

Thus, at this juncture the results of an extensive research program on soil heating are being transferred into a practical, combined package of energy conservation systems for commercial greenhouses. In addition, an Extension bulletin on practical soil heating design considerations is being prepared (7) in order to facilitate the adoption of this valuable technology. This research bulletin was prepared to bring together the present body of information in this area and make it more readily available for future work.

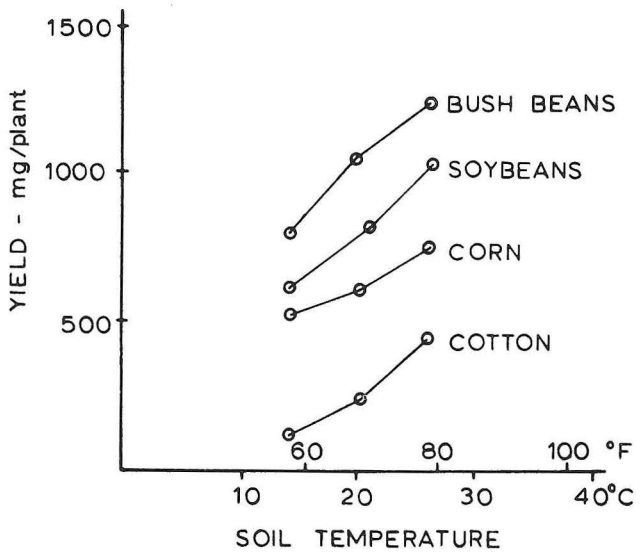


FIG. 1.—Increased yield for plants in nutrient baths at different temperatures (53).

## RESULTS

### A Model of Heat Conduction in a Soil with Fixed Properties

Early studies of various crops had indicated that soil temperature has a significant influence on plant growth (45, 53) as shown, for example, in Figure 1. Therefore, it became desirable to determine the effectiveness of soil warming systems for meeting both agricultural and power plant cooling objectives. The first step in this process was the development of a simplified model for heat conduction in a soil with fixed properties and its use in the evaluation of different proposed heating systems. Specifically, two such designs were considered.

First, a system of buried pipes designed specifically to dissipate heat from power plant condenser water was considered.

The primary objective of such a system was to maintain high heat flux at the pipe surface to enhance heat conduction from the water. This meant that the pipes needed to be *widely* spaced and the pipe diameter needed to be *small* relative to the spacing. Furthermore, the runs of pipe needed to be relatively *long* to allow the water sufficient opportunity to cool as it flows. Also, the pipes needed to be buried *near* the soil surface to reduce the thermal resistance between the pipe wall and the soil surface.

Next, a system designed specifically for agricultural

purposes was considered. An important objective in this case was that the heating effect due to the buried pipes be uniformly distributed throughout the root zone in order to benefit crop growth. A system specifically designed to accomplish this would require *low heat flux* near the pipes, implying that the temperature would not drop off rapidly in the vicinity of the warm pipes. This meant that the pipes needed to be *closely* spaced and the pipe diameter needed to be *sizable* relative to the spacing. Furthermore, it would be desirable that the condenser water flow be nearly *isothermal*, so the temperature potential for heating would be high along the entire length of the field. One way of achieving this would be with relatively *short* pipes. Also, the pipes would need to be buried sufficiently *deep* to allow for proper root formation and cultivation.

It was clear, then, that the design constraints for agriculture and for power plant cooling were somewhat at odds, and that to design for both might not be possible without undue compromise. A major thrust of the study was to investigate if such designs were possible and, if so, under what conditions.

The soil warming system analyzed is illustrated in Figure 2. The system consisted of a series of equally spaced parallel pipes buried at a uniform depth in a level field. To maintain more uniform soil temperature, warm water flowed in opposite directions through adjacent pipes. The purpose of the analysis was to model the heat transfer in the soil around the pipes and to evaluate the heat dissipation rate, under the assumptions of pure heat conduction and constant physical properties of the soil medium.

A steady-state heat conduction model was developed, assuming constant thermal conductivity and insignificant heat transfer in the soil parallel to the pipes, by exploiting the linearity of the two-dimensional *Laplace Equation* governing the heat transfer. Kendrick and Havens (31) solved this model by using the *method of images*, which had been described by Jakob (27). However, for the first time this problem was analyzed in terms of non-dimensional equations (47), a form which

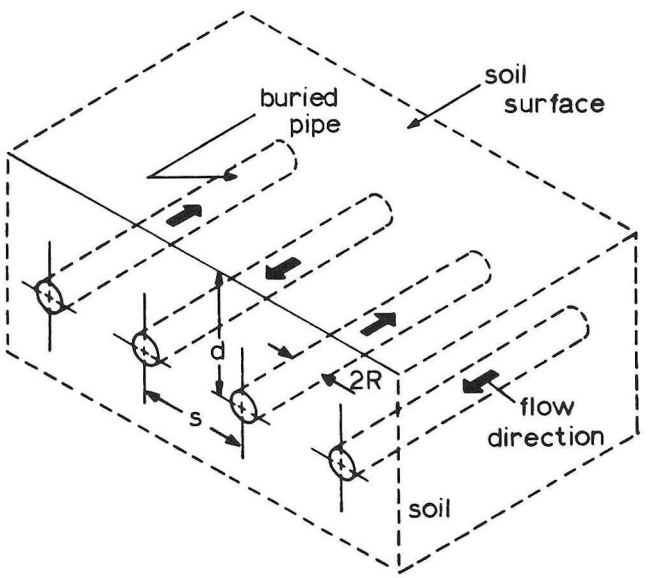


FIG. 2.—Layout of a soil warming system.

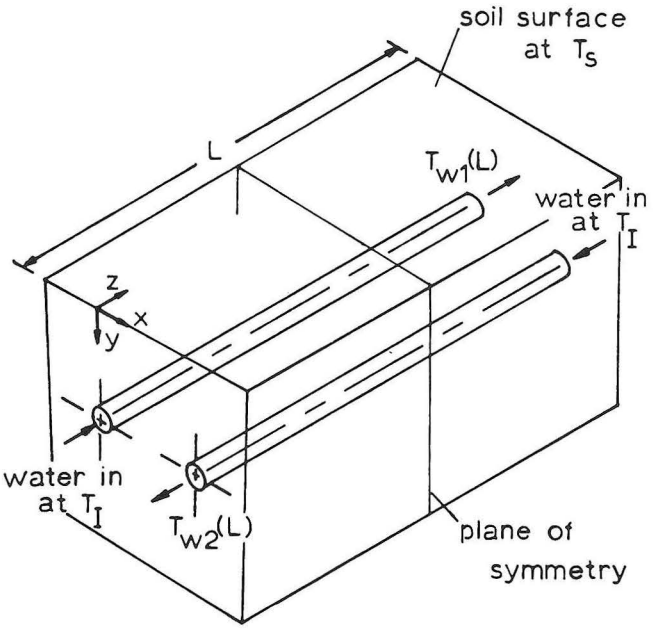


FIG. 3.—Soil warming model.

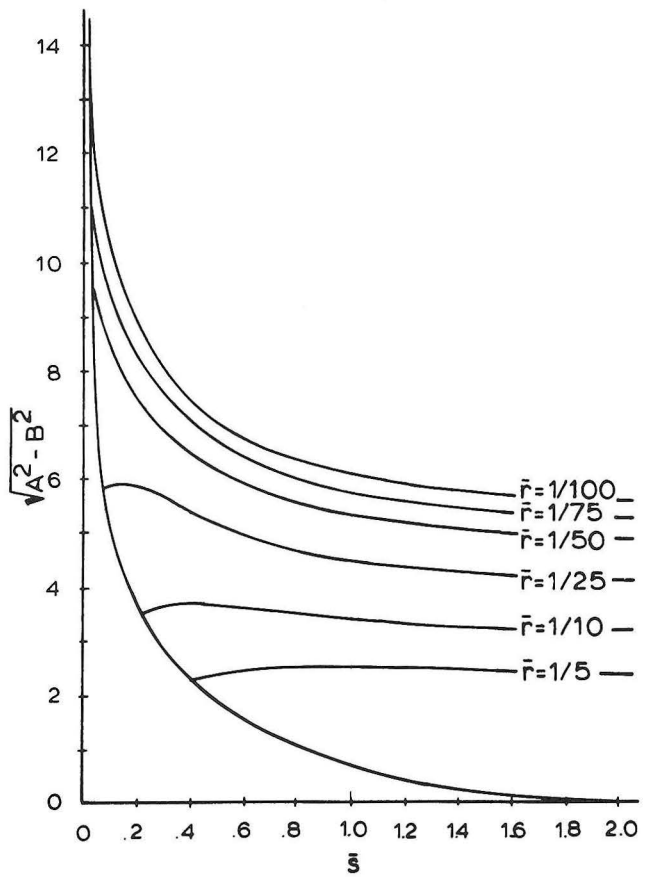


FIG. 4.—Values of the radical $\sqrt{A^2 - B^2}$ as a function of $\bar{s}$ and $\bar{r}$.

facilitated drawing some general conclusions about the operation of the system.

A portion of the soil warming system considered is shown in Figure 3. Water entered at a temperature of $T_I$, coming into adjacent pipes at opposite ends of the field. Since the soil surface temperature $T_s$ was less than $T_I$ when the system was in use, the water cooled as it flowed through the pipes. The temperature at any point in the soil, T (x,y,z), depended on the local water temperatures $T_{w1}$ (z) and $T_{w2}$ (z), as well as on the soil surface temperature. The rate of heat transfer was determined by the local temperature potentials ($T_{w1}$ (z) $- T_s$) and ($T_{w2}$ (z) $- T_s$) and the thermal resistance of the soil. This heat flow, in turn, played a role in determining the water temperatures. Other parameters involved in the heat transfer problem were the mass flow rate in the pipes, $\dot{m}$, and the layout parameters: depth d, spacing s, pipe radius R, and the length of each pipe L.

Kendrick and Havens (31) presented an equation for the soil temperature in the vicinity of 2N + 1 (N is an even number) pipes. The dimensionless form of that equation is:

$$\Phi = \left(\frac{AT_1-BT_2}{A^2-B^2}\right)\left[\ln\sqrt{\frac{\bar{x}^2+(1-\bar{y})^2}{\bar{x}^2+(1+\bar{y})^2}}\right.$$

$$+\sum_{n=1}^{N/2}\ln\sqrt{\frac{(1-\bar{y})^2+(2n\bar{s}-\bar{x})^2}{(1+\bar{y})^2+(2n\bar{s}-\bar{x})^2}}$$

$$\left.+\sum_{n=1}^{N/2}\ln\sqrt{\frac{(1-\bar{y})^2+(2n\bar{s}+\bar{x})^2}{(1+\bar{y})^2+(2n\bar{s}+\bar{x})^2}}\right]$$

$$+\left(\frac{AT_2-BT_1}{A^2-B^2}\right)\left[\sum_{n=1}^{N/2}\ln\sqrt{\frac{(1-\bar{y})^2+((2n-1)\bar{s}-\bar{x})^2}{(1+\bar{y})^2+((2n-1)\bar{s}-\bar{x})^2}}\right.$$

$$\left.+\sum_{n=1}^{N/2}\ln\sqrt{\frac{(1-\bar{y})^2+((2n-1)\bar{s}+\bar{x})^2}{(1+\bar{y})^2+((2n-1)\bar{s}+\bar{x})^2}}\right] \qquad (1)$$

where:

$\Phi = \dfrac{T-T_s}{T_I-T_s}$ . . . . dimensionless soil temperature

$T_1 = \dfrac{T_{w1}-T_s}{T_I-T_s}$, $T_2 = \dfrac{T_{w2}-T_s}{T_I-T_s}$ . . . . dimensionless water temperatures

$\bar{x}=\dfrac{x}{d}, \bar{y}=\dfrac{y}{d}, \bar{z}=\dfrac{z}{d}$ . . . . dimensionless position coordinates

$\bar{r}=R/d$ . . . . dimensionless pipe size parameter ($\bar{r}<1$)

$\bar{s}=s/d$ . . . . dimensionless pipe spacing parameter ($\bar{s}>2\bar{r}$)

and:

$$A(\bar{s},\bar{r}) = \ln(2/\bar{r}-1)+\sum_{n=1}^{N/2}\ln\left[\frac{(2-\bar{r})^2+(2n\bar{s})^2}{\bar{r}+(2n\bar{s})^2}\right] \qquad (2)$$

$$B(\bar{s},\bar{r}) = \sum_{n=1}^{N/2}\ln\left[\frac{(2-\bar{r})^2+(2n-1)^2\bar{s}^2}{\bar{r}+(2n-1)^2\bar{s}^2}\right] \qquad (3)$$

From Equation 1 it can be seen that $\Phi$ is a function of position, local water temperatures $T_1$ and $T_2$, and the layout parameters $\bar{s}$ and $\bar{r}$. Symbolically,

$$\Phi = \Phi(\bar{x}, \bar{y}, T_1, T_2, \bar{s}, \bar{r},) \qquad (4)$$

The dimensionless equation describing water temperature which followed from Kendrick and Havens' development is:

$$T_1 = \cosh(\eta\bar{z}) + \left[\frac{B-A\cosh(\eta)-\sqrt{A^2-B^2}\,\mathrm{Sinh}(\eta)}{A^2-B^2\cosh(\eta)+A\sinh(\eta)}\right]\sinh(\eta\bar{z}) \qquad (5)$$

where:

$$\eta = 2\pi\lambda\, L/\dot{m}C_p\,\sqrt{A^2-B^2}$$

with $\lambda$ being the thermal conductivity of the soil medium and $C_p$ the specific heat of water. A physical interpretation of the dimensionless parameter $\eta$ is given after Figure 5 is presented. The radical $\sqrt{A^2-B^2}$, appearing in Equation 5 and the definition of $\eta$, is a function of $\bar{s}$ and $\bar{r}$ as defined in terms of Equations 2 and 3. This dependence is shown graphically in Figure 4.

Equation 5 shows that $T_1$ depends upon the axial position $\bar{z}$ and the layout parameters $\bar{s}$, $\bar{r}$, and $\eta$. Symbolically,

$$T_1 = T_1(\bar{z}; \bar{s}, \bar{r}, \eta) \qquad (6)$$

Only *one* equation is needed because the symmetry of the system requires that $T_1(\bar{z}) = T_2(1-\bar{z})$ for pipes with local water temperatures $T_{w1}(\bar{z})$ and $T_{w2}(\bar{z})$. Therefore, using Equations 1 and 5, along with the symmetry relationship, the system temperatures are completely described.

Equations 1 and 5 indicate that the soil temperatures depend not only upon the system layout parameters $\bar{s}$, $\bar{r}$,

and $\eta$, but also upon position within the system: $\bar{x}$, $\bar{y}$, $\bar{z}$. However, a convenient set of graphs was developed in order to eliminate this position dependence. The first step in this direction was the identification of certain *critical* locations within the system.

The value of $T_1$ at $\bar{z} = 1$ is a measure of the amount of water temperature drop through the system, where $T_1(1) = 0$ indicates maximum cooling and $T_1(1) = 1$ corresponds to the case of no cooling. When Equation 5 was evaluated at $\bar{z} = 1$, the resulting expression for water temperature drop through the system depended only upon the layout parameters $\bar{s}$, $\bar{r}$, and $\eta$,

$$T_1(1) = T_1(\bar{s}, \bar{r}, \eta) \qquad (7)$$

This relationship is presented graphically in Figure 5.

A physical interpretation of the parameter $\eta$ can be obtained by studying lines of fixed $\bar{s}$ and $\bar{r}$ on Figure 5. For small $\eta$, corresponding to low thermal conductivity, short pipes, and/or a high mass flow rate, there is nearly isothermal flow in the pipes — *i.e.*, $T_1(1) \simeq 1$. On the other hand, when $\eta$ is large, corresponding to higher thermal conductivity, long runs of pipe, and/or a low mass flow rate, there is increased cooling of the water. Thus, $\eta$ can be interpreted as a gauge of the system's ability to cool the water.

For typical field crops, the roots can extend as much as 3 meters into the ground (Fig. 6), and the temperature at which the roots are maintained can influence agricultural yield (Fig. 1). Unfortunately, an essentially uniform, elevated temperature throughout the root zone cannot be achieved with buried pipes. This is shown in Figure 7 which gives experimental data for the variation of soil temperature with depth in a plot heated with *isothermal* cables (46). Figure 7 shows that,

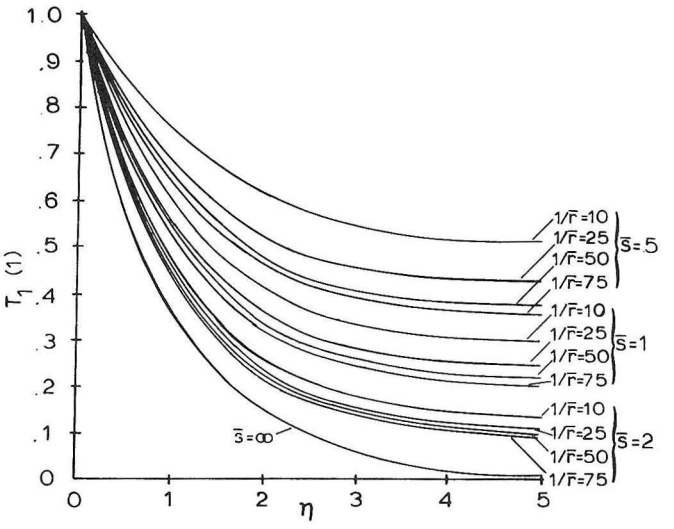


FIG. 5.—Dimensionless water temperature drop as a function of the layout parameters.

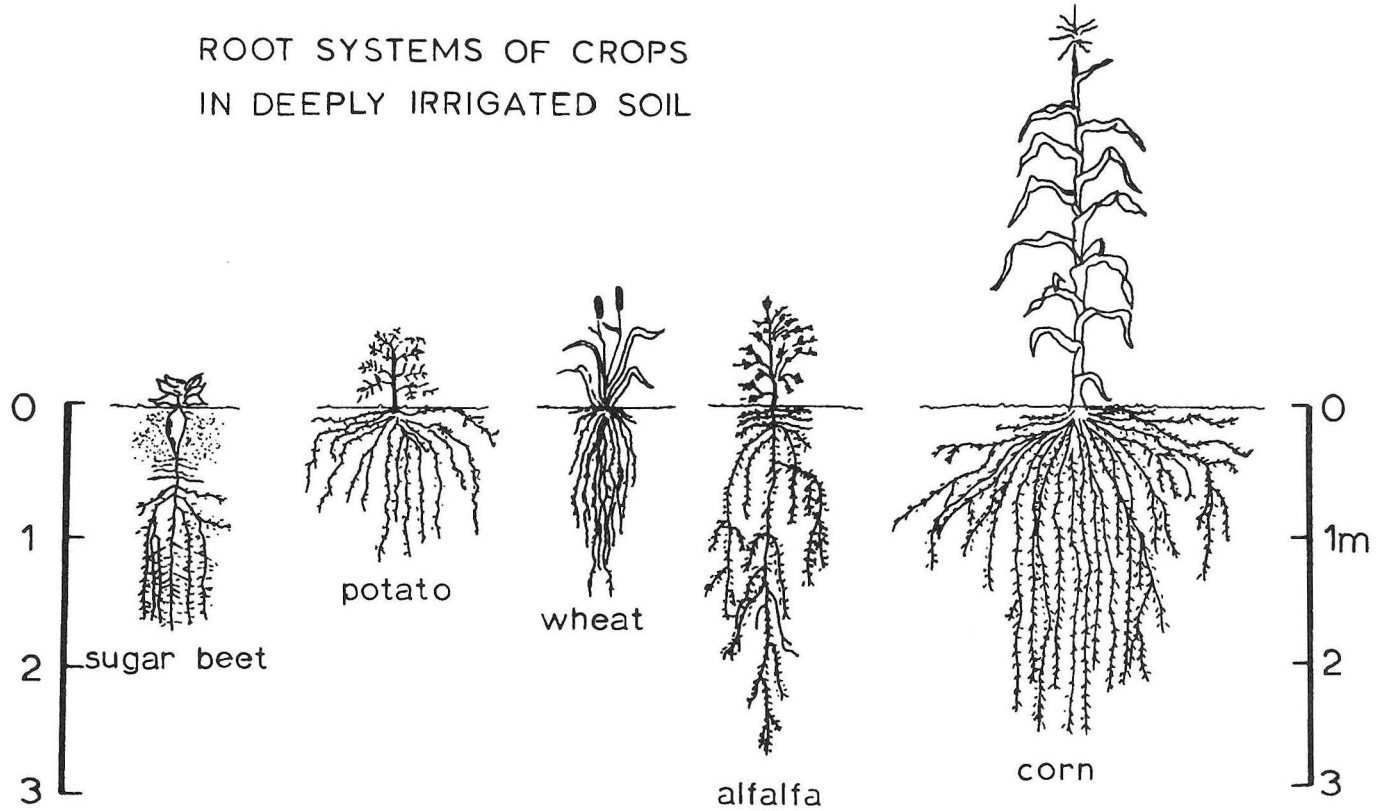


FIG. 6.—Root systems of several crops. (From J. Janick, *Horticultural Science*, 2nd Ed., W. H. Freeman Co., 1972.)

depending upon where the pipes are located in the soil-root system, the roots can experience temperatures anywhere from $T_s$ at the soil surface to $T_I$ at the pipes.

For the purpose of this discussion, it was desirable to have a *single* measure for the temperature of the roots.

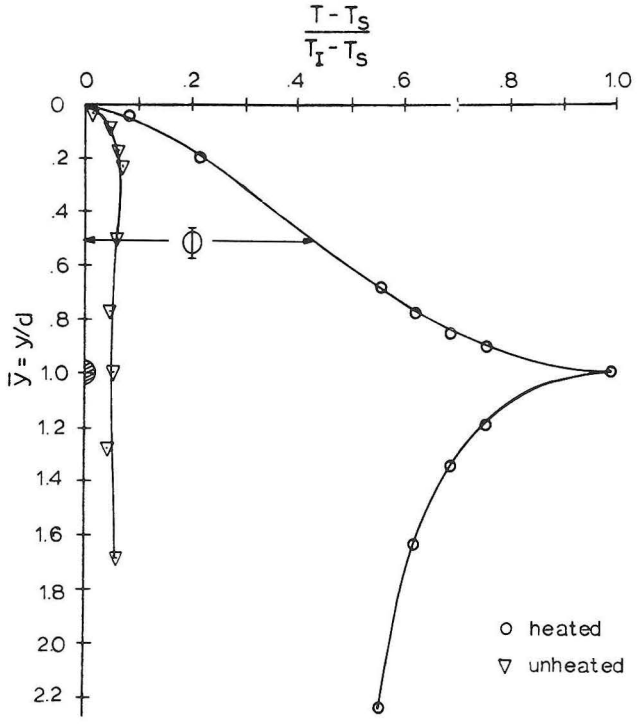


FIG. 7.—Experimental vertical temperature profile about a buried heat source.

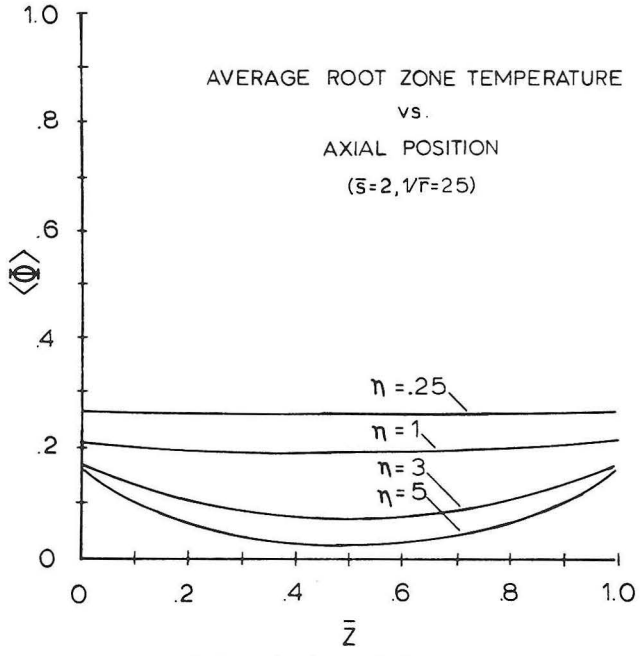


FIG. 8.—Axial variation of dimensionless root zone temperature.

Then, using data such as that presented in Figure 1 as a guide, this measure could be invoked to give some assurance that the temperatures *throughout* the root region would be in a beneficial range. The nearly linear nature of the temperature profile in Figure 7 suggested that the values of $\Phi$ at $\bar{y} = 0.5$, *i.e.*, half the distance from the soil surface to the pipes, would give a satisfactory measure of the average soil temperature. This was arbitrarily called the root zone temperature.

There was a periodic fluctuation of root zone temperature with $\bar{x}$, due to the presence of warm pipes at regular intervals. It was reasonable, however, to eliminate the $\bar{x}$ dependence by averaging across the field. The *average* root zone temperature, then, depended only on $\bar{z}$, when the layout parameters $\bar{s}$, $\bar{r}$, and $\eta$ were fixed. Figure 8 is a set of curves depicting the variation of the average root zone temperature with $\bar{z}$ for the parametric values indicated, and it shows that the values are lowest at midfield. Therefore, for the purpose of the subsequent discussion, $\bar{z} = 0.5$ was chosen as the critical location for soil temperature.

The average midfield root zone temperature, denoted as $\langle\Phi\rangle_c$, had no position dependence and was only a function of $\bar{s}$, $\bar{r}$, and $\eta$. This dependence is presented graphically in Figures 9, 10, and 11 for various values of the parameters. The validity of these graphs is subject to the assumptions of the constant property model, but they can still be studied to determine the ranges of the parametric values which were shown to be most desirable for meeting agricultural and power plant cooling needs.

First, Figures 9, 10, and 11 show that the highest average root zone temperatures (the agricultural objective) were obtained for designs in which $\bar{s}$, $1/\bar{r}$, and $\eta$ were small; these were achieved, for example, when there was close spacing, large pipes, and a short field (and/or large flow rate). Close spacing was also shown to be desirable for temperature uniformity.

Second, turning to the power plant objective, the amount of water cooling by the system was important. Figure 5 shows that large values of $\eta$ effected the most cooling for any given $\bar{s}$ and $\bar{r}$. Also, higher values of $\bar{s}$ and $1/\bar{r}$ lead to greater temperature drops, so that widely spaced, small pipes were the most favorable for maximum cooling. Physically, this was a consequence of the fact that, for such a configuration, the temperature gradients away from the pipes were the steepest. Thus, different parametric ranges were suggested in order to meet the indicated objectives, and it was clear that to design for both requirements would involve some compromises.

The constant property heat conduction model predicted temperature profiles which were in satisfactory agreement with actual data (Fig. 12). This was not unexpected, since the experiments in which the data were obtained included subsurface irrigation near the pipes in order to maintain fairly uniform moisture throughout the soil. Under these conditions, the heat transfer was primarily due to heat conduction, and the thermal conductivity was nearly uniform as well.

Under non-uniform moisture conditions, such as can

occur when no moisture is introduced near the warm pipes, it might be anticipated that the temperature profiles would differ significantly from those calculated via the constant property model. However, data from Gee (24) for steady state, simultaneous heat and mass transfer in *one-dimensional* soil samples indicated that the temperature distribution was not strongly dependent upon moisture content in the particular unsaturated soil used. It appeared, then, that the constant property model was reasonably accurate for calculating the *temperature* variations in the neighborhood of a buried pipe soil warming system.

A particularly useful aspect of the model was that it could be employed to determine accurate upper and

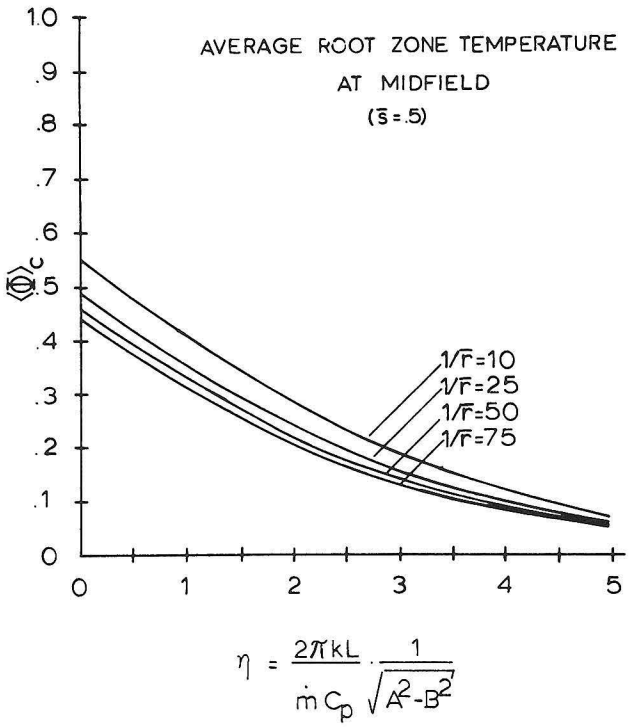


FIG. 9.—Dimensionless soil temperature as a function of the layout parameters.

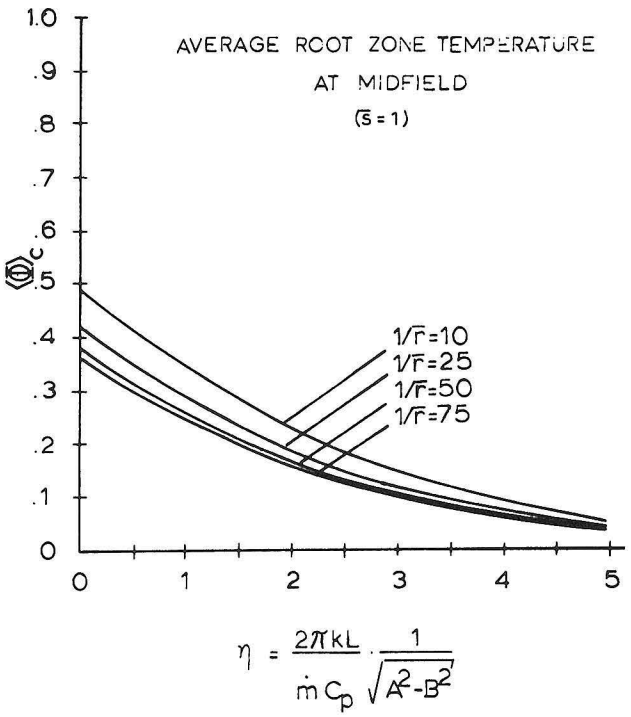


FIG. 10.—Dimensionless soil temperature as a function of the layout parameters.

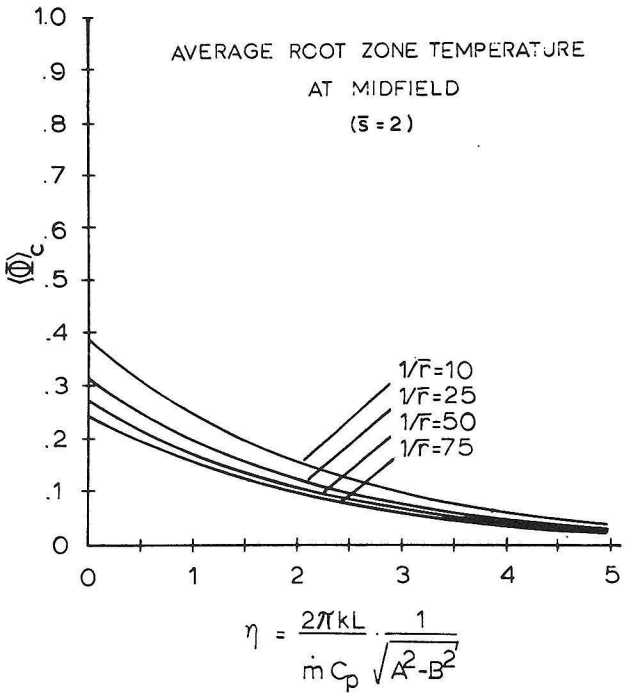


FIG. 11.—Dimensionless soil temperature as a function of the layout parameters.

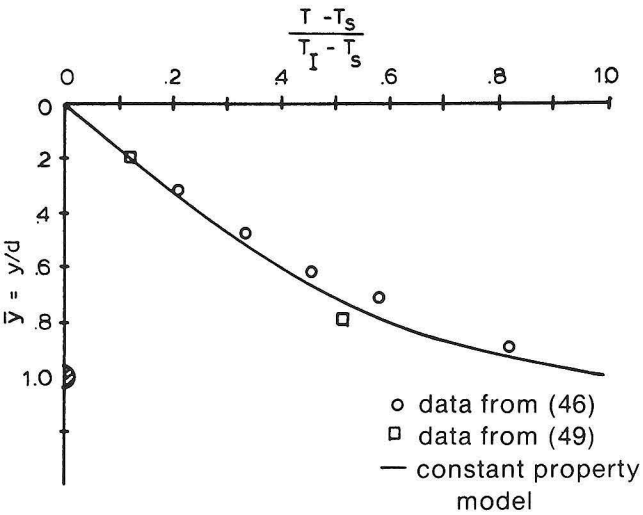


FIG. 12.—Comparison of constant property model with experimental data.

lower limits on the rate of heat dissipation from a given system, or conversely, the size of a system to achieve a given rate of heat dissipation. To obtain these bounds it was necessary to consider the limiting situations of very *dry* soil, wherein the dominant form of heat transfer is conduction and heat transfer is significantly reduced, and of fully *saturated* soil, wherein (under the moderate temperature differences encountered in soil warming applications — up to about 15° C) heat conduction also dominates and heat transfer is high. Specific values depended, of course, on numerical values for soil properties, and since these were evaluated in connection with a more complex, variable property model, the results of both models are presented in the following section.

## A Variable Property Heat and Mass Transport Model

The chief limitation of the previous model was that it required that moisture-related soil parameters be fixed. Except for the limiting conditions of either high or low moisture, this was an inadequate approach since experience indicated that when a moderate temperature difference (*e.g.*, up to 15° C) is impressed across a moist porous material, the moisture in the pores *migrates* from regions of high temperature to regions of lower temperature. Simultaneously, the presence of moisture gradients tends to cause redistribution of moisture from regions of high moisture to regions of lower moisture content (8, 34, 44) These two effects are superimposed according to the magnitudes of the gradients of temperature and moisture content. The net effect is a slow migration which, along with heat conduction, tends to redistribute energy and mass in the porous medium.

In order to deal with these considerations, differential equations for conservation of mass and energy can be written for every point in a porous medium. However, due to the inhomogeneity of the medium, integration of the equations would require knowledge of the exact pore geometry. To avoid the complexity of such an approach, *volume-averaged* properties were associated with each point in the porous medium, and then differential equations for conservation of mass and energy were cast in terms of volume-averaged properties. The details of this procedure were given in Shapiro (47). The resultant, nonlinear simultaneous differential equations did not include a gravity effect (due to its relative unimportance in the silt loam soil being studied) and were:

**1. Moisture Equation**

$$\frac{\partial}{\partial t}(\rho_L+\rho_V)=\rho_L\nabla\cdot\left[(D_{TV}+D_{TL})\nabla T+(D_{\theta V}+D_{\theta L})\nabla\theta\right] \quad (8)$$

**2. Energy Equation**

$$\frac{\partial}{\partial t}\left[(\rho u)_L+(\rho u)_V+(\rho u)_S\right] = -\nabla\cdot\left[\left[\lambda_{eff}+\rho_L(D_{TV}h_V+D_{TL}h_L)\right]\cdot\nabla T + \rho_L(D_{\theta V}h_V+(D_{\theta L}h_L)\cdot\nabla\theta\right] \quad (9)$$

where:

| | | |
|---|---|---|
| $\rho$ | = | mass density, kg/m$^3$ |
| $\lambda_{eff}$ | = | effective thermal conductivity, w/mK |
| u | = | specific internal energy, J/kg |
| h | = | specific enthalpy, J/kg |
| L, S, V | = | subscripts for liquid, solid, and vapor phases, respectively |
| and | | |
| $D_T$, $D_\theta$ | = | temperature and moisture dependent transport coefficients, respectively. |

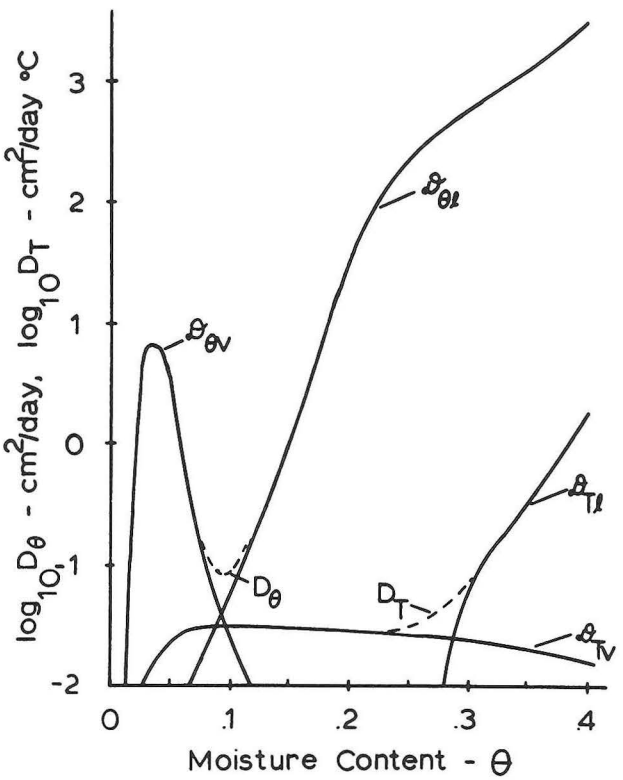


FIG. 13.—Theoretical transport coefficients for Palouse silt loam.

The evaluation of these transport coefficients was undertaken on both a theoretical and an empirical basis. The theoretical method was due to Philip and de Vries (41). It was based upon a theoretical explanation of the mechanism of heat and mass transport in the pores, and the results of these calculations are shown in Figure 13. Although the method was regarded to be valid *qualitatively*, several investigators (4, 21, 24, 29) had pointed out that the predicted coefficients, when used in the constitutive relationships (Equations 8 and 9), did not give values of the liquid and vapor *fluxes* within experimental accuracy.

In addition, temperature and moisture *profiles* could not be accurately predicted using Philip and de Vries' coefficients. For example, Gee (24) presented experimental, one-dimensional temperature and moisture

profiles in a Palouse silt loam soil. Using the coefficients calculated from the theory, and other data to be presented shortly, Equations 8 and 9 were cast in finite difference form and solved on a digital computer [see Shapiro (47) for details]. The result of the numerical integration for one set of boundary conditions is given in Figure 14. Inspection of Figure 14 indicated that while there was qualitative agreement, the curves deviated significantly from the experimental data, particularly in the drier end of the sample. In order to overcome this difficulty, an empirical approach of fitting the basic theoretical forms to the experimental data was adopted.

Figure 15 shows the experimental values of $D_\theta$, obtained by Gee (24) in an isothermal evaporation experiment using the technique of Gardner and Miklich (23), and the theoretical curves of $D_{\theta v}$ and $D_{\theta l}$ (Fig. 13). It can be seen that the sum, $D_\theta$, of the *theoretical* curves for $D_{\theta v}$ and $D_{\theta l}$ exhibits a minimum at $\theta \simeq 0.1$, and that for small $\theta$, $D_\theta \simeq D_{\theta v}$, while for large $\theta$, $D_\theta \simeq D_{\theta l}$. Jury's (29) data for $D_{\theta v}$ and $D_{\theta l}$ for a Plainfield sand exhibited similar characteristics. In addition, Philip and de Vries' (41) calculated values for Yolo light clay showed like trends. With these considerations in mind, the solid curves on Figure 15 were accepted as valid approximations of $D_{\theta v}$ and $D_{\theta l}$ for the present soil. Using these values for $D_\theta$, along with values for $d\bar{T}/dx$ and $d_\theta/dx$ determined graphically from experimental temperature and moisture profiles, $D_{T v}$ and $D_{T l}$ were then de-

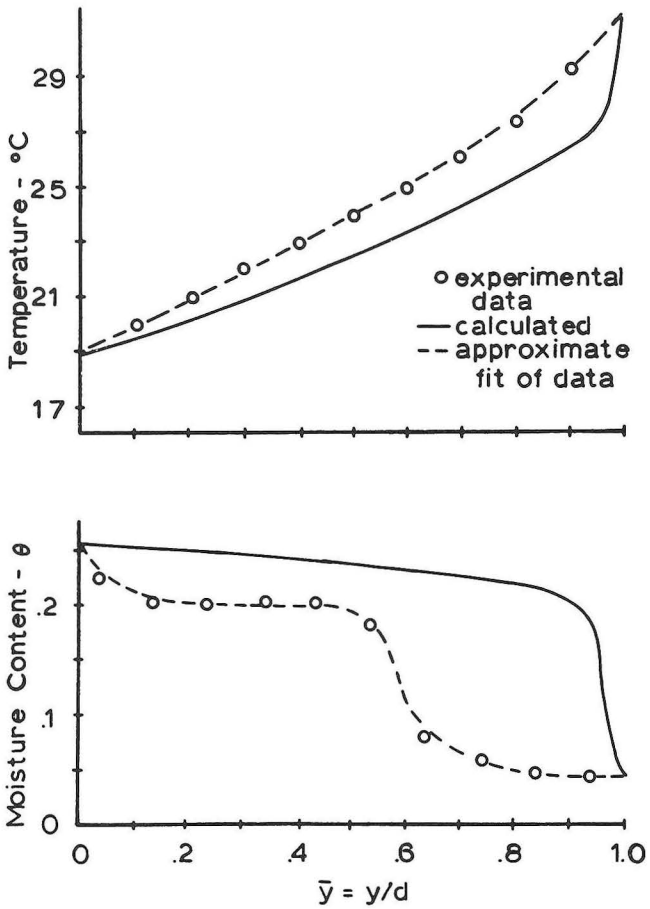


FIG. 14.—Experimental and theoretical temperature and moisture profiles in a one-dimensional soil sample.

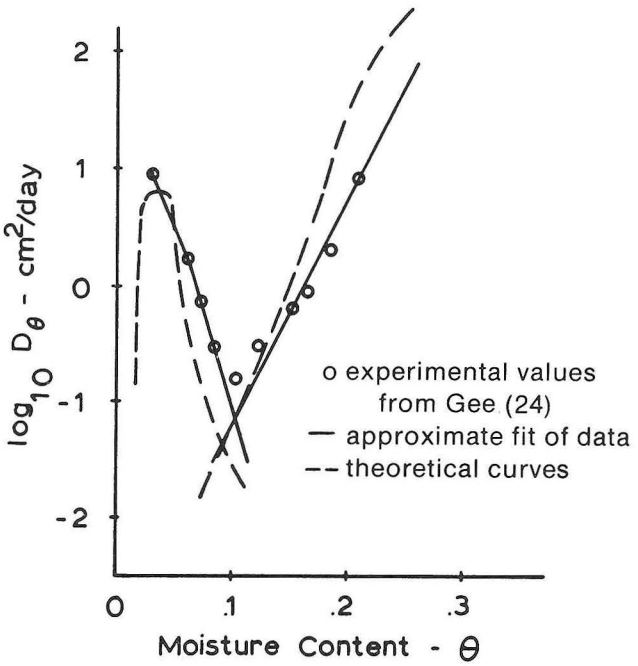


FIG. 15.—Transport coefficients for moisture-induced flow.

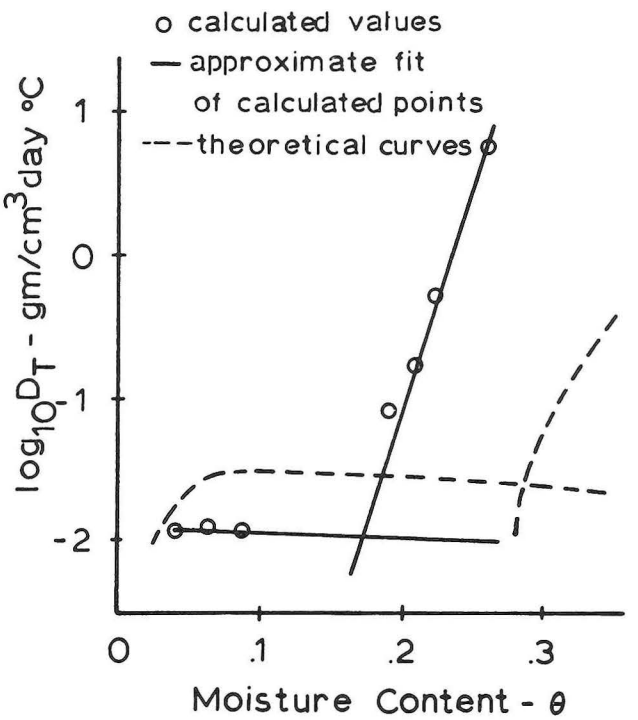


FIG. 16.—Transport coefficients for temperature-induced flow.

termined via the steady state version of Equation 8. Figure 16 shows these values along with the previously determined theoretical curves (Fig. 13).

The effective thermal conductivity for a silt loam soil,

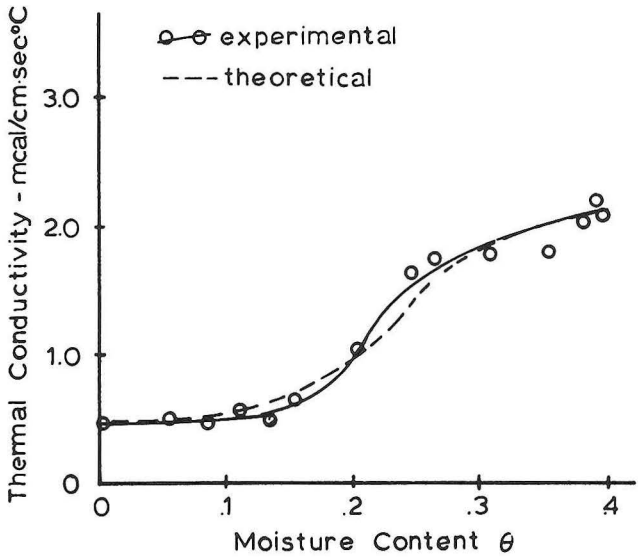


FIG. 17.—Thermal conductivity for silt loam soil at 25° C.

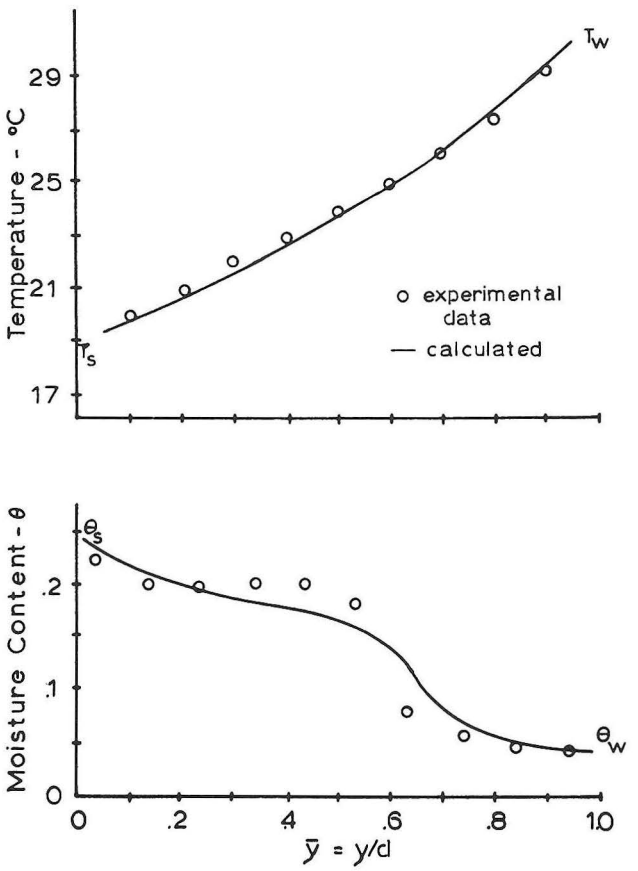


FIG. 18.—Calculated one-dimensional temperature and moisture profiles.

taken from Boersma *et al.* (4) (Gee did not give values for $\lambda_{eff}$), is shown in Figure 17. The solid line is an approximate fit to the data. For comparison, the dashed curve is the theoretical variation of thermal conductivity according to the method of de Vries (12), as reported in Boersma *et al.* (4). It can be seen that there is good agreement.

The enthalpies of the liquid and vapor were evaluated using the thermodynamic relationships:

$$h_l \simeq (C_p)_l (T - T_o)$$

$$h_v \simeq (C_p)_v (T - T_o) + h_{fgo}$$

where $(C_p)_l$ and $(C_p)_v$ are the specific heats for the liquid and vapor, $T_o$ is a reference temperature for enthalpy, and $h_{fgo}$ is the enthalpy of vaporization at the reference temperature.

In order to determine the validity of the empirical values for the transport coefficients, the finite difference forms of Equations 8 and 9 were again solved on the computer with these new input values. Figure 18 shows the results of these calculations in comparison with Gee's experimental results and can be compared with the previous theoretical results shown in Figure 14. It can be seen that there was a considerable improvement in the agreement obtained from using the empirically obtained coefficients. Computer solutions for other moisture and temperature conditions which were studied experimentally by Gee were also obtained, and the agreement was good for these cases as well.

Finally, the now complete, finite differences computer formulation [(47), Appendix A] of the transport problem was solved for various conditions using an IBM-370/165 digital computer. The temperature solution for dry soil ($\theta = 0.04$ at the boundaries) was compared with the limiting solution of the constant property model. These results were in agreement to within ± 0.5%, and this suggested that the formulation of the variable property transport problem was valid and that its computational routines were correct. Thus, for the conditions applicable to the transport coefficients used (silt loam soil with moisture content between 0.04 and 0.26), the results of the calculations were expected to provide useful information on the interactions between soil heat and moisture transport.

Temperature profiles obtained with the variable property model were considered first. The temperature predictions of the variable property analysis for the case in which the moisture content was allowed to vary due to the imposed temperature gradient from the surface, $\theta_s = 0.15$, to the lower boundary, $\theta_b = 0.20$, were compared with the corresponding predictions of the constant property solution (Fig. 19). The equilibrium moisture content at the pipe nodes was calculated to be $\theta = 0.08$ under the condition that no moisture was introduced at the pipe. Comparison of the temperatures at the node points for the variable and constant property cases showed that the solutions differ by at most 3% throughout the region. This indicated that temperature profiles are not *strongly* dependent upon the

moisture distribution, a conclusion in agreement with one stated earlier based upon Gee's one-dimensional data. This observation was a *significant* result of Shapiro's study (47).

Due to the observed insensitivity of the temperature profiles to varying moisture conditions, the constant property model was considered to be adequate for evaluation of the heating effect of a soil warming system. Thus, the *qualitative* conclusions based upon the constant property model were regarded to be valid under variable property conditions as well, and no further discussion of the temperature profiles was necessary at this point. Attention was then focused upon the moisture profiles in the soil.

Moisture profiles were obtained from the variable property model only for the case of isothermal flow in the pipes. This case imposed the greatest temperature difference on the soil around each pipe and therefore had the greatest potential for drying out this soil. For a given system ($\bar{s}$ and $\bar{r}$ specified) and for a given temperature potential, the equilibrium moisture distribution depends on the moisture at the lower boundary, $\theta_b$, and the steady-state moisture content at the soil surface, $\theta_s$. A reasonable value for $\theta_s$, 0.15, was determined from available data (4, 46). The lower boundary was set at $\bar{y}_b = 2$, where available data (4) indicated nearly uniform

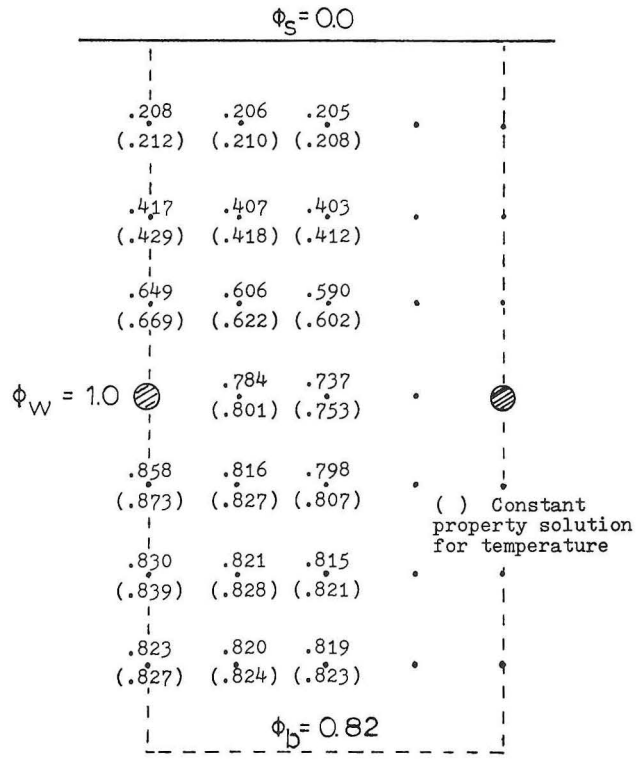


FIG. 19.—Temperature solutions of the variable and constant property models.

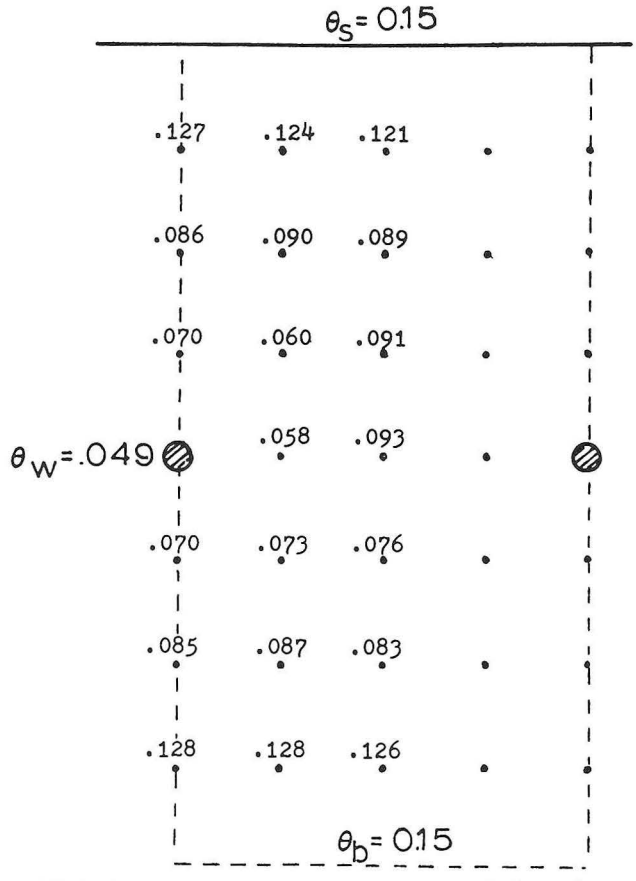


FIG. 20.—Variable property model moisture content solution ($\theta_b = 0.15$).

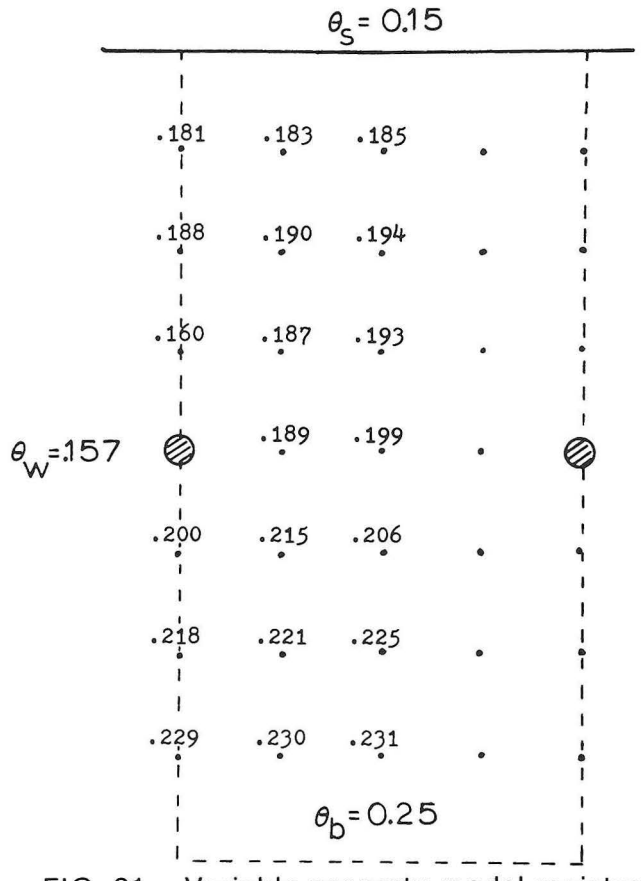


FIG. 21.—Variable property model moisture content solution ($\theta_b = 0.25$).

moisture content in soil warming applications, and $\theta_b$ was set at various levels to simulate different conditions in different runs. The results of two of these runs are shown in Figures 20 and 21.

The moisture distributions shown in these figures indicated that no single value of moisture content characterized the moisture level throughout the entire soil region under consideration. However, for soil warming applications it was reasonable to focus attention on the soil between the pipes and the surface, since that region is likely to encompass the bulk of the root zone. Two parameters were used to characterize the moisture level in that region. One was the equilibrium moisture content at the pipe nodes, $\theta_w$, and the second was the average moisture content in the root zone, $<\theta>_c$. The values of these parameters, at least in a gross way, are indicative of the moisture available for plant growth. The effects of systematically varying the parameters $\theta_b$, $\bar{s}$, and $T_I - T_s$ upon the calculated values of $\theta_w$ and $<\theta>_c$ were investigated. Representative computed results are given in Table 1. Some qualitative conclusions were drawn from these results regarding the effects of parametric variations upon soil drying, which were in accord with expectations from physical reasoning.

The results in Table 1 show that for $\theta_b$ of 0.15 and 0.20, the soil nearest the pipe is very dry ($\theta_w < 0.1$). Furthermore, as can be seen in Figure 20, there was considerable drying over a large part of the root region. However, Table 1 and Figure 21 indicate that a relatively small additional increase in $\theta_b$ to 0.25 virtually eliminated the dry region. This increase in $\theta_b$ shifted the moisture level in the entire region to the range where liquid effects rather than vapor effects dominate moisture movement (Figs. 15 and 16). Therefore, the change in character of the solution was attributed directly to different transport coefficients becoming dominant.

Another direct, and not unexpected, effect was that soil drying decreased when $T_I - T_s$ was reduced. Since the water will cool as it flows through the pipes, this meant that there can be variation in drying throughout the field due to the change in temperature potential. It can also be seen from Table 1 that as $\bar{s}$ was varied from 0.5 to 2.0, the moisture at the pipes, $\theta_w$, and the average moisture content in the root zone, $<\theta>_c$, changed only slightly. Furthermore, the values did not increase as $\bar{s}$ increased, but changed somewhat erratically because the calculational grid had to be changed for different values of $\bar{s}$, and the effective dimensionless pipe radius $\bar{r}$ could not be held constant. The significance of these results was that large changes in $\bar{s}$ coupled with small variations in $\bar{r}$ did not *significantly* affect the values of $\theta_w$ and $<\theta>_c$. Therefore, the dimensionless pipe spacing $\bar{s}$ is not a critical parameter for determining the extent of soil drying.

A realistic lower limit for soil moisture content for agricultural purposes is the so-called *permanent wilting* point, at which the moisture requirements of the plants exceed the amount of moisture available in the soil. If the moisture level of the soil, as characterized by the average root zone moisture content $<\theta>_c$, is above this limiting value, then there is some assurance that crop growth can be sustained without recourse to subsurface irrigation in the neighborhood of the warm pipes. Data for silt loam soils show that the permanent wilting point is approximately 0.1 (33, 52). Based on this value, Table 1 indicates that for $T_I - T_s = 15°$ C, the minimum acceptable value of $\theta_b$ for agricultural purposes is about 0.15. This value should not be interpreted as a universal requirement for soil warming applications, but it did represent an estimate of the acceptable parametric range for the soil under consideration.

Once the specific parameters of the variable property model had been determined and the solutions to moisture and temperature profiles had been obtained, it became possible to return in a more specific way to the basic problem of the ability of a soil warming system to meet either or both of the agricultural and power plant objectives. For illustrative purposes, a system aimed at meeting the agricultural objectives was first considered. It was assumed that the pipes were 1.0 m deep and had $\bar{r} = 0.04$, that warm water entered the system at $T_I = 31.5°$ C, and that the minimum soil surface temperature $T_s$ was

**TABLE 1.—Parametric Study of the Moisture Content Variation.**

| Parametric Values | | | Calculated Values | |
|---|---|---|---|---|
| Spacing $\bar{s}$ | Moisture at Lower Boundary $\theta_b$ | Temperature Potential (°C) $T_I - T_s$ | Equilibrium Moisture Content $\theta_w$ | Average Moisture Content $<\theta>_c$ |
| 0.5 | 0.20 | 15 | 0.0614 | 0.1314 |
| 1.0 | 0.20 | 15 | 0.0771 | 0.1436 |
| 2.0 | 0.20 | 15 | 0.0555 | 0.1127 |
| 1.0 | 0.15 | 15 | 0.0487 | 0.0998 |
| 1.0 | 0.20 | 15 | 0.0771 | 0.1436 |
| 1.0 | 0.25 | 15 | 0.1566 | 0.1760 |
| 1.0 | 0.20 | 15 | 0.0771 | 0.1436 |
| 1.0 | 0.20 | 5 | 0.1241 | 0.1379 |

expected to be 16.5° C. If the average, midfield root-zone temperature was to be no less than 21° C, then there would be some assurance that the soil temperatures throughout the root-zone would, for a crop such as corn, be in the beneficial range. This implied that $\langle\Phi\rangle_c \geq 0.3$. Figure 22 shows values of $\langle\Phi\rangle_c$ based on Equation 1 for several values of $\bar{s}$. It can be seen that there was a maximum value of $\bar{s}$ above which the criterion $\langle\Phi\rangle_c \geq 0.3$ cannot be met. Then, for any $\bar{s}$ less than this maximum, there was a $\eta_u(\bar{s})$ which represented an upper bound on the operating conditions of the system. In particular, the ratio of pipe length to flow rate in each pipe was limited by:

$$\frac{L}{\dot{m}} \leq \frac{1}{\lambda}\left[\frac{\eta_u\, C_p\, \sqrt{A^2-B^2}}{2\pi}\right] = \frac{\text{constant}}{\lambda} \qquad (10)$$

If, for example, $\bar{s}$ was chosen to be 1.0, then $A^2 - B^2 = 4.50$ and $\eta_u \cong 0.9$ so that:

$$\frac{L}{\dot{m}} \leq \frac{0.644}{\lambda} \quad \frac{\text{cm}}{\text{g/sec}}$$

Taking $\lambda = 3.0$ mcal/cm sec °C for wet silt loam soil as a conservative choice, the result was:

$$\frac{L}{\dot{m}} \leq 215 \quad \frac{\text{cm}}{\text{g/sec}}$$

where the value of the constant depended upon $\bar{s}$, $\bar{r}$, and $\eta$.

Any combination of pipe length L and flow rate $\dot{m}$ which satisfies Equation 10 would meet the temperature specification of $\langle\Phi\rangle_c \geq 0.3$. For a given flow rate, the maximum allowable pipe length could be calculated. If the actual thermal conductivity was lower than the value for saturated soil, the maximum length would increase, since then the water would not tend to cool as readily. In addition, a smaller value of $\bar{s}$ (*i.e.*, closer pipe spacing) would result in a higher value of $\eta_u$, also increasing the limits of pipe length. It is important to emphasize that operating with *any* length *less* than the maximum allowable would meet the temperature specification that $\langle\Phi\rangle_c \geq 0.3$. This indicated that there would be considerable flexibility in the final selection of design parameters when only soil temperature constraints had to be met.

From this example and the previous general discussion of soil moisture, it was concluded that it is possible to design a soil warming system which will significantly raise the soil temperature without drying it to such an extent that additional moisture may be needed near the buried pipes. It was also noted that the ability to heat the soil rests mainly upon the choice of appropriate values for the layout parameters, whereas the availability of adequate moisture in the root zone rests primarily with the moisture content at the lower boundary. The latter depends mainly upon the conditions at the site chosen and the magnitude of the temperature potential, rather than the layout parameters.

The feasibility of satisfying both the agricultural and power plant requirements with a single system was then considered. This example had the same soil temperature requirement, $\langle\Phi\rangle_c \geq 0.3$, as in the previous one, but it also had the significant additional constraint that the system must cool the condenser water by at least 5° C. This latter constraint translated to the condition that:

$$T_1(1) = \frac{T_{w1}(1) - T_s}{T_I - T_s} \leq \frac{26.5-16.5}{31.5-16.5} = 0.667$$

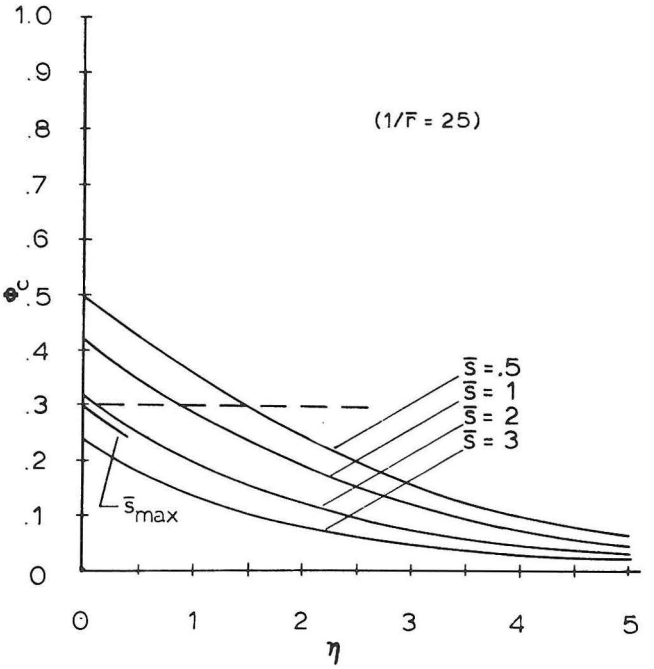


FIG. 22.—Possible solutions for dimensionless soil temperature.

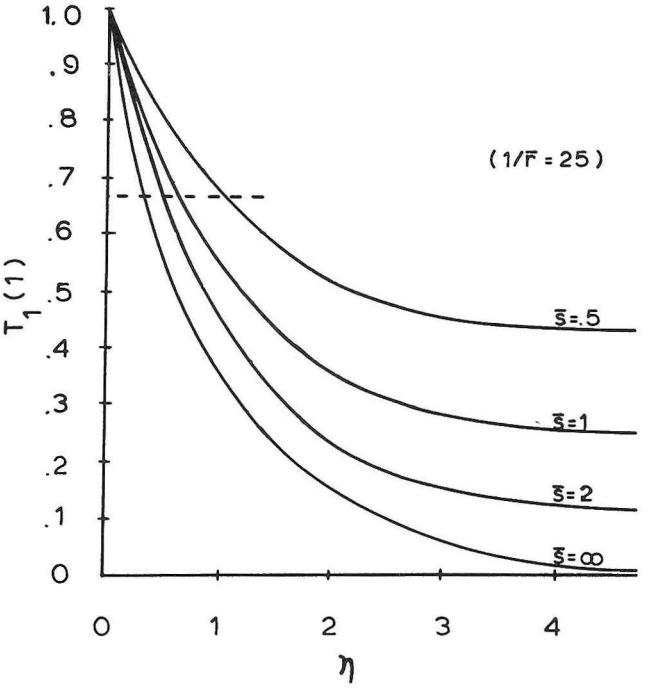


FIG. 23.—Possible solutions for dimensionless water temperature drop.

Figure 23 shows the relationship between $T_1$ (1) and $\eta$ for various values of $\bar{s}$. Thus, in addition to the upper bound imposed on $\eta$, $\eta_u$ ($\bar{s}$), from Figure 22, there was now a lower bound, $\eta_l(\bar{s})$, from Figure 23. In particular, for $\bar{s} = 1$, $\eta_u \simeq 0.9$ and $\eta_l \simeq 0.7$ so that the possible range for acceptable values of $\eta$ was severely restricted. It was also noted that for some values of $\bar{s}$ which satisfy the soil temperature criterion (*i.e.*, $\bar{s} = 2$), the $\eta$ restriction values conflicted and could not be met simultaneously. Taking $\bar{s} = 1$, $\bar{r} = 1/25$, and $\lambda = 0.5$ mcal/cm sec °C (dry silt loam) yielded:

$$1000 \leq \frac{L}{\dot{m}} \leq 1287 \frac{\text{cm}}{\text{g/sec}}$$

If the flow velocity in the pipes was only 11 cm/sec (Reynolds' number of approximately 10,000), then m = 552 g/sec and

$$5.52 \text{ km} \leq L \leq 7.11 \text{ km},$$

and even if wet soil were considered, this length would have been roughly 1 km.

From this second example it was concluded that, when both agricultural *and* power plant objectives must be met by a single system, there is little flexibility in selecting values for the system parameters. Nevertheless, it is technically feasible to meet both objectives with some designs, but the practicality of the systems is questionable. Specifically, it was found that even though all of the constraints can be met, the required length of each pipe is likely to be excessive. Because of this conclusion, all of the succeeding work has been directed at considering the agricultural objectives of soil heating.

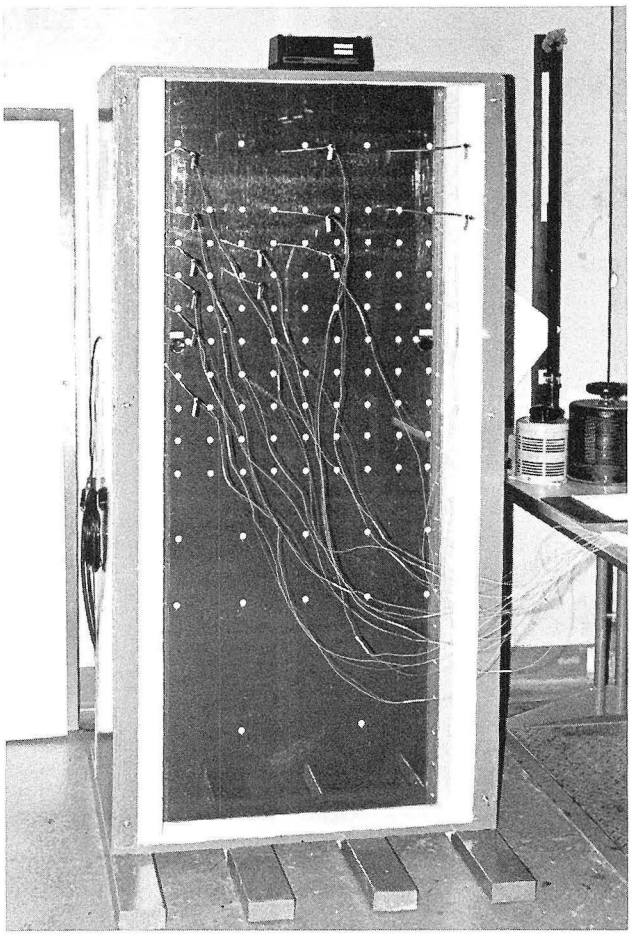

FIG. 24.—Laboratory soil heating system (front cover and insulation removed).

The major significance of the variable property model was that it could compute soil moisture and predict soil drying. Specifically, it could calculate the equilibrium moisture content at the heating pipes and determine the moisture migration effect in the surrounding soil. This model appeared to be the first attempt to address analytically the question of how extensive the dry region would be and to identify the important controlling parameters. Its generality was limited. However, the model established a basis for continued research in this area. One significant limitation was the lack of experimental verification of its predictions. Another limitation was the use of transport coefficients for a specific soil and valid only in a particular moisture range. Because of this, the predictions could not be compared quantitatively with published data for soil warming systems using different soils. In addition, the computer analysis did not represent an exhaustive numerical treatment, even for the particular soil considered. The inherent complexity of the numerical solution required a considerable amount of storage and execution time and limited the number of cases which could be run.

The conclusions drawn from the initial variable property model regarding moisture migration could at best be considered *qualitative* observations which were only quantitatively valid for the case under consideration. It is important, however, to stress that the approach developed by Shapiro (47) was valid and applicable to other soils and soil warming analyses.

## Verification of Predictions for Silt Loam Soil

Johnson (28) studied temperature variation and moisture distribution in silt loam soil in a controlled laboratory system. Figure 24 shows this system with the front cover and insulation removed. The soil sample itself was 0.20 m thick, 0.57 m wide, and 1.52 m deep. The heating sources were electrically heated copper tubes 2.5 cm in diameter placed 0.54 m apart (symmetrically across the width of the system), 0.54 m deep, and extending through the full thickness of the soil. Thermocouple temperature probes could be inserted into the soil at 96 locations throughout the face of the system. By varying depth of insertion, it was determined that the sidewall insulation did indeed reduce the longitudinal temperature variation in the soil to less than 1% of the imposed temperature difference created by the heat pipes. Thus, it appeared that the laboratory unit validly represented a section of a large scale, practical system heated with uniform temperature pipes.

Nine experimental runs were made with this labora-

tory unit. These runs lasted at least 6 days and both of the approaches to temperature and moisture equilibrium were studied. In the first two runs, the overall moisture was kept at a relatively modest level, $\theta = 0.21$, and an effective pipe separation to depth ratio of $\bar{s} = 1$ was achieved by heating both pipes. Figures 25 and 26 show the measured steady-state temperatures for these two runs. In the second, higher temperature run, the heat flux away from the heat pipes was sufficient to form a cylindrical, dry core region approximately 9 cm in diameter around each pipe. This produced very considerable reduction of the soil thermal conductivity in the dry region, and hence very steep temperature gradients around the pipes. Further details on these and the other runs were presented in Johnson (28).

Soil moisture content was determined gravimetrically using oven-dried samples. However, considerable effort was directed toward *in situ* determination of moisture content in the undisturbed soil. The dry cores were observed visually when the insulating cover of the system was removed. However, while the distinction between dry and moist soil was quite clear visually, this technique provided no information of a more continuous, quantitative nature on gradual changes. To overcome this limitation, an adaptation of gamma ray absorption spectroscopy was utilized with partial success.

The absorption of gamma rays is sensitive only to density when transmitted through a homogenous medium. The degree to which a beam of monoenergetic gamma rays is attenuated while passing through a soil sample depends upon the overall density of the sample. Thus, if the spatial distribution of the dry soil material was uniform throughout the sample, changes in the attenuation would have represented changes in water content, and a single gamma ray source would have sufficed for evaluation of the moisture content. Unfortunately, soil density variations from point to point were pronounced. Consequently, the single source method would have been inadequate and *two* gamma

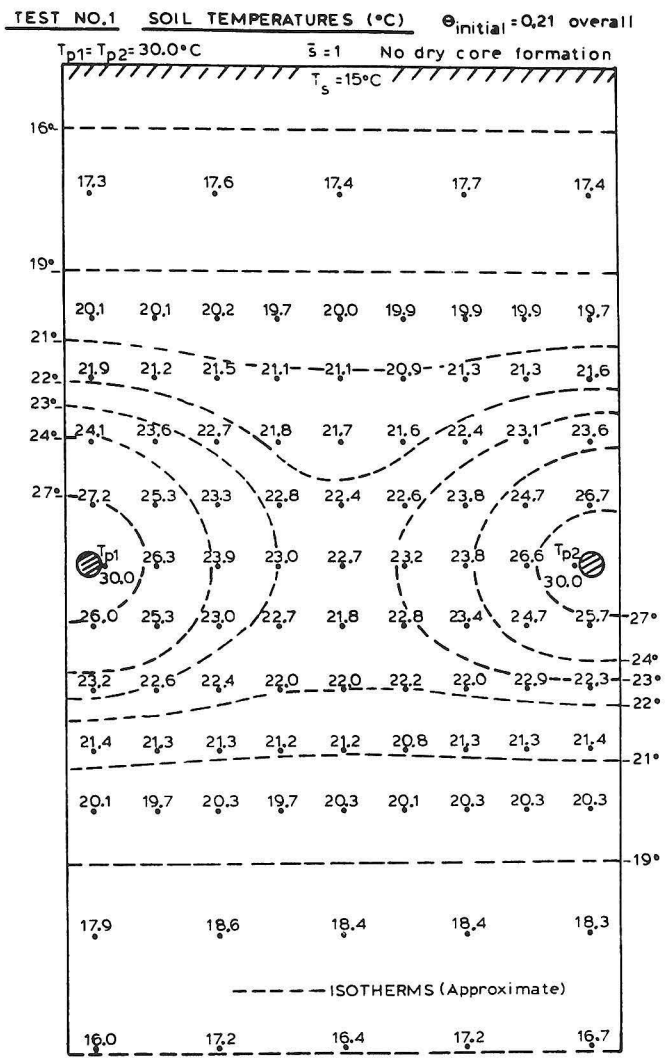


FIG. 25.—Experimental steady-state temperatures (°C), Test No. 1.

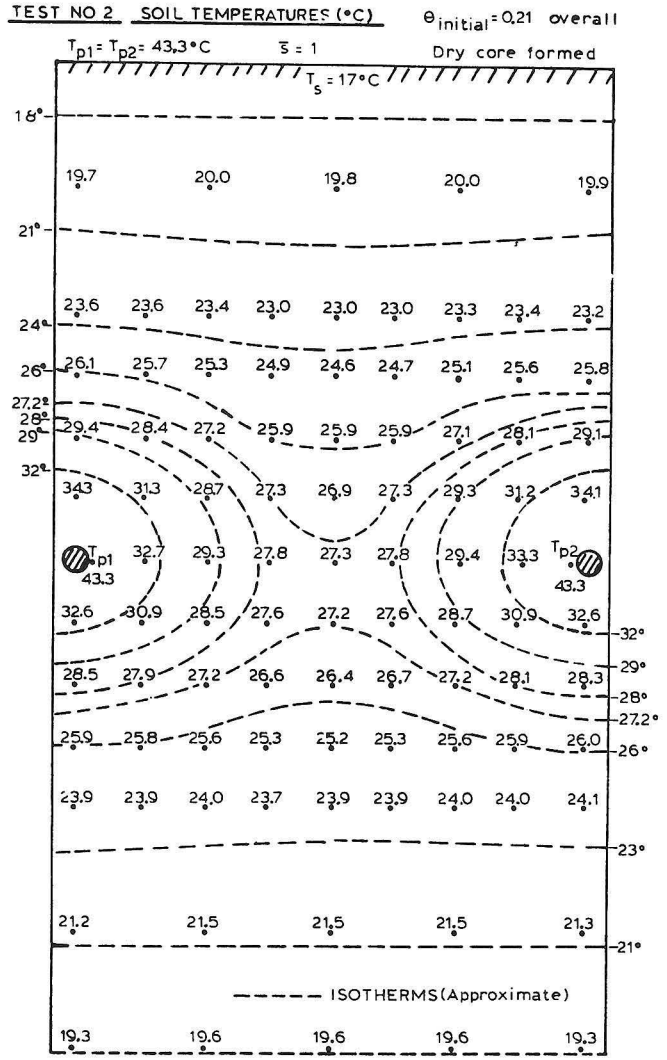


FIG. 26.—Experimental steady-state temperatures (°C), Test No. 2.

ray sources were needed to measure soil density and soil moisture *simultaneously*. This measurement problem was discussed in detail by Johnson (28).

At the outset of Johnson's study, a major objective was to measure soil moisture content via the *dual* gamma ray technique just described. However, after considerable effort it was found that the method was not feasible. The study explained why the method could not be applied to the laboratory model. In addition, an alternate scheme was devised for measuring *changes* in soil moisture at a *fixed* point in the soil warming unit using gamma rays from a *single* source. This allowed at least some *in situ* information on soil moisture behavior to be obtained. First, it was determined that even when overall soil moisture was high and no dry core was formed around the heating pipes, there was a small amount of moisture migration away from the heat source ($\Delta\theta = -4.4\%$ of $\theta$ near the pipe) and no significant change elsewhere. Second, when a dry core formed around a heat pipe, there was a *slight* increase in the moisture content in the region outside the core. Thus, when dry cores formed there were two distinct moisture regimes: a dry core surrounded by relatively unchanged wet soil.

The principal objective of this study was accomplished by evaluating experimentally two conclusions drawn from theoretical considerations by Shapiro (47). First, Shapiro concluded that soil temperature distribution was not strongly dependent upon soil moisture content for a silt loam soil, and that therefore a constant property model would be reasonably accurate for calculating temperature variations in the neighborhood of a buried pipe soil warming system. Experimentally, it was found that if there were *no* substantial dry core formations around the heat sources (*i.e.*, when pipe temperatures were relatively moderate, ~ 30° C, and/or the overall soil moisture content was high, $\theta = 0.32$ $cm^3/cm^3$), then the temperatures predicted by the constant property model agreed well with the experimental steady-state temperatures. Thus, if no dry cores formed, temperature distributions appeared not to be strongly dependent upon soil moisture content. These findings supported Shapiro's conclusions. However, for the case of high pipe temperatures (~ 40° C) in a soil medium of moderate soil moisture content ($\theta \approx 0.21$ $cm^3/cm^3$), dry cores formed, and the constant property model was inadequate for calculating system temperatures. Since these high pipe temperature cases were not considered among the numerical solutions to the variable property model reported by Shapiro, it was recommended that the variable property model be applied for the maximum pipe temperatures considered in this investigation with the objective of evaluating the correspondence of these experimental findings with those predicted by theoretical considerations when dry cores form.

Second, Shapiro concluded that soil warming can be feasible without introducing moisture near the pipes to prevent drying. The experimental results of this study supported this contention, too. Specifically, even when dry cores formed, the system temperatures throughout the bulk of the soil in the laboratory model were elevated enough to be beneficial to plant growth. Also, it was felt that the small moisture changes measured during the experiments would have a minimal adverse effect on the water available in the plant root zone.

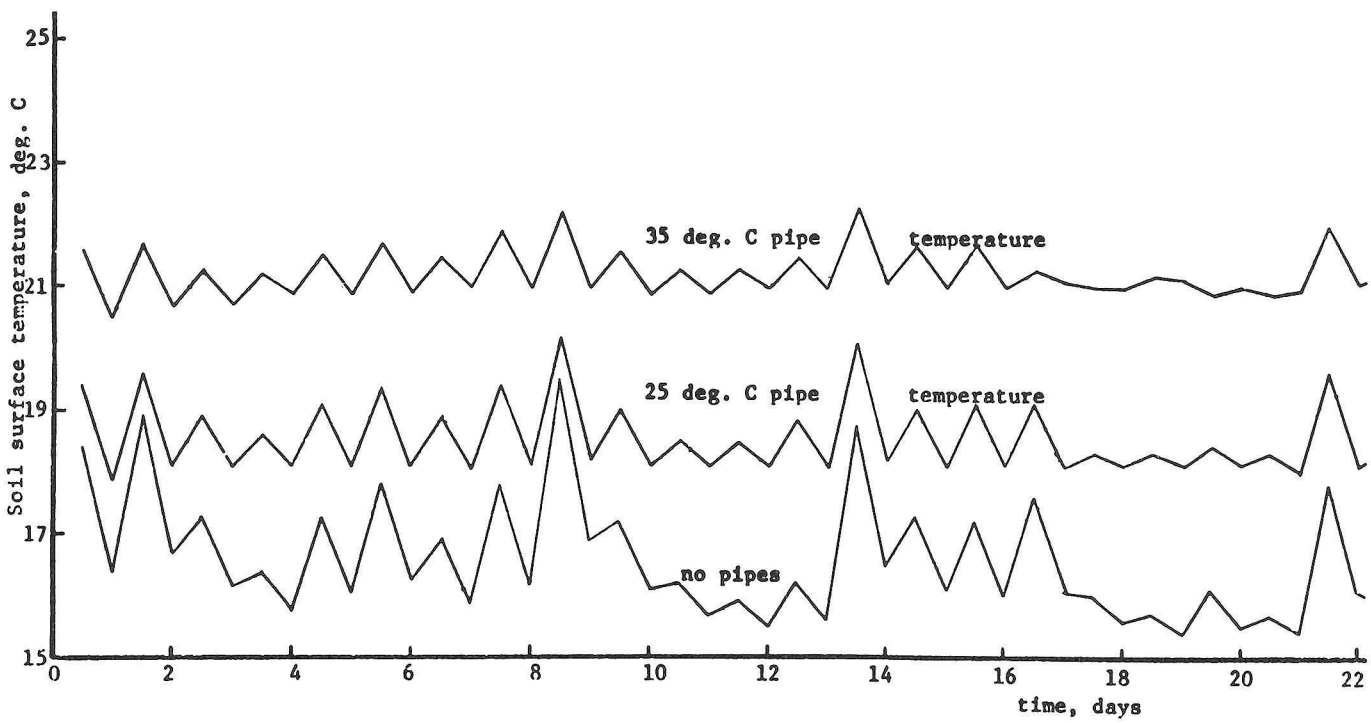


FIG. 27.—Soil surface temperature variations.

## Coupling Soil Heating with Greenhouse Operation

Once soil heating for agricultural purposes had been judged to be feasible, it became important to establish a framework in which the practicality of some area of agricultural application could be considered. The high productivity and energy intensiveness of greenhouse operations made this a logical area to consider, and such a study was undertaken by Parker (38) and Parker *et al.* (39). This study required both the development of a soil heat and mass transfer model capable of handling transient behavior and the coupling of it to a greenhouse heat balance model also capable of handling transient responses.

The conditions which Parker (38) imposed on the soil heat model were rather different from those which Shapiro (47) had used. In particular, he included the effects of temperature-induced vapor flow and soil-water-potential-induced liquid flow. To this end, information from Wescott and Wierenga (54), Gurr *et al.* (25), Bruce (6), Kersten (32), de Vries (13), and Rollins *et al.* (44) was used to produce a new set of equations and parameters which were capable of predicting transient temperature and moisture profiles. An improved, finite differences scheme was used to implement this model in CSMP/360 on an IBM 375/165 computer. The improvements included both a finer mesh grid with more nodes and the development of a parabolic approximation scheme for rectangular grids. The details of Parker's (38) work, however, are not included here since they do not bear directly on the general development of the soil heating research.

Parker coupled his model to a plastic bubble model of a greenhouse which Soribe (50) and Soribe and Curry (51) had developed. This was a one-dimensional model for vertical heat transfer, and the coupling assumed that the pipes were 0.4 m deep and 1 m apart. The basic heat balance equation from the bubble model for the top layer of soil was retained and applied to a surface layer 1 cm thick. In this way, the soil surface temperature was allowed to vary continuously as a dependent variable of both the greenhouse and soil models.

Three different situations were simulated: Case I, without buried pipes; Case II, with 25° C buried pipes; and Case III, with 35° C buried pipes. In each case, weather data for Wooster, Ohio, for the period from Nov. 16 to Dec. 7, 1972, were used. Figure 27 shows the computed soil surface temperatures at 12-hour intervals. The standard deviations of these temperatures about their respective means were 1.00, 0.60, and 0.41° C. The two cases with warming had 1.97 and 4.64° C higher mean soil surface temperatures, respectively.

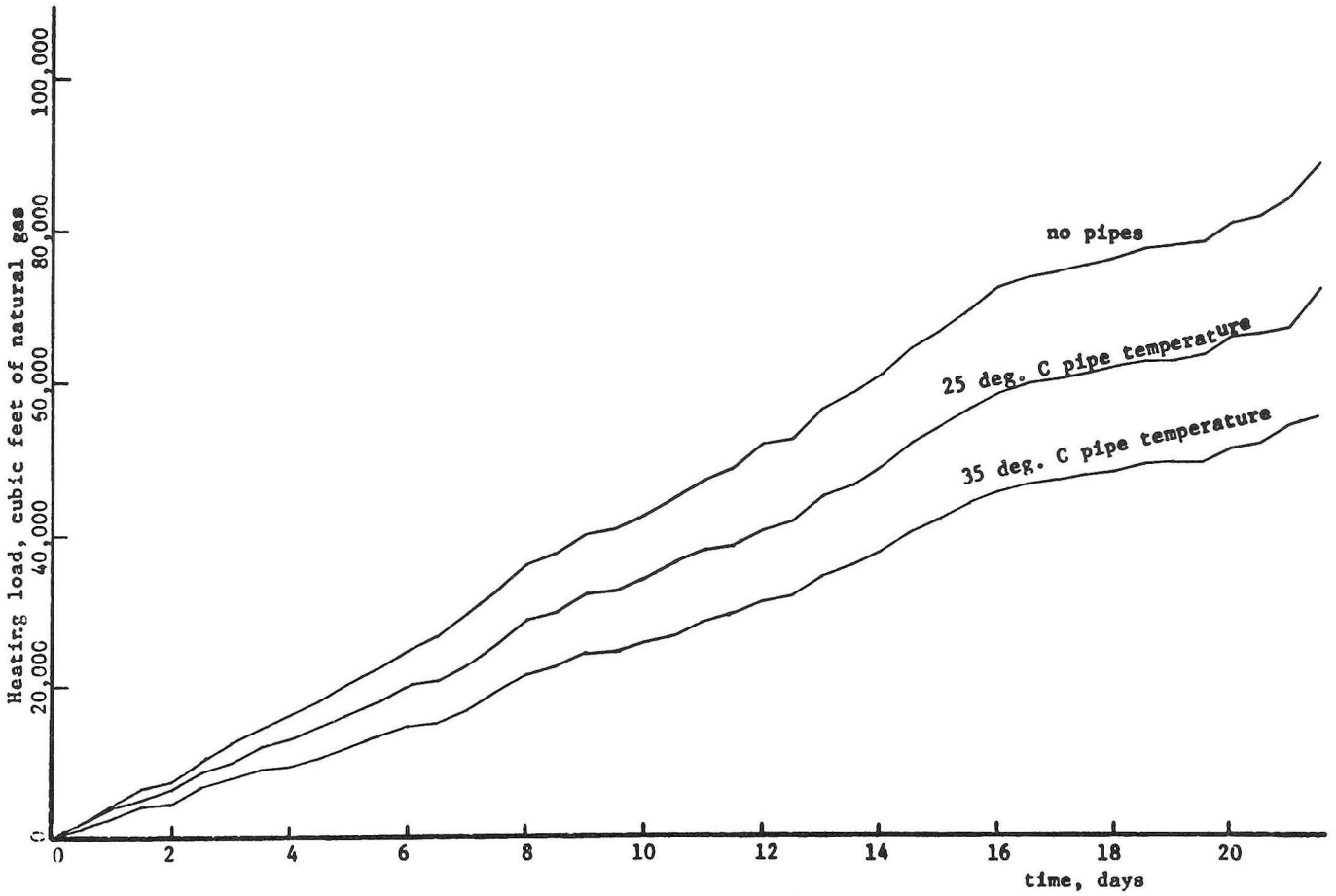


FIG. 28.—Cumulative bubble heating load requirements.

Thus, as the temperature of the pipe system increased, the soil surface temperature also increased and became somewhat less erratic. Both of these effects ought to be beneficial for at least some greenhouse crops.

Greenhouse air temperatures for the three cases were calculated and were found to be quite close (within 0.4° C). The computed cumulative heat load requirements of the greenhouse under these conditions (Fig. 28) show that the savings in the heating requirements for Cases II and III compared to Case I were more than 18 and 35%, respectively. A more generalized view of these results is presented in Figure 29. The average of the outside temperatures for each simulated 6-hour period was computed, as well as the heat load for that particular period. Only the nighttime hours of each of the 22 days were included in order to eliminate extreme scattering of points due to sunny and cloudy days of the same temperature. Some scattering still existed, however, due to such factors as the on-off nature of the heating system and wind velocity variations. The linear regression of the heating load on the outside air temperature is shown for each of the three cases. These results indicated that soil heat can significantly reduce overall greenhouse heating requirements.

## Experimental Soil Heat Studies

The indicated potential for the successful application of soil heating to greenhouse production made it important to take the work out of the laboratory and put it into a practical situation where a detailed examination of actual operation could take place. To some extent the first part of this need had been met with the

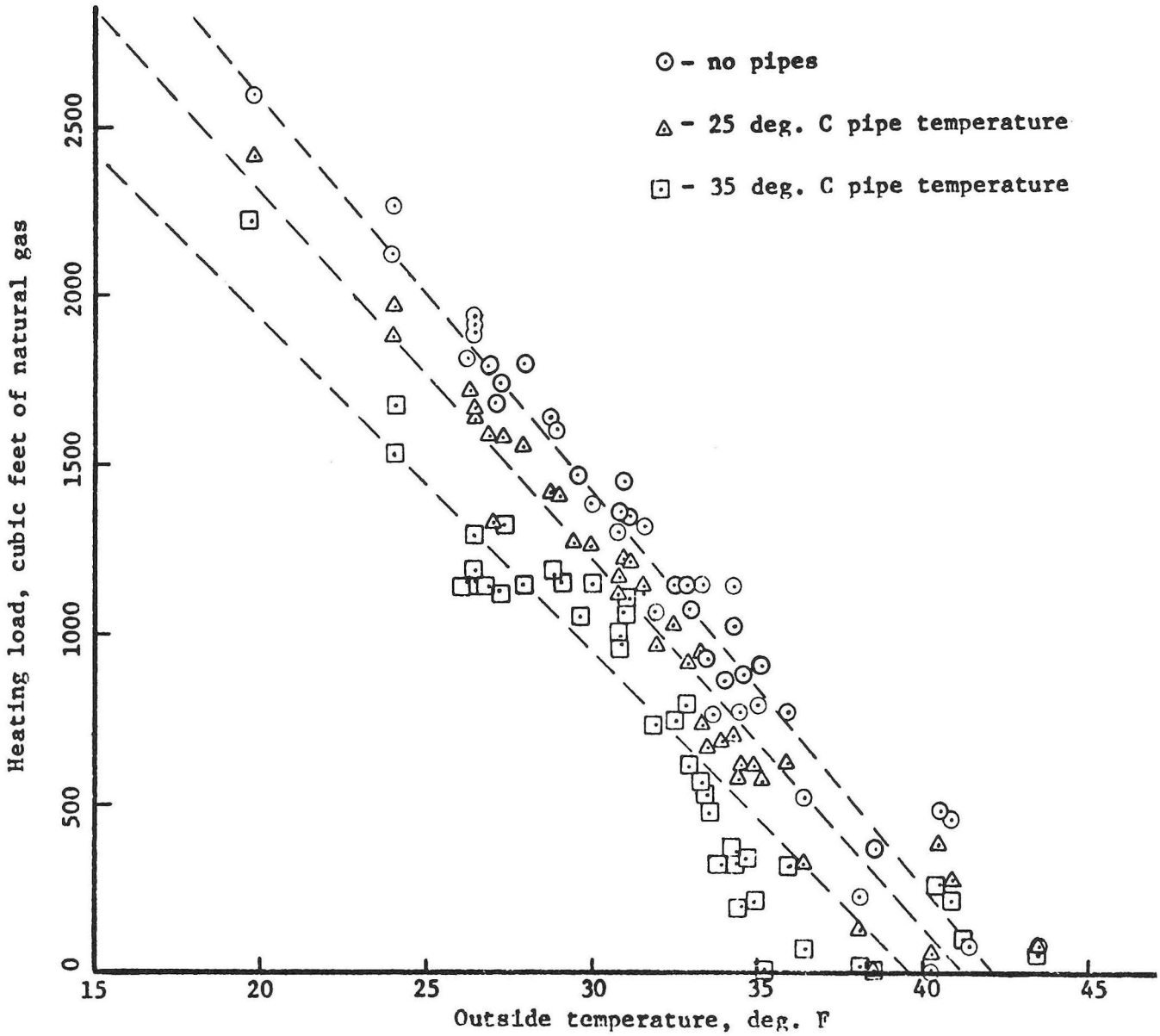


FIG. 29.—Bubble heating load requirements as a function of outside air temperature.

inclusion of Shapiro's (47) basic soil heating design into the Sherco waste heat demonstration greenhouse (5). However, while this project was a very successful demonstration of waste heat utilization, its overall scope precluded a detailed examination of the specific heating contributions obtained through the soil. Therefore, under funding from the Electric Power Research Institute, a series of detailed experiments was initiated in small scale greenhouse plots which contained three very different but representative soil media (42, 43).

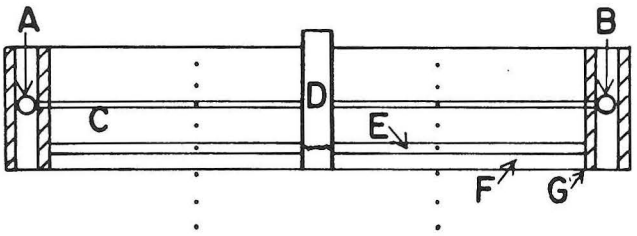


FIG. 30.—Vertical section of an experimental soil warming plot showing the depths at which the thermocouples (•) are located. The hatch marks represent styrofoam insulation. (A) is the supply header, (B) is the return header, (C) is one of the ten heating pipes, (D) is a stand pipe for controlling the water level, (E) is an inch of sand, (F) is 3 inches of pea gravel, and (G) is an impermeable membrane.

## Experimental Facilities and Procedures

These waste heat studies were conducted during the three winters from 1977 to 1980 in a two-bay, gutter connected, double plastic covered greenhouse. Each bay was 5.5 m wide by 29 m long (18.5 x 96 ft) and the two bays were separated into independently heated aerial environments by a clear plastic divider. The southern

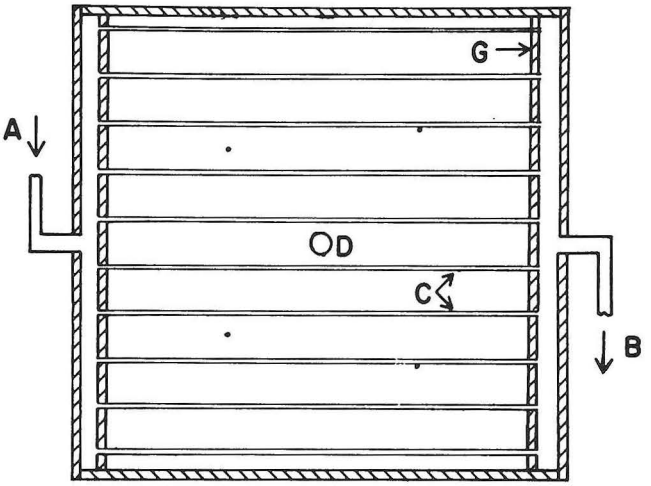


FIG. 31.—Horizontal view of a plot showing two sets of thermocouples on the pipes and two sets between the heating pipes. The labeling is the same as in Fig. 30.

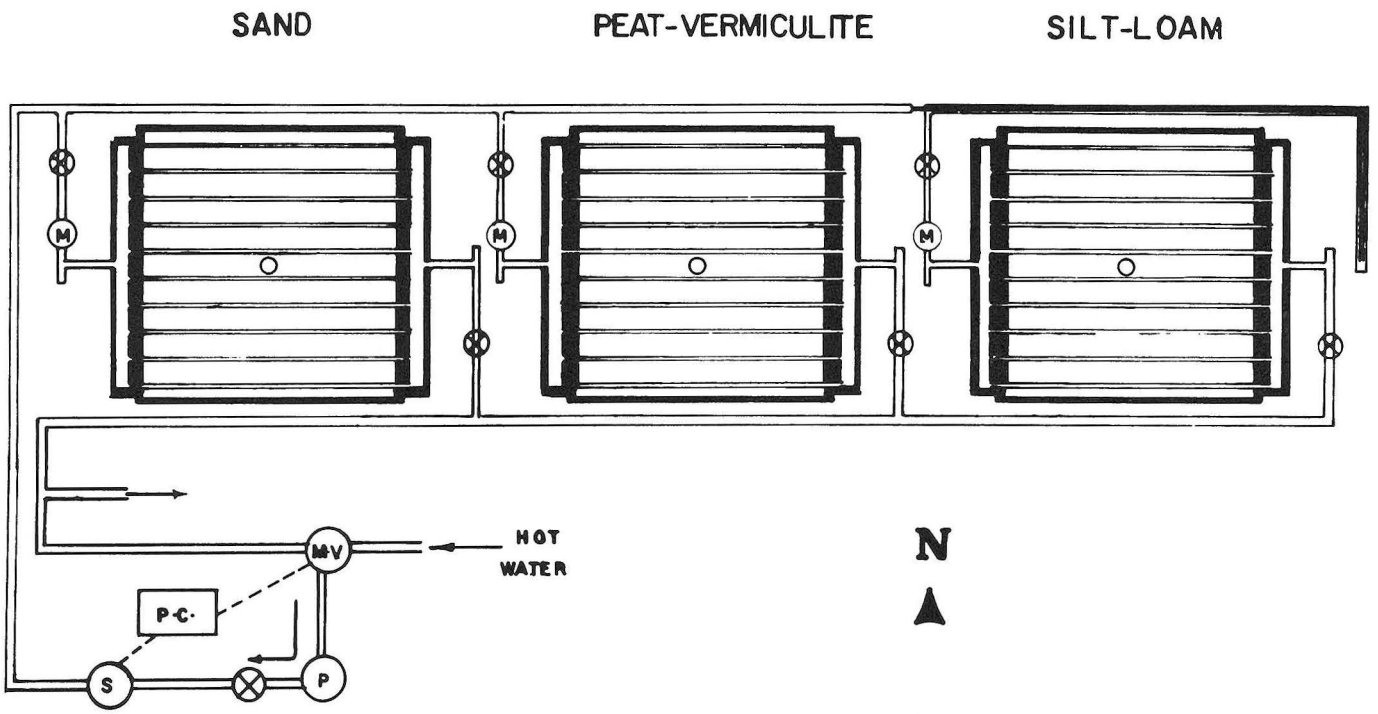


FIG. 32.—Horizontal view of heated soil plots showing general heating pipe configuration and schematic layout of heating control system. (M) is the flow meter on the input side of each plot, (MV) is the mixing valve which regulates water temperature, (P) is the circulation pump, (P• C•) is the Honeywell pressure controller, and (s) is a sensor to determine water temperature.

bay had four 2.9 x 3.0 m (9.5 x 10 ft) soil plots. Three of these plots were heated, provided with sub-soil irrigation (Fig. 30), and contained sand, peat-vermiculite, and Wooster silt loam soils, respectively. The fourth plot was unheated, surface irrigated, contained Wooster silt loam, and served as a control for purposes of comparison.

A plastic liner was placed at a depth of 0.6 m (24 in.) in the three test plots (and up to the surface around their perimeters) to prevent moisture loss to the underlying soil. The bottom 0.1 m (4 in.) of these plots was filled with pea gravel topped with coarse sand to allow for rapid, horizontal, water table equalization, and the remaining 0.5 m (20 in.) was filled with one of the soils indicated above. A constant-level water table was maintained at the 0.5 m depth by an automatic irrigation system and water usage was recorded manually from flow meters.

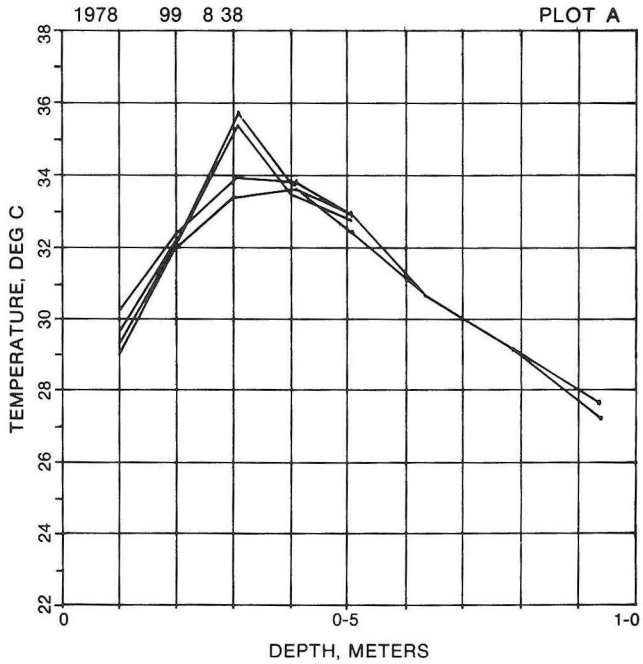


FIG. 33.—Computer-plotted temperature profile.

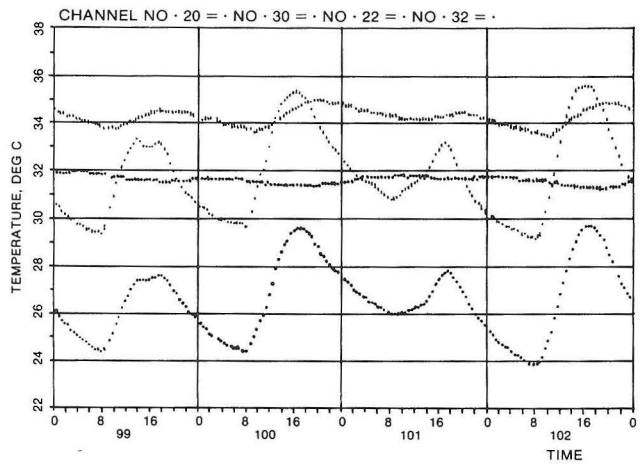


FIG. 34.—Computer plot of various thermocouple readings vs. time.

In an entirely separate, closed loop system, constant temperature heating water was supplied to the heated test plots through a mixing valve controlled by a Honeywell air pressure regulator (Fig. 32). The heated water was circulated to and from the plots through 0.05 m (2 in.) i.d. plastic pipes, and this circulation system supplied, through flow meters and 0.1 m (4 in.) headers, ten 0.025 m (1.0 in.) i.d. ABS plastic heating pipes which passed through the soil in each plot. The depth of and lateral separation between these pipes was 0.3 m (12 in.) (Figs. 30 and 31). The plots were insulated around all four sides with 0.05 m (2 in.) of polystyrene insulation board in order to minimize edge effects on the heat flow in the soil (Fig. 31).

Type T thermocouples, sealed against moisture, were buried in the three heated plots at the various locations indicated in Figures 30 and 31. Each heated plot had 26 temperature recording sites and the unheated plot had 10 such sites. In addition, a 10-junction thermopile was connected across each plot, radiometers were located both inside and outside the greenhouse, and wet-bulb/dry-bulb stations were located at appropriate points in the greenhouse. The readings from these various sensors were monitored automatically by a Kaye Instruments System 8000 datalogger and were recorded on magnetic tape for computer analysis (Figs. 33 and 34).

During each of the three winters of this study, a series of heating water temperature plateaus was maintained such that each temperature level was held constant for 4 to 7 weeks depending on experimental requirements. Four temperatures: 25, 30, 35, and 40° C (77, 86, 95, and 104° F) were used to provide a range of information which would cover the temperature levels normally encountered in power plant cooling water.

The first winter of these studies, 1977-78, was used to determine the physical parameters of heat and moisture transfer in the selected soils (15). The second winter of this work continued the collection of physical parameter data, and in addition examined the effect of soil temperature on lettuce plant growth under standard greenhouse operating conditions. Leaf lettuce, variety HR-5, which is similar to Grand Rapids curly leaf lettuce, was used for this work. Finally, during the third winter the lettuce growth studies were repeated, but this time the minimum nighttime air temperature maintained in the greenhouse was lowered from the standard 13° C (55° F) to an energy saving 7° C (45° F) in order to determine the interaction between air and soil temperatures in their effect on lettuce growth.

## Experimental Results

### *Soil Properties*

The Wooster silt loam was composed of 25% sand (primarily very fine sand, 0.1 to 0.05 mm), 60% silt, and 15% clay. This was fairly close to the composition of the

silt loam used by Johnson (28) in the earlier laboratory studies (Fig. 35). The Wooster silt loam was found to have a dry density of 1.32 g/cm$^3$ and a porosity (based on saturated water content) of 0.44. The sand "soil" was composed of 99+% quartz with approximately 55% of the particles in the medium sand range (0.25 to 0.5 mm) and the remaining 45% being fine sand (0.1 to 0.25 mm). It had a dry density of 1.63 g/cm$^3$ and a porosity of 0.38. The peat-vermiculite mixture was composed of approximately 50% (by volume) commercially available sphagnum peat moss (no further analysis was attempted) and 50% vermiculite particles. It had a dry density of 0.16 g/cm$^3$ and a porosity of 0.81.

### *Moisture*

The irrigation system was designed in such a way that, at equilibrium, all moisture supplied to the water table by the water level controller (Fig. 30) in each plot had to be balanced by an equivalent amount of evaporation from its surface. Due to various contingencies associated with requirements of plant growth, equilibrium conditions were best approximated in the first winter of this study. Figure 36 shows the irrigation supply rates obtained under these circumstances. The values obtained for the silt loam soil were in excellent agreement with Sepaskah *et al.* (46), but the present results for sand were approximately 15 times smaller than those reported there. This discrepancy indicated the relative significance of gravitational potential energy in the determination of fluid flow in these two soils. The fine particle size in silt loam made capillary forces predominate (at moderate moisture content) over gravitational ones so that moisture moved (nearly) as readily upward (as in the configuration studied here) as downward (the configuration studied by Sepaskah). On the other hand, capillary forces in the relatively coarse sand were less significant than gravitational ones, and moisture tended to drain downward much more readily than it could be drawn upward. One effect of this was the formation of a completely dry surface layer in the sand as shown by the lowest line in Figure 37. Thus, it was necessary to supply surface irrigation to the sand in the subsequent studies in order to support lettuce growth. This irrigation was at a rate of at least 19 L/day (5 gal/day or 0.6 in./wk) and eliminated the dry surface layer as shown in Figure 37.

The moisture profiles shown in Figure 37 were obtained from core sample drying data. The figure indicates two separate comparisons which were obtained from these data: first, the drying effects detected in the first winter's physical studies, and second, the variations from the first winter's equilibrium values which occurred during the subsequent growth studies and were related to these growth studies. Each curve shown resulted from a composite of at least two, and usually four, cores per heating period. Cores were taken both adjacent to and midway between heating pipes, each core was divided into 0.025 m (1.0 in.) segments, and the resultant scatter of the individual data points about the lines shown was generally less than ± 0.03 g/cm$^3$.

Due to the considerable effect that soil drying in the region of the heating pipes can have on system heat transfer, drying in this region was carefully studied. The dashed lines in Figure 37 show the drying effects which were detected. This drying was minimal and

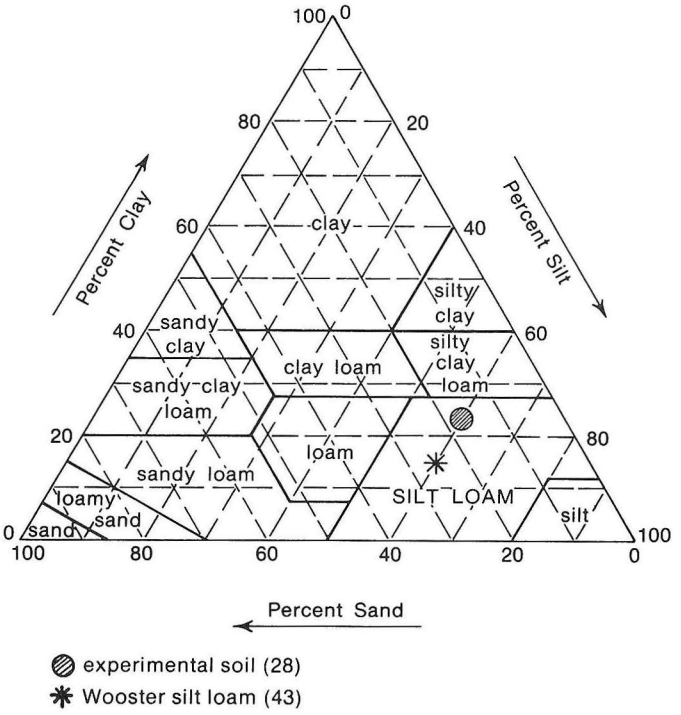


FIG. 35.—Textural classification for soil (14).

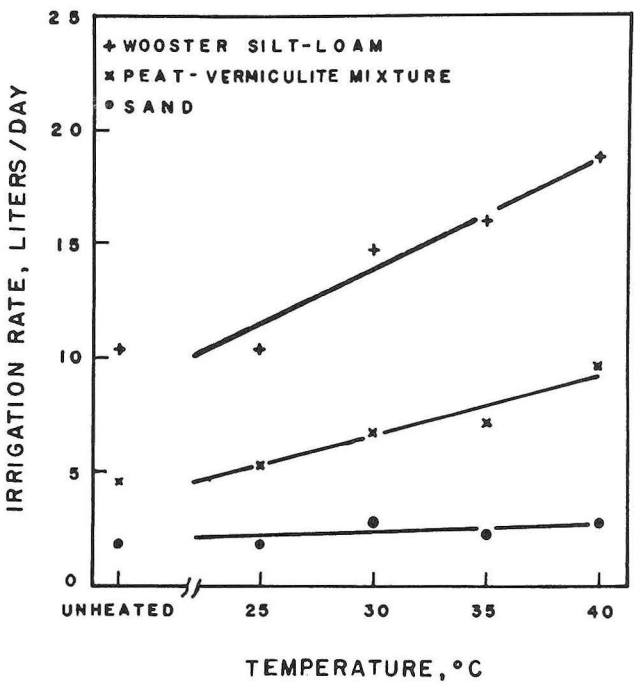


FIG. 36.—Irrigation water supply rate at the different heating levels as determined in the first year of the study.

only occurred in the peat-vermiculite and silt loam soils at the temperature levels indicated. Thus, it was determined that a water table maintained 0.2 m (8 in.) below the heating pipes was able to support adequate moisture around the heating pipes in the temperature range considered. However, it also seemed likely that at higher temperatures this method would prove to be inadequate and that this adequacy would vary with soil type. In addition, the presence of plants in the peat-vermiculite soil seemed to have reduced the moisture in the root zone (down to 0.2 m deep), and it seemed reasonable to associate this reduction with greater moisture withdrawal due to plant transpiration.

### *Heat*

Total heat flow through the soil was determined from two independent sets of data. First, the heat loss from the water in the heating pipes was calculated from the temperature drop of the heating water across the plots (obtained from thermopile readings) and from the flow rates through the heating pipes. Second, the heat transfer in the soil was obtained from measured temperature profiles and from values of thermal conductivity available in the literature (12, 37). For the results of the first winter of this 3-year study, the agreement between the two approaches was generally within ± 5%. In the subsequent work, where various contingencies associated with plant growth made for somewhat less control of soil conditions, the difference between the results of these two techniques was as much as 15%, with a distinct tendency for the heating water heat loss calculations to yield the larger of the two values in each case. However, insufficient detail in the data and lack of known results in the literature made it impossible to tell if this was merely an artifact of the greater uncertainty in the data or an indication of a real effect on thermal conductivity due to root activity.

The results from these heating rate calculations are shown in Figure 38, and the scatter of the data about the lines shown was roughly ± 4 W/m$^2$. The values obtained for sand in the second and third winters were consistently higher than those which were obtained in the first year due to the higher surface moisture values

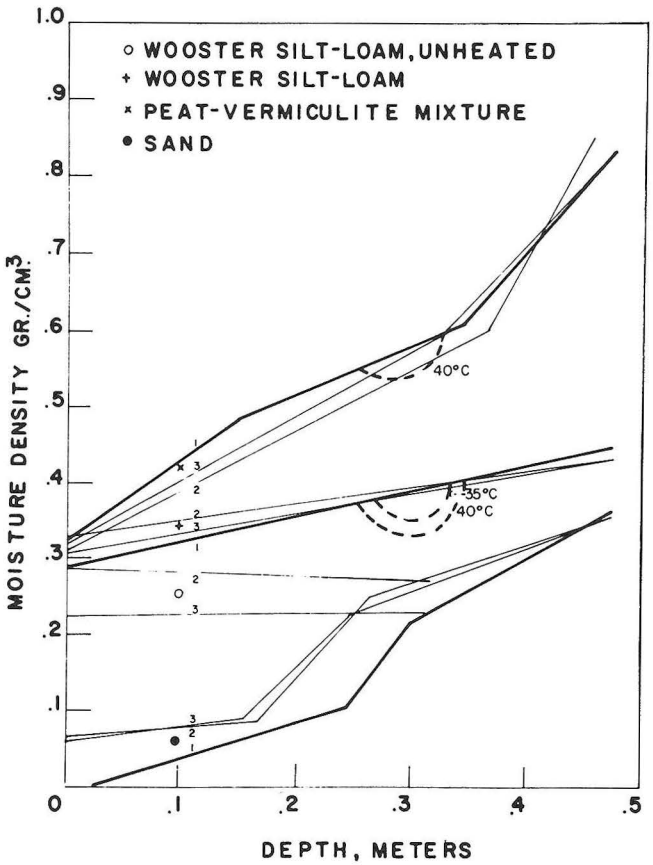


FIG. 37.—Moisture profiles. The dashed lines indicate the drying effects mentioned in the text. The small numerals indicate the year to which a particular line applies.

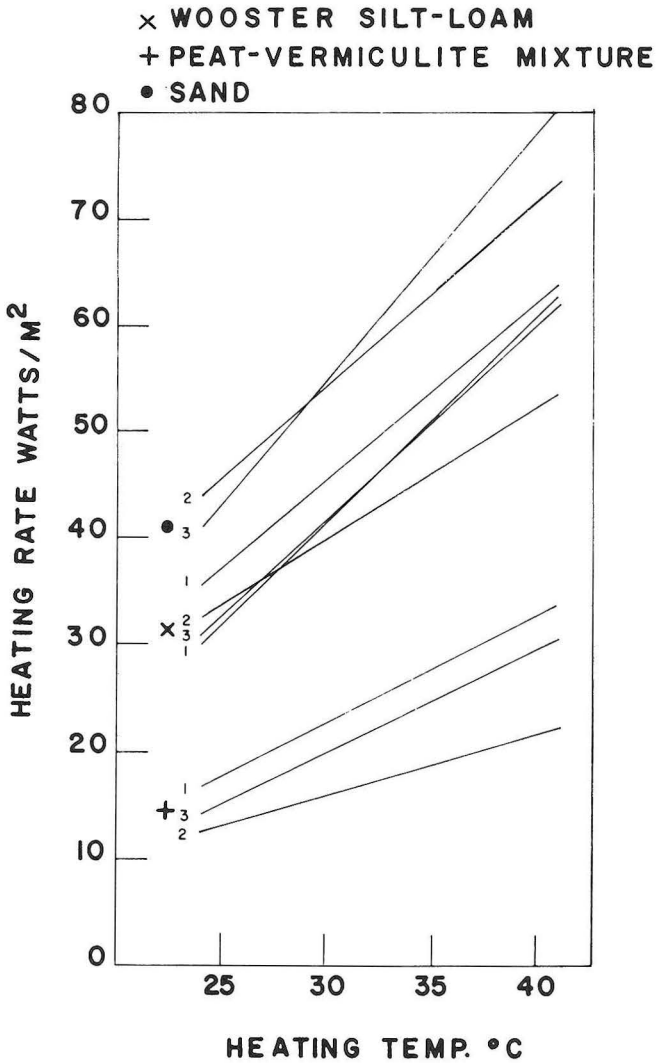


FIG. 38.—Rate of heat absorption from the heating pipes in each of the soil plots. The small numerals indicate the year of the study to which each line applies.

maintained for growth purposes and due to the resultant increase in thermal conductivity. The values obtained for silt loam were in generally good agreement throughout this study, and the differences at higher temperatures in the second winter's values were probably due to a combination of experimental uncertainty and imposed variations caused by the need for soil removal and sterilization. The values for peat-vermiculite were consistently lower in the later work than those observed during the first winter, and since there was considerable evidence that the thermal conductivity of the peat-vermiculite mixture was sensitive to moisture content, it seemed reasonable to associate this with the corresponding lowering of moisture noted earlier. However, more detailed information beyond that presently available (35, 36) on the properties of peat-vermiculite mixtures would be very useful, particularly if computer modeling is to be applied in this case.

The portion of the heat which left the heating pipes and then flowed upward to the soil surface depended on, among other variables, the temperature of the soil beneath the plots. This was an important shortcoming of the small scale plots since it meant that the soil heat flow patterns were to some extent dependent on outside air temperature, an effect which would have been considerably less important in a full scale system. Nevertheless, the then available figures (42, 16) did indicate (even with this "edge effect") that up to 23% of the total, maximum, greenhouse heating requirement (215 $W/m^2$; 1650 $Btu/ft^2/day$) could be met through soil heating, and that on a seasonal averaged basis, up to 40% of the total heating fuel requirement could be replaced in this way. It should be noted, however, that these figures were based entirely on soil heat conductance numbers derived from temperature profiles and that precisely how this heat would have affected the aerial environment could not be determined from the available information.

Figure 39 shows the effect that the soil heating had on the soil temperature at a depth of 0.1 m (4 in.) below the surface. This depth was selected as a useful and convenient representation of the root-zone environment since the bulk of the roots of a lettuce plant grow in the top 0.2 m (8 in.) of the soil and since frequent readings were obtained from each plot at this depth. The particular results shown in this figure are from the second winter of the study (since it does not make sense to make comparisons between years when different heating levels occurred at different times), but the basic effect was the same in all cases. The heated soils remained significantly warmer (see following section) than the unheated soil.

### *Plant Growth*

Various kinds of information were obtained as indicators of plant growth. The most important of these for the above ground (yield) portion of the lettuce plants were wet (fresh) weight, dry weight, and leaf area. It was found that these properties remained in constant proportion to each other throughout the study, and wet weight was chosen as the primary growth indicator since it could be more accurately determined and since it is the normal measure of productive yield. The root systems of various plants were also studied qualitatively. In every case where good leaf growth occurred, there was thick root growth in the top 0.15 m (6 in.) of soil and significant root growth down to the water table.

The lettuce was planted in square patterns with 0.2 m (8 in.) between plants and with 14 rows of 15 plants each

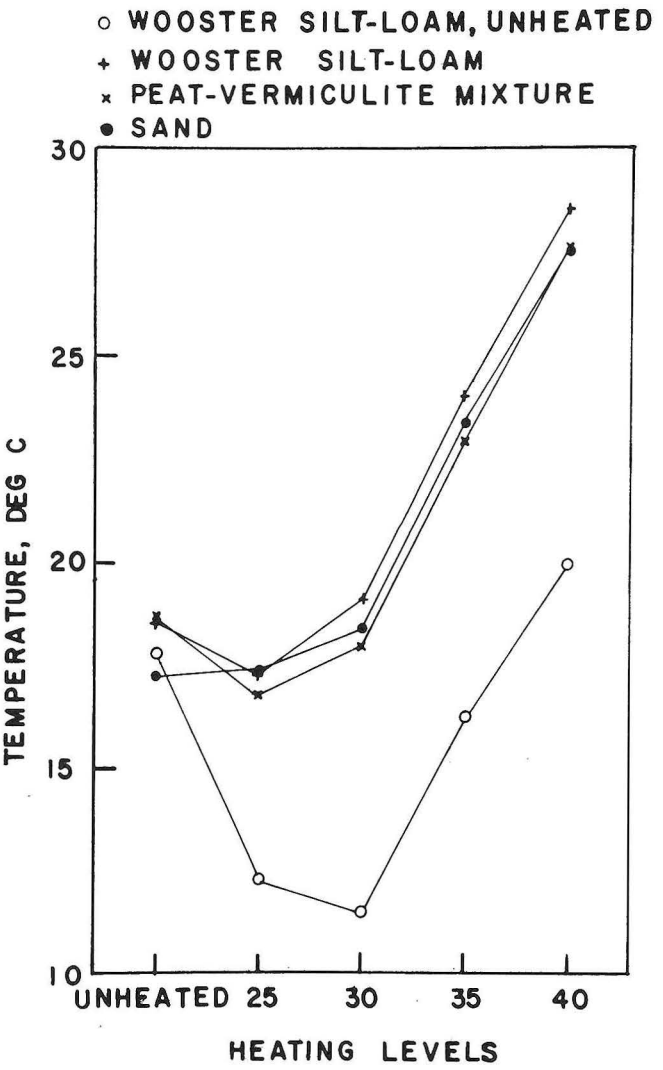


FIG. 39.—Soil temperature as a function of heating water temperature level. The soil temperatures were determined 0.1 m below the surface of the soil and were averaged over each heating period. The results shown here are from the second year of the study. During the fall of that year, all four plots were studied in the unheated state, and then successively higher heating levels were studied through the winter (causing the lower, unheated silt loam temperatures) and into the spring.

(210 plants) in each plot. Six sampling sites of six plants each were designated in each plot according to a predetermined scheme. The layout of these sites was such that each sample area always had a "buffer zone" at least two rows wide completely around it (Fig. 40). Midway through each growth period, 12 lettuce plants were cropped from two of these sample sites on each plot, and at the end of each growth period the same procedure was applied to two additional sites on each plot. In every case the corresponding sites were cropped in each of the four plots, and throughout the growth periods selection of the sites was rotated randomly among the available areas. Thus, while a "double blind" selection system was not maintained, this procedure, combined with the general uniformity of growth in each plot, provided a reasonable degree of assurance that operator bias did not detract from the significance of the results.

For each of the growth periods, the average plant yield from each of the heated soil plots was compared as a ratio with the average from the unheated soil plot. The results for the year when normal greenhouse operating conditions were maintained showed ratios, at a given point in time, which ranged from one (when no heating water was being used) to as high as five in the middle of the winter. Since lettuce growth is exponential with time, this did not mean that lettuce grown on heated soil could reach marketable size in as little as one-fifth the time needed in unheated soil. It did, however, mean that the time required to grow a marketable crop could be significantly reduced by this technique. The results for the year when the minimum nighttime temperature was lowered to 7° C (45° F) showed ratios as great as 10-to-1, primarily due to very slow growth of the crop in the unheated soil.

The significance of these ratios depended to a considerable extent on the absolute values of the yield and on the factors which could be related to these values. One factor which can have an important effect on lettuce growth is the amount of light received by the plant during its growth period, and low growth rates obtained by Ohio lettuce producers during the winter months had traditionally been explained in terms of insufficient light availability. The work of Soribe (50), however, indicated that lettuce growth response saturates at

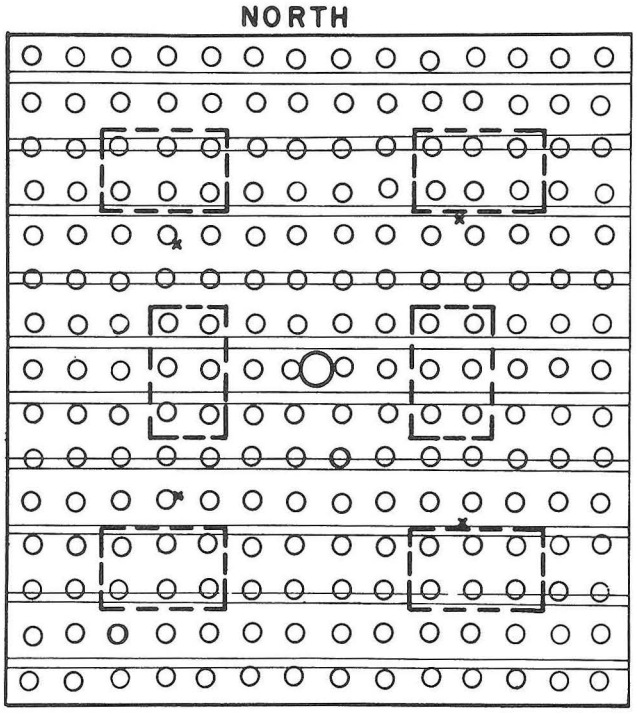


FIG. 40.—Basic layout of each lettuce plot. The lettuce plants (circles) are spaced 0.2 m (8 in.) apart in 14 rows of 15 plants each. The locations of the heating pipes are shown as pairs of light, horizontal lines, and the positions of the thermocouple strings are shown as x's. The six cropping sites are indicated by heavy, dashed lines.

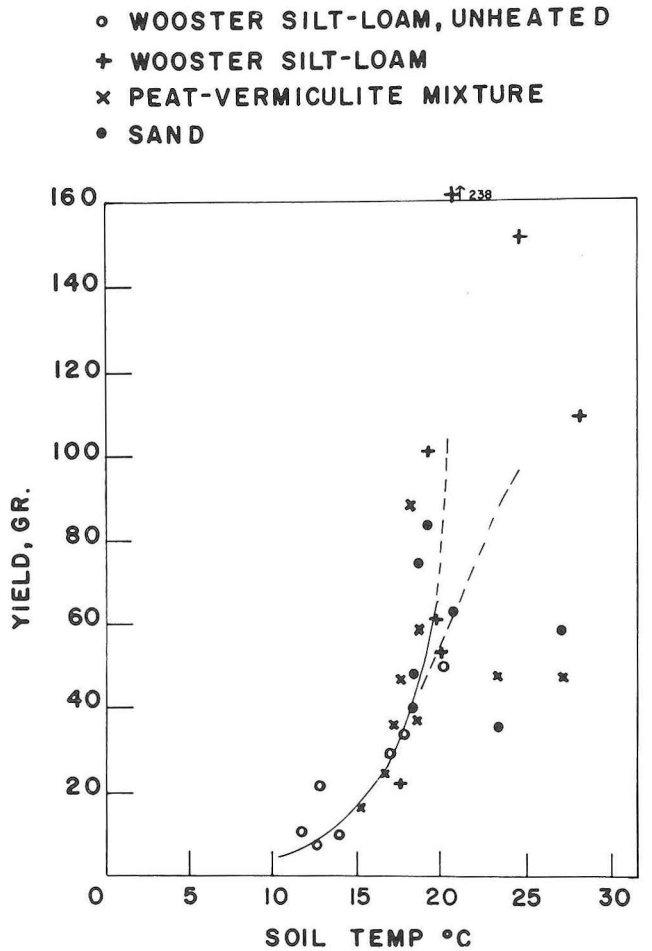


FIG. 41.—Plant yield as a function of soil temperature. The significance of the lines shown is discussed in the text. These results apply to fresh weight yield after 6 weeks of growth. All of the results from the second and third years of the study are shown.

relatively low light levels. In addition, the small plot results (many of which were obtained at "low" winter light levels, but all of which applied to times of sufficient light availability in terms of Soribe's saturation values) indicated good growth response in the heated soil at light levels which were only 60% as great as those that applied for some of the trials where poor growth was obtained in the unheated soil. Therefore, it seemed plausible to conclude that light is not (under Ohio greenhouse operating conditions) the most important factor in limiting winter lettuce growth.

Figure 41 shows plant yield, after 6 weeks of growth, as a function of soil temperature (Fig. 39). The points which fall below and to the right of the main body of the data were results which had been limited by fungus (pythium) and manganese toxicity problems. Thus, all of the results applying to normal lettuce plants fell on a general curve which indicates a strong relationship between soil, root-zone temperature, and plant growth rate. In particular, when soil temperatures fell below 16° C (60° F), lettuce growth was severely restricted. However, when soil temperature was above 19° C (65° F) (up to some high temperature limit not determined by this work), the potential for excellent growth response was present. Thus, in this warmer region other factors, probably of a horticultural nature, produced various limitations which led to the spread in results indicated by the dashed lines.

Two conclusions were drawn from these data. First, it is likely that the long, midwinter growth period required to produce a commercial lettuce crop in Ohio (as much as 13 weeks) is a result of low soil temperatures, and, at most, only a secondary effect of low light levels. Second, with sufficiently warm soil (above 19° C) it should be possible for a commercial lettuce crop to be grown in 6 or 7 weeks even in the middle of winter. This means that a soil-heated greenhouse should be able to produce one additional crop (five instead of the four normally achieved) per year. Such a gain in production ought to be (very roughly) sufficient to pay for the cost of the soil heating equipment in about a year.

Finally, one purpose of the small plot studies was to determine whether satisfactory lettuce growth could be achieved in a lowered nighttime temperature greenhouse. Figure 41 shows growth data obtained under normal nighttime air temperatures (second winter of study) and under lowered nighttime air temperatures (third winter of study), and there is no significant difference between the two sets of results for the two conditions. Thus, clearly, good growth was achieved when soil temperatures were maintained above the critical values already noted and independently of the air temperature differences. This means that energy can be conserved on the basis of a lowered heating requirement (a reduction, corrected for degree day difference, of approximately 25% was achieved in the comparison which took place during this study) and that the soil heating equipment ought to be able to, again very roughly, also pay for itself in this way in less than a year.

## Final Computer Simulation

Ahmed's (1, 2) computer studies made use of the equations of Philip and de Vries (41) and de Vries (11) for moisture transfer in soil. These equations were an extension of diffusion theory which accounted for the thermal and isothermal components of vapor transfer in porous media and separated the fluid flux into components due to temperature gradient, moisture gradient, and gravitational potential.

$$\frac{\partial \theta}{\partial t} = \nabla \cdot (D_T \nabla T) + \nabla \cdot (D_\theta \nabla \theta) + \frac{\partial k_\theta}{\partial z} \qquad (11)$$

component of moisture flux due to temperature gradient + component of moisture flux due to moisture gradient + component of liquid flux due to gravity

where:

$\theta$ = Total volumetric moisture content, $cm^3/cm^3$
$D_T$ = Thermal moisture diffusivity, $cm^2 sec\,°C$
$D_\theta$ = Isothermal moisture diffusivity, $cm^2/sec$
$k_\theta$ = Unsaturated hydraulic conductivity, cm/sec

The thermal and isothermal moisture diffusivities were further broken into liquid and vapor components:

$$D_T = D_{TL} + D_{TV} \qquad (12)$$

$$D_\theta = D_{\theta L} + D_{\theta V} \qquad (13)$$

The two liquid diffusivities ($D_{TL}$ and $D_{\theta L}$) tend to dominate at high moisture contents, while the two vapor diffusivities ($D_{TV}$ and $D_{\theta V}$) dominate at low moisture content. These equations also separated heat transfer in porous media into components due to temperature and moisture gradient.

$$C \frac{\partial T}{\partial t} = \nabla \cdot (\lambda \nabla T) - L \nabla (D_{\theta V} \nabla \theta) \qquad (14)$$

where:

C = Volumetric heat capacity, $cal/cm^3$
$\lambda$ = Soil thermal conductivity, cal/sec cm °C
L = Heat of vaporization, cal/g

Cassel *et al.* (9) and Dempsey (10) applied Equations 11 and 14 to a soil column and concluded that they provided the most comprehensive basis for predicting transient heat and moisture flow in porous media.

It was necessary to know accurate values for the transport properties of a particular soil to apply these equations. The following relationships were used to calculate the theoretical values of the four diffusivity terms (9, 24, 40).

**Isothermal liquid diffusivity, $D_{\theta L}$**

$$D_{\theta L} = \kappa \frac{\partial \psi}{\partial \theta} \qquad (15)$$

where:

$\kappa$ = Unsaturated hydraulic conductivity, cm/hr
$\psi$ = Soil water pressure head, function of moisture content, cm

**Isothermal vapor diffusivity, $D_{\theta V}$**

$$D_{\theta V} = \frac{D_{atm} \alpha \rho_a g P}{(P-p)\rho_w} \frac{\partial \psi}{\partial \theta} \qquad (16)$$

where:

$D_{atm}$ = The molecular diffusivity of water vapor in air, $cm^2/hr$
P = Total air pressure, mm Hg
p = Vapor partial pressure, mm Hg
$\alpha$ = A tortuosity factor taken as 0.66, dimensionless
a = Volumetric void fraction, $cm^3/cm^3$
g = Gravitational acceleration, $cm/sec^2$
$\rho_w$ = Density of liquid water, $g/cm^3$
R = Gas constant, ergs/gK
$\theta$ = Soil water content, $cm^3/cm^3$
T = Temperature, K

**Thermal liquid diffusivity, $D_{TL}$**

$$D_{TL} = \kappa \gamma \psi \qquad (17)$$

where:

$\gamma = \frac{1}{\sigma} \frac{d\sigma}{dT}$ = temperature coefficient of surface tension of water, $°C^{-1}$
$\sigma$ = Water surface tension, dynes/cm

**Thermal vapor diffusivity, $D_{TV}$, $cm^2/hr\ °C$**

$$D_{TV} = \frac{(a+f \cdot \theta)\ D_{atm}\ P\ h}{\rho\ (P-p)} \frac{\nabla T_a}{\nabla T} \frac{\partial \rho_o}{\partial T} \qquad (18)$$

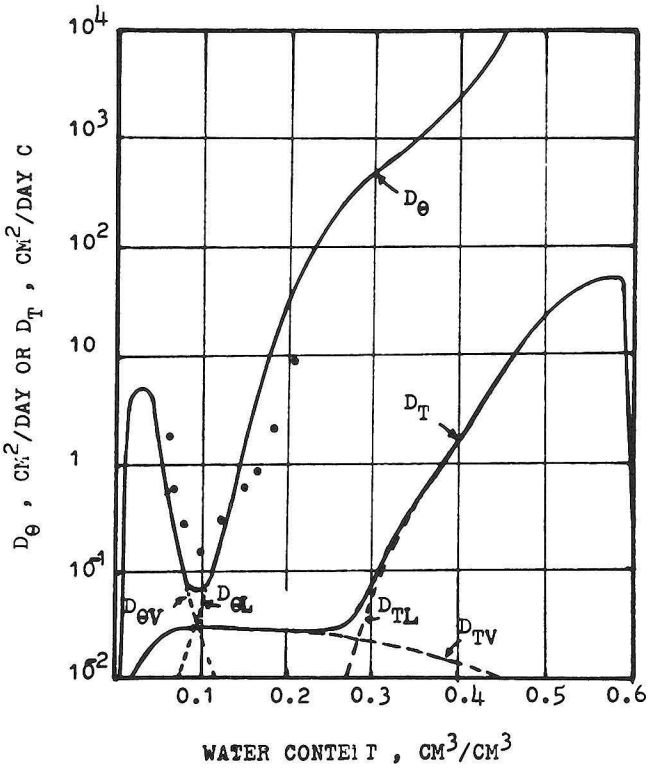


FIG. 42.—Theoretical and experimental values of the transport coefficients for Palouse silt loam (24).

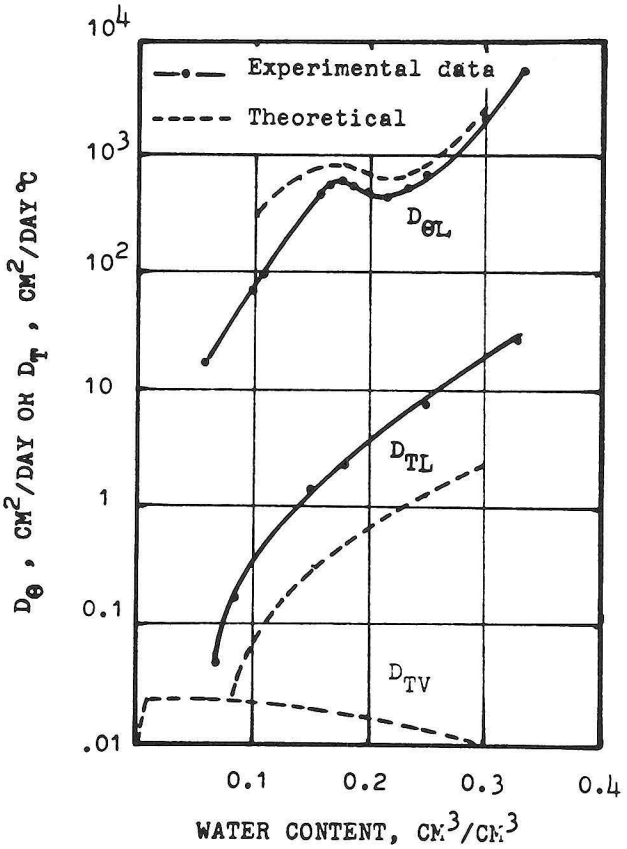


FIG. 43.—Theoretical and experimental values of the transport coefficients for a medium sand (30).

where:

$a$ = $\theta_s - \theta$, $\theta_s$ = saturated moisture content

$f$ = $\begin{cases} a/a_k \text{ for } 0 < a < a_k \\ 1 \text{ for } a \geq a_k \end{cases}$

$a_k$ : value of $a$ at which liquid continuity in pores no longer exists

$h$ = $p/p_o$, the relative vapor pressure of air, mm Hg

$\rho_o$ = Density of saturated vapor, $g/cm^3$

$P_o$ = Saturated vapor pressure of air, mm Hg

$T$ = Temperature, °C

$\nabla T_a$ = Mean temperature gradient in air-filled pores, °C/cm

$\nabla T$ = Overall temperature gradient, °C/cm

Gee (24) used the non-destructive neutron water-content measurement method on a silt loam soil in a closed column to determine the component diffusivities of Equations 12 and 13. A comparison between the calculated and the experimental values of the four diffusivity terms is shown in Figure 42. Jury and Miller (30) measured the primary and cross-coupling transport coefficients for the simultaneous flow of heat and moisture through a medium sand in the liquid-dominated regime of moisture flow. The calculated and the experimental values of these diffusivity coefficients are shown in Figure 43.

A finite differences computer modeling approach was used to solve the transport equations. The modeled rectangular soil region was divided into a grid of rectangles (Fig. 44). Rectangles above the pipes were equal and had one height; those below the pipes were also equal but had a different height. All rectangles had the same width. Nodes were taken to be at the corners of the rectangles. Node temperature and moisture content were determined from the equations except at the upper and lower boundaries, where experimentally recorded values were used, and except in the case of temperature, at the pipe node where an assigned (driving) value was used. This procedure yielded an equal number of equations and unknowns and therefore provided a unique solution to the problem. A parabolic approximation method, developed by Hamdy and Barre (26) in spherical coordinates and modified by Parker (38) for use in two-dimensional Cartesian coordinates, was used to approximate the space partial derivatives in the equations. This method approximated the profile of a dependent variable around a node in the direction of the space derivative of each independent variable by a parabolic curve. The three coefficients of this curve were calculated for interior nodes such that the parabola agreed with the dependent variable at the node and at the adjacent node on each side. The three coefficients were calculated for nodes on the vertical boundaries such that the parabola agreed with the dependent variable at the node and at the adjacent interior node, and its gradient agreed with the gradient at the node. The parabola was then differentiated as often as necessary to approximate the partial derivatives with respect to the space variable at the node. It was also integrated over the space variable to determine the average temperature and moisture content.

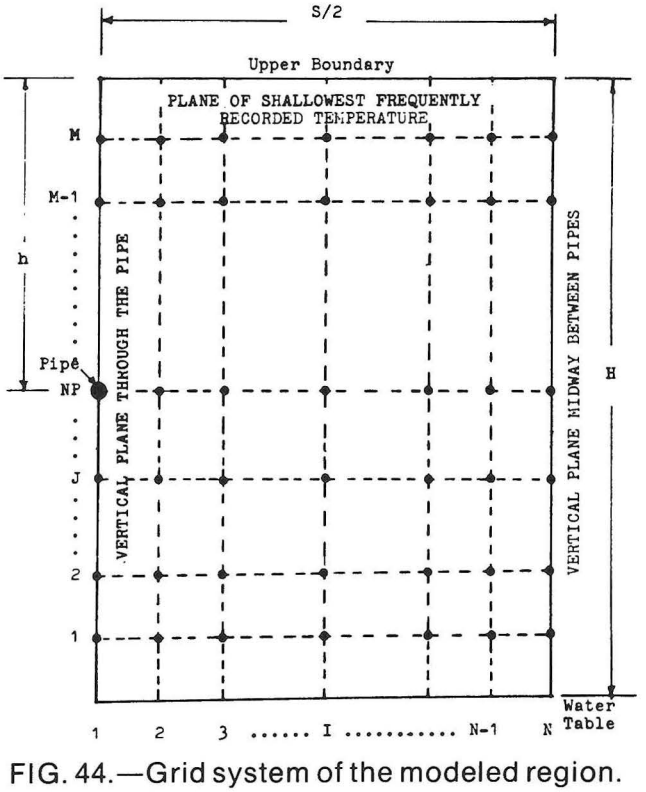


FIG. 44.—Grid system of the modeled region.

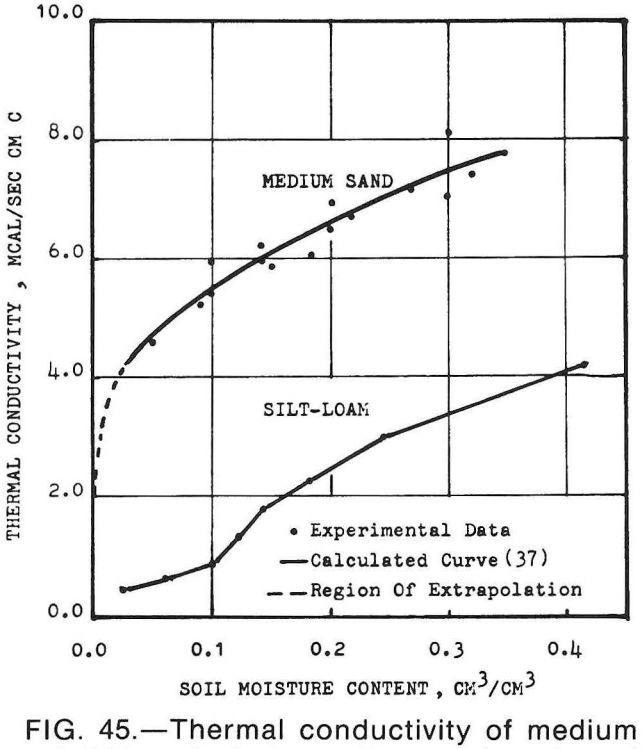


FIG. 45.—Thermal conductivity of medium sand (30) and silt loam (3) as a function of moisture content.

The transport coefficients for silt loam (Fig. 42) and sand (Fig. 43), their thermal conductivities (Fig. 45), and the sand hydraulic conductivity (Fig. 46) were stored as functions of the soil moisture content on function generators in the computer program (Appendix B). The thermal capacity was calculated by the program as a function of soil moisture and bulk density. The bulk density and latent heat of vaporization were input parameters incorporated into the program.

Figure 47 shows a comparison of the computed, steady state, vertical temperature profiles in the silt loam soil with the first year's experimentally measured values for the same quantity. Experimentally measured values at the 0.1 m and 0.5 m depths and at the surface of the heating pipes were used as the boundary conditions for the computer calculations, and the root mean square deviation of the intermediate points was only 0.1° C. Similar comparisons for all three experimental soils at the 25° C heating level are shown in Figure 48.

Figure 49 shows the transient temperature in the sand soil midway between two adjacent heating pipes. The upper and lower dotted "lines" were the experimental values which were used as input boundary conditions. Initial conditions fed into the model were arbitrary and *did not* correspond to observed soil temperatures. Thus, during the first 12 hours there was considerable deviation between observed and calculated values which compensated for the initial differences. However, for the final 72 hours the root mean square deviation is a respectable 0.2° C. In addition, the fact that the experimental points tend to be higher than the calculated ones could result from small displacements of the thermocouples from their theoretical positions.

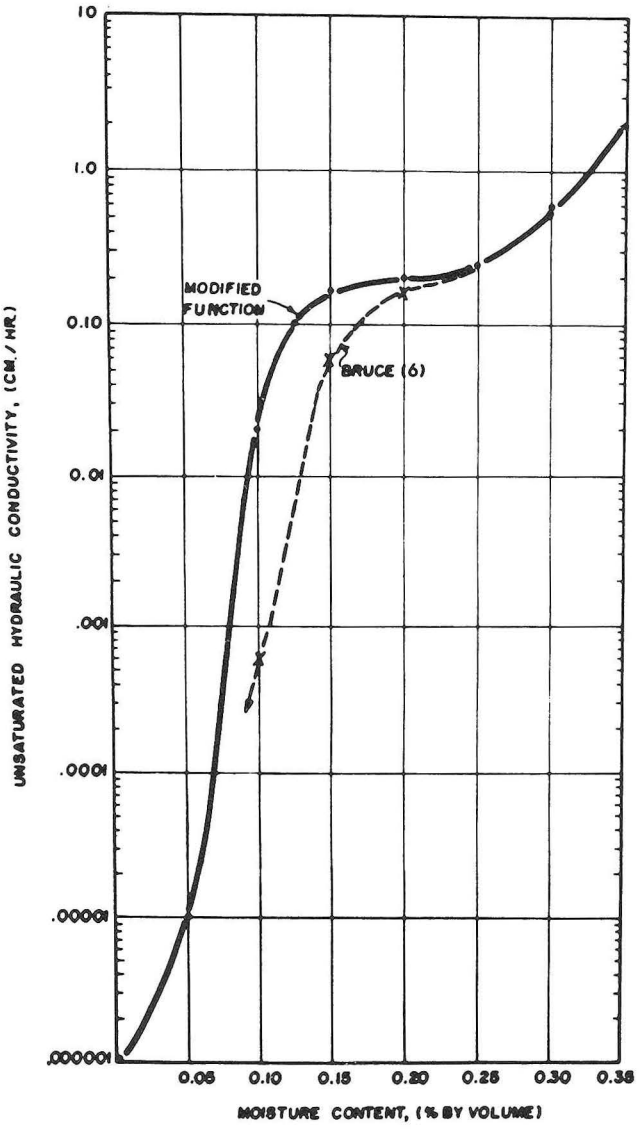


FIG. 46.—Hydraulic conductivity for the sand plot.

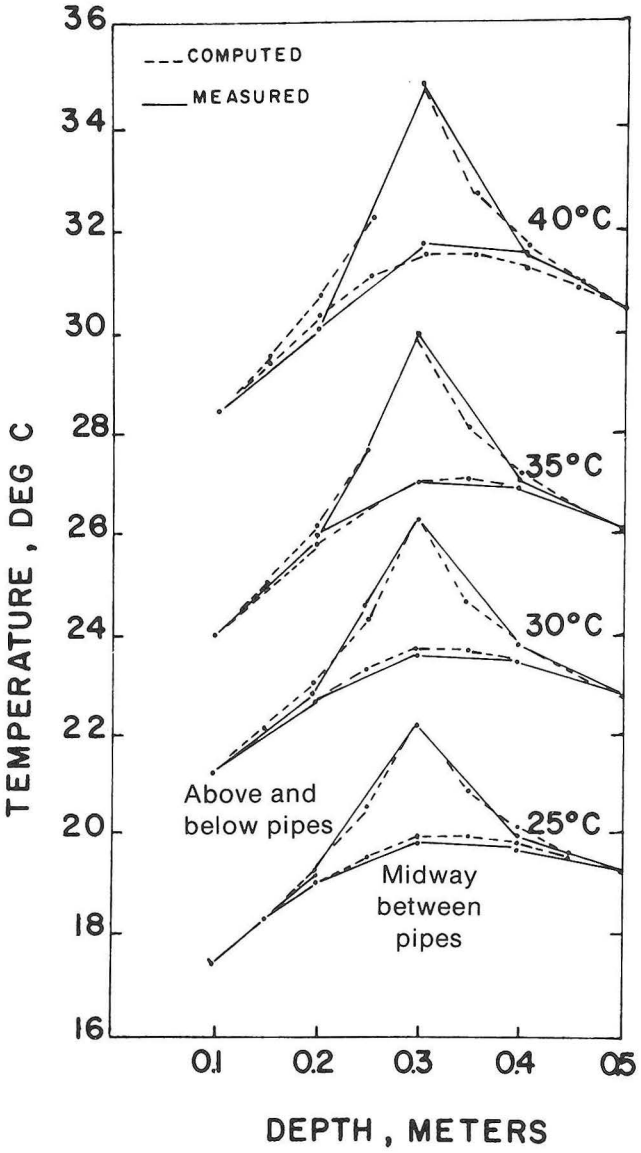


FIG. 47.—Steady-state temperature profiles for the silt loam soil based on the first year's results.

**TABLE 2.—Heat Absorption Rates by the Test Plots from the Heating Pipes at Different Heating Levels.**

| Heating Level | Average Heat Absorption Rate, watts/m² | | | | | | |
|---|---|---|---|---|---|---|---|
| | Silt-Loam | | | Sand | | | P. V.* |
| | T/P | O/P | C/P | T/P | O/P | C/P | T/P |
| 25° C | 30.0 | 36.26 | 38.01 | 35.3 | 42.97 | 41.81 | 17.7 |
| 30° C | 41.9 | 39.15 | 40.72 | 50.4 | 49.11 | 51.80 | 22.5 |
| 35° C | 51.1 | 46.21 | 48.83 | 52.3 | 52.56 | 53.71 | 27.2 |
| 40° C | 61.4 | 50.58 | 50.40 | 58.0 | 57.94 | 57.99 | 30.7 |

T/P: Based on thermopile readings.
O/P: Based on observed average temperature profiles.
C/P: Based on computed steady state temperature profiles.
*Rates based on profiles could not be calculated for lack of information on peat-vermiculite (mixture) thermal conductivity.

Table 2 gives the rates of heat flow away from the heating pipes (heat absorption rate) for each of the four heating levels observed during the first year and the computer simulation calculations of the same quantities. The agreement of values along any given line is generally quite good. Comparisons between lines are discouraged since the air temperatures above the soils were different in each case due to changes in solar intensity and outside air temperature.

Figure 50 shows a comparison between the experimentally obtained moisture profile for the sand soil without surface irrigation (first year's results) and the computer calculation of the same quantity. This particular comparison is of considerable importance in the evaluation of the model's capabilities because of the distinct lack of linearity of the results involved. It was originally believed that this lack of linearity might be a response to heat flow from the pipes, but neither the computer calculations nor the experimental results supported such a hypothesis. In fact, later experimental work indicated that the distinct changes in the slope of the moisture profile occurred at particular moisture contents (Fig. 37) and were not related to the heating pipes. To account for this, it proved necessary to modify the hydraulic conductivity figures which were fed into

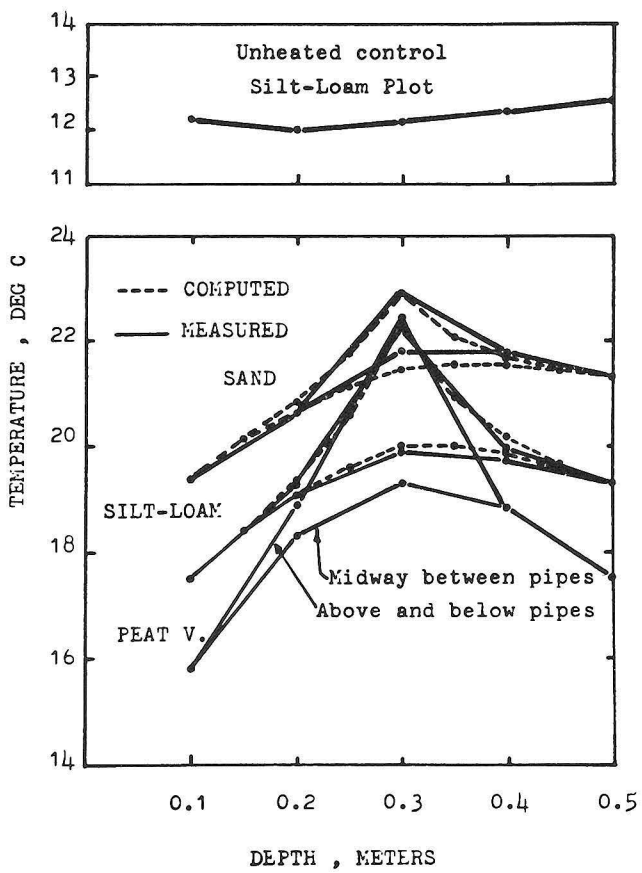


FIG. 48.—Measured average and computed steady-state vertical temperature profiles at the 25° C heating level (–8.5° C average outside temperature).

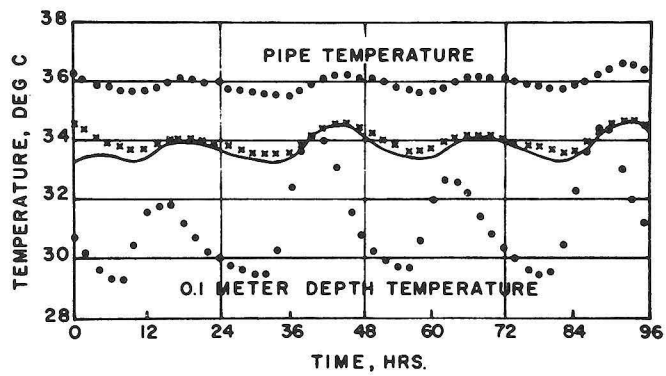


FIG. 49.—Temperature variation in the sand soil over a 4-day period. The dots show experimental values for the temperatures at the surface of the heating pipes and at the 0.1 m (4 in.)depth in the soil, amd these values were used as input boundary conditions for the computer model. The experimental points (x) and computer values (solid line) are for temperatures midway between the pipes.

**TABLE 3.—Average Water Consumption Rate by Test Plots in liters/m$^2$ per Day.**

| Heating Level | Silt-Loam | | | | | Sand | | | Peat-Vermiculite |
|---|---|---|---|---|---|---|---|---|---|
| | | Gee (24) | | Revised | | | Jury and Miller (30) | | |
| | Meter | O/P | C/P | O/P | C/P | Meter | O/P | C/P | Meter |
| Unheated | 1.20 | | | | | 0.22 | | | 0.53 |
| 25° C | 1.21 | 21.48 | 31.28 | 2.00 | 2.80 | 0.22 | 0.15 | 0.21 | 0.61 |
| 30° C | 1.69 | 21.41 | 31.29 | 1.99 | 2.80 | 0.31 | 0.16 | 0.22 | 0.78 |
| 35° C | 1.85 | 21.56 | 31.42 | 2.15 | 2.95 | 0.24 | 0.16 | 0.22 | 0.83 |
| 40° C | 2.15 | 21.45 | 31.44 | 2.04 | 2.98 | 0.32 | 0.16 | 0.22 | 1.09 |

O/P: Based on observed profiles.
C/P: Based on computed profiles.

the computer program as shown in Figure 46. It was only when the upper curve was used that the agreement shown in Figure 50 was obtained. These modified values were subsequently compared with the hydraulic conductivities obtained by Bruce (6) for various types of sand. The higher values shown in Figure 46 correspond to those given in that paper for a "graded" rather than for a "fine" sand, and the physical soil properties of the sand used in the present experiments were quite close to those given for "graded" sand. Thus, the computer model proved to be both sufficiently sensitive to simulate an interesting experimental result and sufficiently discriminating to require accurate input information. Such performance indicated the considerable capabilities which have been achieved in this modeling work.

Table 3 gives the rates of irrigation water consumption observed during the first year of the study and presented in a slightly different form in Figure 36. The same quantity was also calculated from observed and computed moisture profiles on the basis of isothermal diffusivity values obtained from the literature. The agreement in the sand soil using figures from Jury and Miller (30) was reasonably good, but reasonable agreement was obtained in the silt loam soil only when the figures obtained from Gee (24) were revised downward by an order of magnitude as shown in Figure 51.

The final calculation made with the soil model was directed at determining the effect which raising the

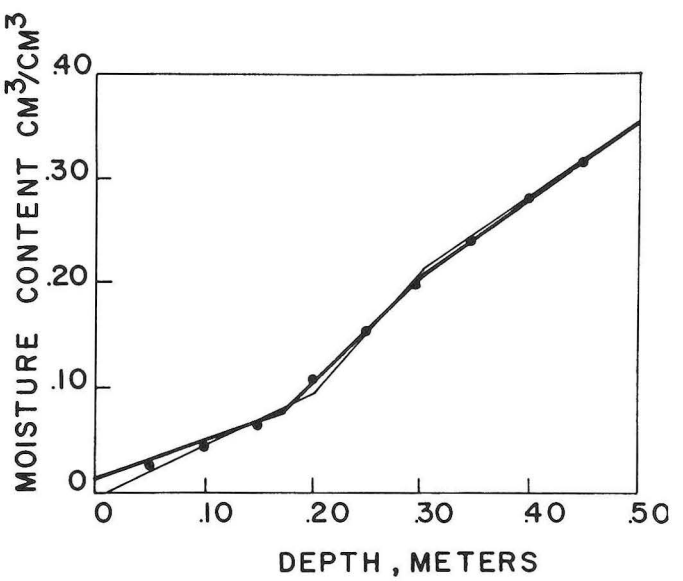


FIG. 50.—Computed moisture profile for the sand soil. The light line indicates the corresponding experimental results.

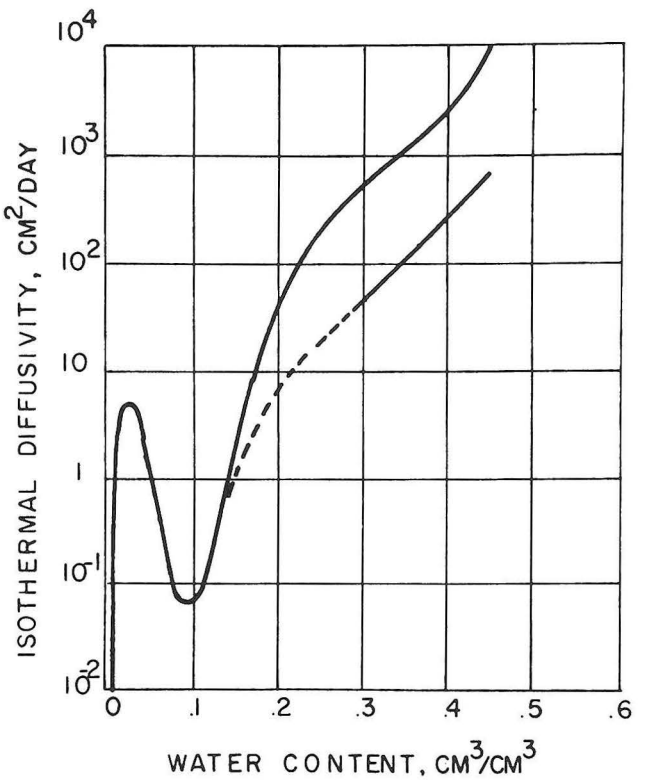


FIG. 51.—Isothermal diffusivity for silt loam soil (24). The lower lines indicate the revisions discussed in the text.

level of the water table would have on the sand moisture profile. Figure 52 shows the results of the computer soil moisture profile calculations for three different water table depths. These results indicated that adequate surface moisture could be maintained in sand if a shallower plot depth was adopted, and that this could serve as a basis for future system design improvements.

## Full Scale System

In 1982, the small scale plots were replaced with a full scale, 5.6 m x 27 m, soil heating system which nearly filled one bay of a two-bay greenhouse (Fig. 53). This system was part of a total energy conservation package for greenhouses which also included solar energy collection and nighttime insulation. A separate publication on solar ponds (22) is available on the solar energy portion of this package, and various research publications have been and are being prepared on the use of polystyrene pellets for intermittent insulation (19, 20).

The new soil heating layout was in moist sand (since it was designed to take advantage of the earlier determination that moist sand provided the best heat transfer) and was in a shallower configuration than used previously (Fig. 54). In this configuration, 0.02 m (3/4 in.) diameter heating pipes were buried 0.2 m (8 in.) deep and 0.2 m apart, and warm water was circulated at 1.0 liter per second (15.5 gpm) through the total pipe

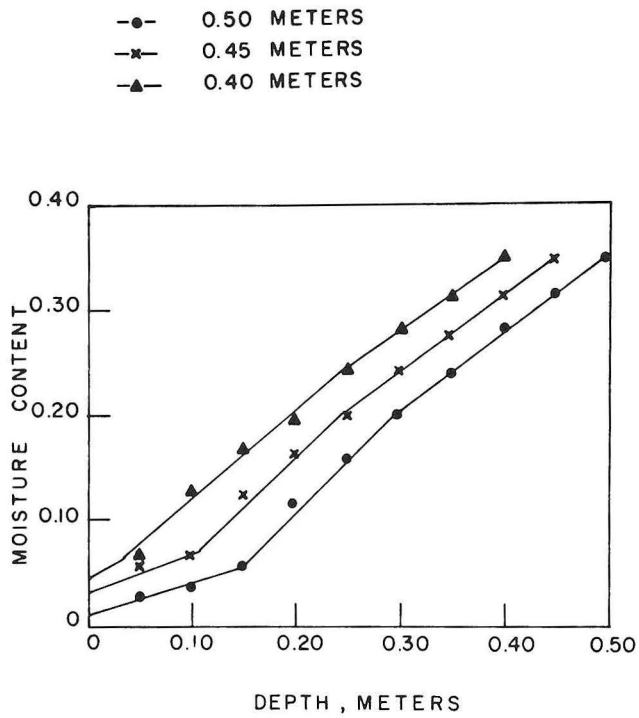


FIG. 52.—Calculated sand moisture profiles for water tables of different depths.

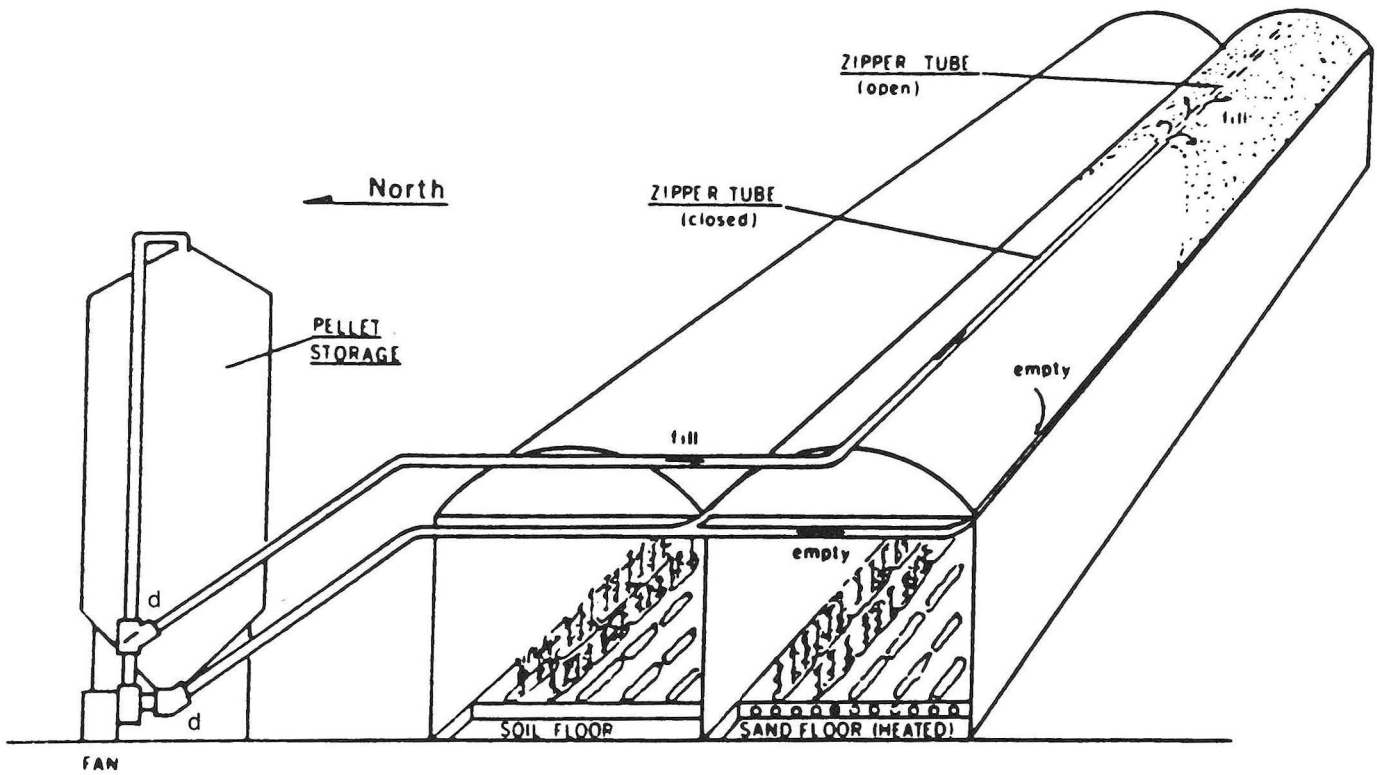


FIG. 53.—Diagram of the demonstration greenhouse showing the basic layout of the pellet handling system. The two diverters (d) allowed for either: 1) fan suction pulling pellets out of the bottom of the storage tank and blowing them into the top of the greenhouse, or 2) removal from the bottom sides of the roof and blowing them into the top of the storage tank.

network. The water table was held at the depth of the heating pipes. In addition, during the winter of 1982-83, tomato plants (variety CR-6 at commercial density of one plant every 4 square feet) were grown in peat-vermiculite bags laid on the sand surface.

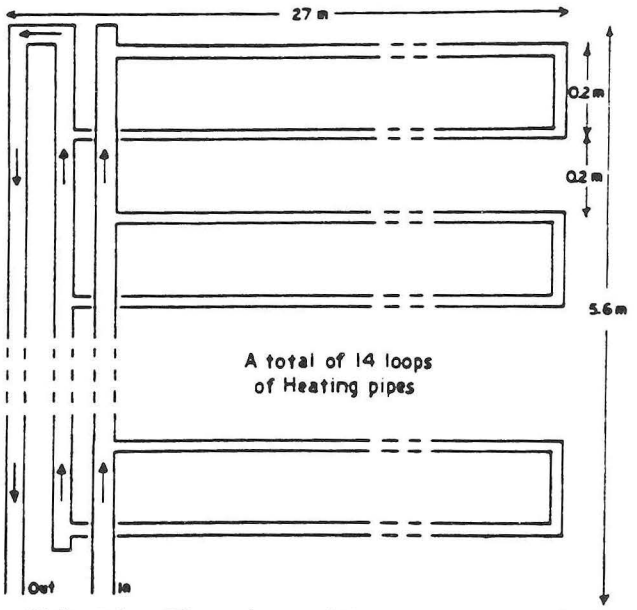


FIG. 54.—Plan view of the pipe layout in the 5.6 x 29 m greenhouse. The heating pipes were high density polyethlylene, 0.02 m in diameter and buried 0.2 m deep in moist sand.

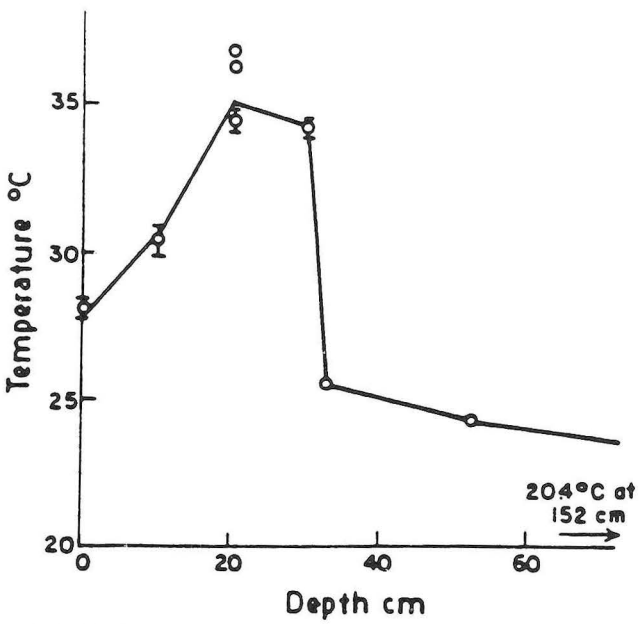


FIG. 55.—A typical temperature profile in the heated sand soil. The two highest points were the outer surface temperatures of an adjacent pair of supply and return pipes halfway along the length of the greenhouse. The strong temperature drop at the 30 cm depth was caused by a layer of insulation.

The soil heating system was insulated with a 2.5 cm (1 in.) thick layer of Thermax, polyisocyanurate insulation under the moisture retention liner in order to prevent excessive heat loss to the deep soil. A typical soil temperature profile (Fig. 55) thus shows a very strong temperature decrease at the depth of the insulation. Because of this, the heat lost to the deep soil was only about 10% of the heat supplied by the pipes, as opposed to the 30% to 40% observed in the uninsulated small plots. Since the soil heat represented about 40% of the total, uninsulated greenhouse heat load (see below), the soil insulation savings were about 10% of this latter, overall load. Therefore, the economic benefit of the soil insulation can be taken to be about 10% of the cost of heating a greenhouse, and typically this would be about one-third of the cost of the insulation and would imply a reasonable return on investment. However, if other conservation measures, particularly nighttime roof

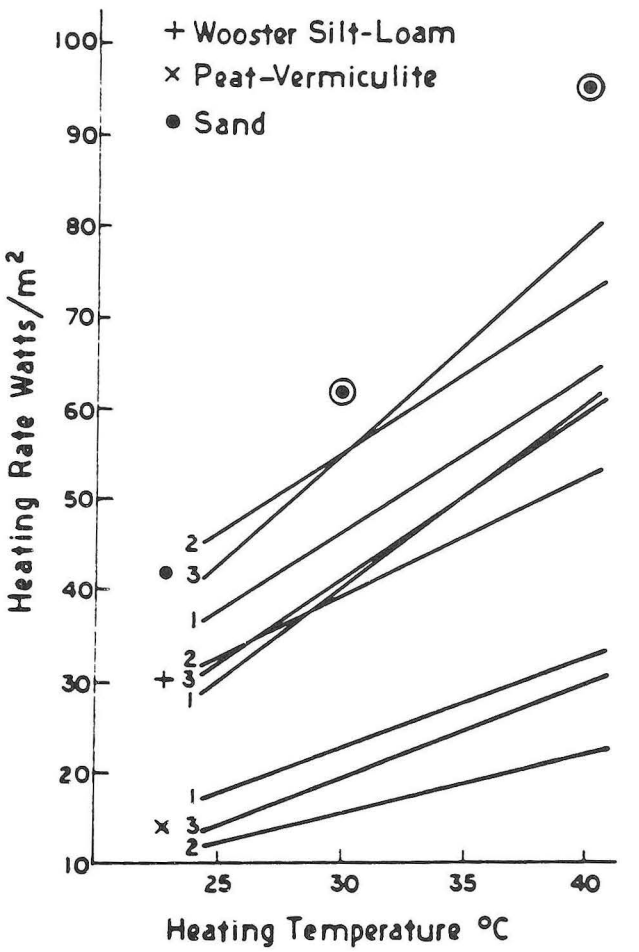


FIG. 56.—Heat transfer rate from the heating pipes to the soil per unit of greenhouse floor area. The straight lines are the earlier results presented in (16) (see Fig. 38), and the circled points are the values observed during the full-scale study.

insulation, were to be undertaken along with the introduction of a soil heat system, then there would be conditions under which the soil heating temperature (and hence soil temperature) would need to be reduced. This would affect the heat loss figures, and because of this the economics of soil insulation have not yet been completely determined.

Figure 56 shows the heat transfer rates from the soil heat pipes obtained in the new, full-scale configuration in comparison to the previous values. The new values are higher than the old ones, both because the pipes were closer to the surface and because the sand was wetter in the new configuration. Relative to the previously noted maximum, uninsulated greenhouse heating requirement (215 $W/m^2$), the new figures indicate that up to 41% of the instantaneous heat load can be met with soil heating, which on a seasonal average basis would translate to about 65% replacement of the direct air heating requirement. This represents a very considerable contribution to the heat needs of a greenhouse.

In addition, the use of nighttime insulation, while it is not the subject of this bulletin, was shown to significantly improve the effect soil heating can have on overall greenhouse operation. In particular, studies with 10 to 15 cm of polystyrene insulation showed that the heating requirement was reduced by 90%. Thus, the use of nighttime insulation between the two plastic sheets which form the roof of a greenhouse changed the energy requirement so significantly that soil heating was shown to be capable of meeting all of the greenhouse needs.

Only very basic horticultural data on tomato production was gathered during these studies. From this it was determined that the total fruit yield from early October (transplant) to the end of April was equivalent (on a year-long basis) to 90 tons/acre/year (200 tonnes/hectare/year). This observed production was considered to be good for this darkest portion of the year.

Humidity levels in the floor-heated, pellet-insulated bay of the greenhouse at day and night were typically 5-10% higher than those in the control bay (Table 4). The daytime increases were probably due to increased transpiration from warmer, more active roots, but may have also been influenced by increased evaporation from the open portions of the sand floor. Nighttime humidities were always 90-93% in the insulated bay, but the inside surface of the plastic glazing was always relatively dry so that no dripping from the roof was observed. Thus, this high humidity at night was not observed to be detrimental to plant growth or conducive to disease organism spread.

Both the soil surface and bag temperatures in the south bay were raised above the corresponding values in the north bay by 10-11° C when the highest temperature (40° C) heating water was used. Thus, in particular, the temperatures in the middle of the growth bags in January and early February were in the 16-17° C range in the north bay while they were as high as 27-28° C in the south bay. Smaller temperature increases were observed with cooler water in the heating pipes, but in all cases the increase was in the range which had previously been shown to be beneficial for vegetative growth of lettuce plants.

## BASIC DESIGN CONSIDERATIONS

For an uninsulated greenhouse, and under Ohio weather conditions except for the very mild periods in early fall and late spring, the heat requirement of a greenhouse is likely to exceed the amount of heat available from soil heating by quite a bit. Typically, at peak demand an Ohio, double-poly greenhouse may require 215 $W/m^2$ (1650 $Btu/ft^2/day$) and soil heating can only be expected to supply about one-third of this requirement. Thus, soil heating should be undertaken only as part of an overall greenhouse heating system.

The simplest and least expensive method of transferring heat to the soil is to circulate warm water through flexible plastic pipes buried in moist sand. Maintenance of adequate moisture in the sand around the pipes is particularly important for good heat transfer. In order to meet this requirement, it is advisable to design the system so that a water table can be maintained at, or just below, the level of the heat pipes and also to use warm water at a temperature of 40° C (104° F) or less.

If the heated soil is to be used directly as the growth medium, then the heating pipes must be buried sufficiently deep to prevent damage by tillage equipment. Otherwise, as with the use of growth bags placed on the soil surface, pipes spaced 20 cm (8 in.) apart and 10 to 20 cm (4 to 8 in.) deep should provide both adequate heat distribution throughout the soil and maximum heat transfer to the air of the greenhouse. A greater spacing, up to 40 cm (16 in.), will reduce system cost but will also reduce performance somewhat.

Operating experience has shown that 2 cm (3/4 in.) diameter, flexible, high-density polyethylene pipe (or similar plastic pipe suitable for operation at water main pressures and moderate temperatures) is appropriate for soil heating applications. Individual pipe runs, from supply header to return header (Fig. 57), should be no more than 120 m (400 ft) long, and the flow rate of water in each run should be approximately 0.1 L/s (1.5 gpm) or greater. Water temperature can be controlled as shown in Figure 58.

The circulation pump should be designed for continuous operation with warm water and sized to provide the total circulation needed (number of runs times flow per run) against a pressure head of 10 to 15 psi. The

**TABLE 4.—Relative Humidity of Air in a Polystyrene-Pellet Insulated Greenhouse with a Tomato Crop.**

| | Double Plastic Greenhouse | Pellet Insulated and Floor Heated Greenhouse |
|---|---|---|
| Daytime | 72 - 93% | 81 - 94% |
| Nighttime | 75 - 88% | 90 - 93% |

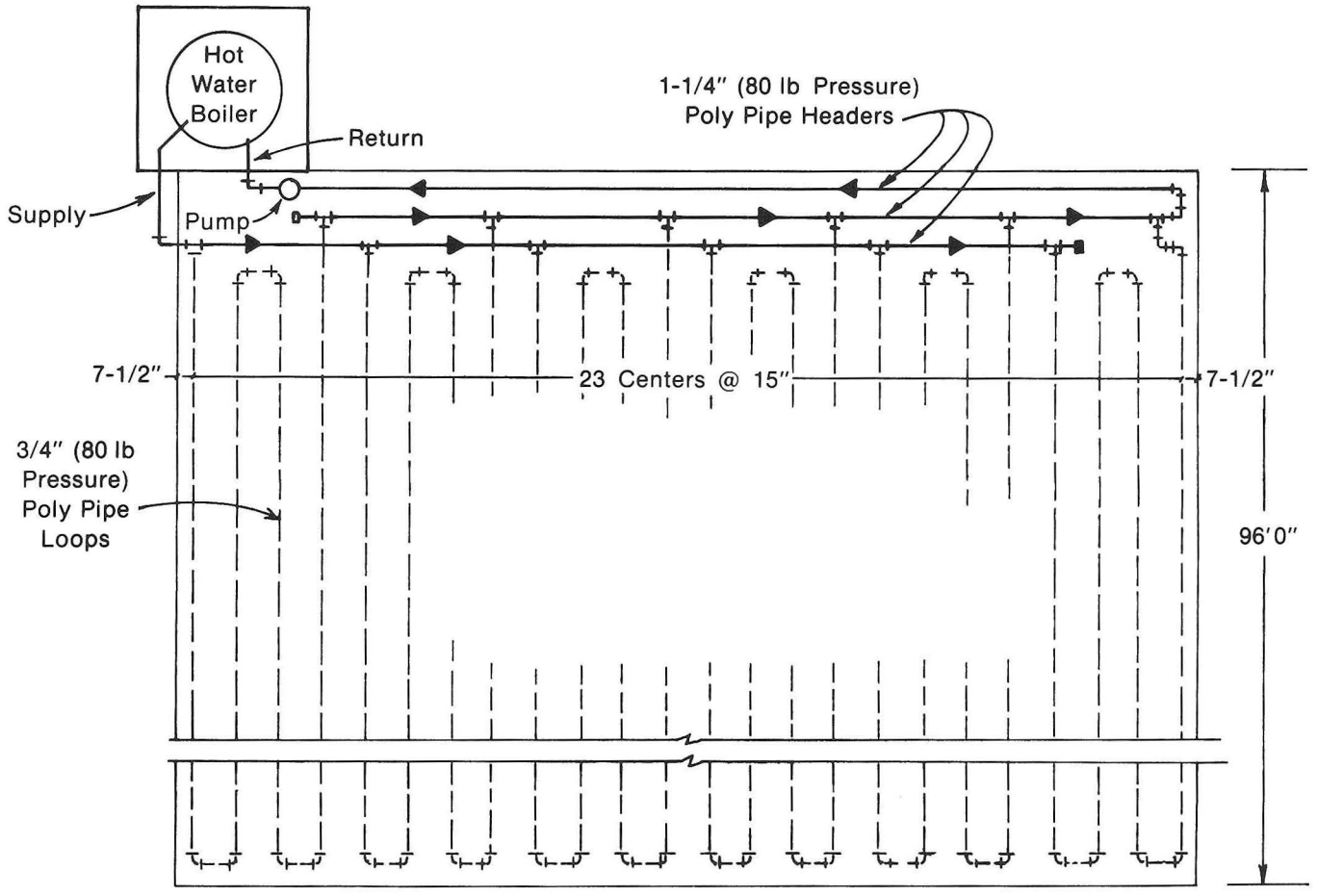


FIG. 57.—Plan diagram.

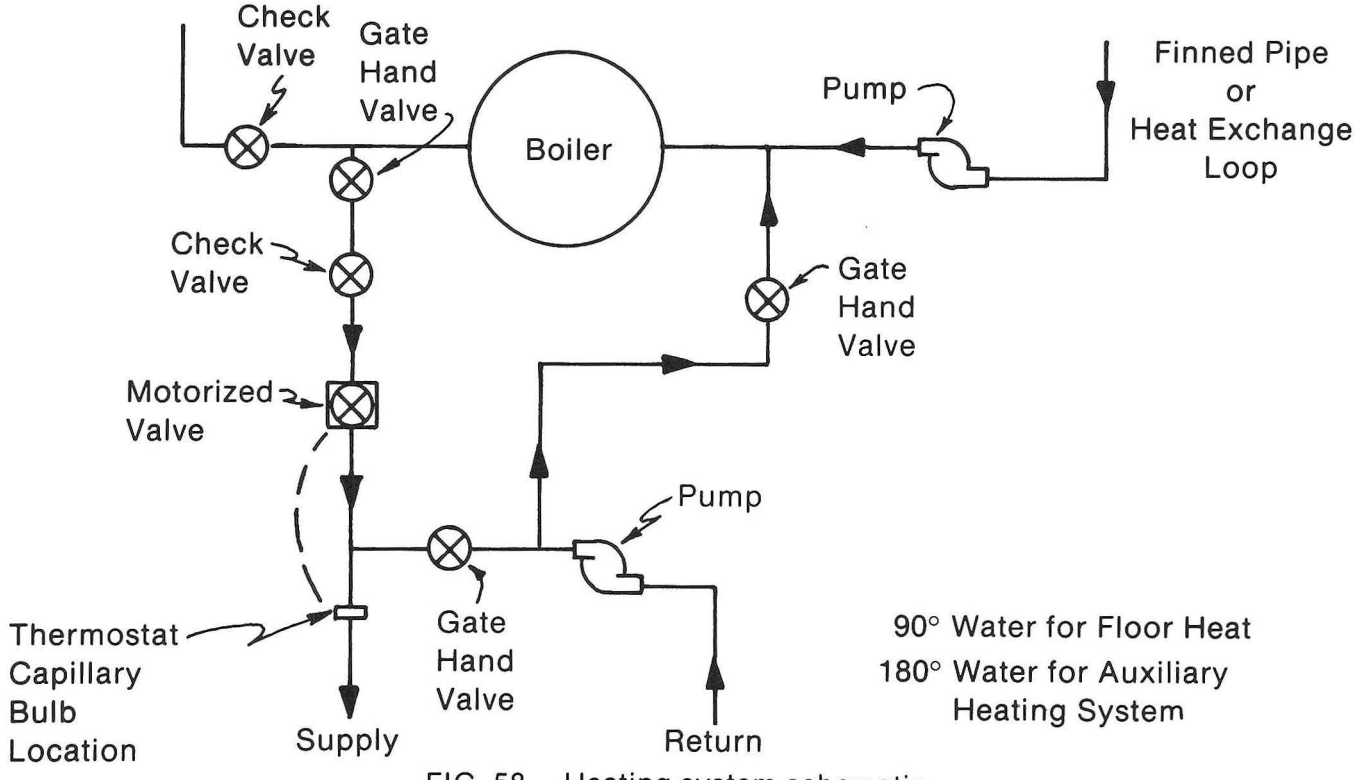


FIG. 58.—Heating system schematic.

heating system should provide hot water for mixing at temperatures above 50° C (120° F) and should have a capacity of around 130 W/m$^2$ (40 Btu/hr/ft$^2$) of greenhouse to be heated.

Finally, a warm moist floor can increase the humidity of the greenhouse air, and some form of moisture barrier at the soil surface is desirable. A simple, white (for light reflection), plastic mulch should serve this purpose without significantly affecting heat transfer.

## CONCLUSION

This bulletin has set forth the results of a decade of soil heating research at OSU/OARDC. The basic scientific information in this area is now reasonably well established and is being incorporated into technological designs. The benefits of soil heating are also presently being studied in terms of their effect within total greenhouse energy conservation schemes. Within this context, it is anticipated that soil heating will make an important contribution to the future of the greenhouse industry.

## REFERENCES


1. Ahmed, A. E. 1980. Simulation of simultaneous heat and moisture transfer in soils heated by buried pipes. Ph.D. dissertation, The Ohio State Univ. 120 pp.
2. Ahmed, A. E., M. Y. Hamdy, W. L. Roller, and D. L. Elwell. 1983. Technical feasibility of utilizing reject heat from power stations in greenhouses. Trans., ASAE, 26(1):200-206, 210.
3. Alnakshabandi, G. A. and H. Kohnke. Thermal conductivity and diffusivity of soils as related to moisture tension and other physical properties. Agri. Meteorol., 2:271-279.
4. Boersma, L., L. R. Davis, G. M. Reistad, J. D. Ringle, and W. E. Schmisseur. 1974. A systems analysis of the economic utilization of warm water discharge from power generating stations—final report. Oregon State Univ., Agri. Exp. Sta., Bull. 48.
5. Boyd, L. L., R. V. Stansfield, G. C. Ashley, J. S. Hietala, and T. R. D. Toukinson. 1977. Greenhouse heating with warm water from electric generating plants. A demonstration project. Proc., International Symposium on Controlled Environment Agriculture, Univ. of Arizona, Tucson, pp. 169-183.
6. Bruce, R. R. 1972. Hydraulic conductivity evaluation of the soil profile from soil water retention relations. Soil Sci. Soc. Amer. Proc., 36:555-561.
7. Brugger, M. F. 1983. Design guidelines for soil heating in greenhouses. Preliminary publication. Ohio Coop. Ext. Serv., The Ohio State Univ.
8. Cary, J. W. and S. A. Taylor. 1962. Thermally driven liquid and vapor phase transfer of water and energy in soil. Soil Sci. Soc. Amer. Proc., 26:417-420.
9. Cassel, D. K., D. R. Nielsen, and J. W. Biggar. 1969. Soil-water movement in response to imposed temperature gradients. Soil Sci. Soc. Amer. Proc., 33:493-500.
10. Dempsey, B. J. 1978. A mathematical model for predicting coupled heat and water movement in unsaturated soil. Int. J. for Numerical and Analytical Methods in Geomechanics, 2:19-34.
11. de Vries, D. A. 1958. Simultaneous transfer of heat and moisture in porous media. Trans. Amer. Geophys. Union, 39(5).
12. de Vries, D. A. 1963. Thermal properties of soils. *In:* W.R. van Wijk (ed), Physics of Plant Environment. John Wiley and Sons, New York.
13. de Vries, D. A. 1966. Thermal properties of soils. *In:* W.R. van Wijk (ed), Physics of Plant Environment, pp. 210-235. North Holland Publishing Co., Amsterdam, The Netherlands.
14. Donahue, R. L. 1958. Soils, An Introduction to Soils and Plant Growth, pp. 20-22. Prentice-Hall, Inc.
15. Elwell, D. L., W. L. Roller, and A. E. Ahmed. 1978. Waste heat for root-zone heating — a physical study of heat and moisture transfer. Proc., Second Conference on Waste Heat Management and Utilization, IV-B, pp. 28-38. Univ. of Miami.
16. Elwell, D. L., W. L. Roller, and A. E. Ahmed. 1982. Waste heat utilization for soil heating in greenhouses. Trans., ASAE, 25(3):773-778, 784.
17. Elwell, D. L., W. L. Roller, and T. H. Short. 1984. Heat and moisture transfer in heated greenhouse soils and floors. Proc., Third International Symposium on Energy in Protected Cultivation. Acta Horticulturae, 148, pp. 377-384.
18. Elwell, D. L., T. H. Short, and R. P. Fynn. 1984. A double-plastic greenhouse with a polystyrene-pellet energy screen and floor heating for winter tomato production. Proc., Third International Symposium on Energy in Protected Cultivation. Acta Horticulturae, 148, pp. 461-467.
19. Elwell, D. L., T. H. Short, and R. P. Fynn. 1983. Winter operation of a polystyrene-pellet-insulated and warm-floor-heated greenhouse. Presented at Chicago, December. Amer. Soc. Agri. Eng., St. Joseph, Mich., ASAE Paper No. 83-4524.
20. Elwell, D. L., T. H. Short, and W. L. Roller. 1983. A warm floor solar greenhouse insulated at night with polystyrene pellets. Proc., Third Annual Solar and Biomass Workshop, Atlanta, Ga., pp. 67-70.
21. Fritton, D. D., D. Kirkham, and R. H. Shaw. 1970. Division S-1—Soil Physics. Soil water evaporation, isothermal diffusion, and heat and water transfer. Soil Sci. Soc. Am. Proc., 34(2):183-188.
22. Fynn, R. P. and T. H. Short. 1983. The salt stabilized solar pond for space heating—a practical manual. Ohio Agri. Res. and Dev. Ctr., Spec. Circ. 106, 40 pp.
23. Gardner, W. R. and F. J. Miklich. 1962. Unsaturated conductivity and diffusivity measurements by a constant flux method. Soil Sci., 93:271-274.
24. Gee, G. W. 1966. Water movement in soils as influenced by temperature gradient. Ph.D. dissertation, Washington State Univ.

25. Gurr, C. G., T. J. Marshall, and T. T. Hutton. 1952. Movement of water in soil due to a temperature gradient. Soil Sci., 74:335-345.
26. Hamdy, M. Y. and H. J. Barre. 1969. Evaluation of film coefficient in single kernel drying. Trans., ASAE, 12(2):205-208.
27. Jakob, M. 1957. Heat Transfer, Vol. II. John Wiley and Sons, New York.
28. Johnson, S. E. 1976. Soil temperature and moisture content measurements for a system of subsurface heating pipes. M.S. thesis, The Ohio State Univ. 153 pp.
29. Jury, W. A. 1973. Simultaneous transport of heat and moisture through a medium sand. Ph.D. dissertation, Univ. of Wisconsin.
30. Jury, W. A. and E. E. Miller. 1974. Measurement of the transport coefficients for coupled flow of heat and moisture in medium sand. Soil Sci. Soc. Amer. Proc., 38:551-557.
31. Kendrick, J. H. and J. A. Havens. 1973. Heat transfer models for a sub-surface, water pipe, soil-warming system. J. Env. Qual., 2(2):188-196.
32. Kersten, M. S. 1949. Thermal properties of soils. Univ. of Minnesota, Inst. of Technol., Eng. Exp. Sta., Bull. 28.
33. Kohnke, H. 1968. Soil Physics. McGraw-Hill Pub. Co., New York.
34. Luikov, A. V. 1975. Systems of differential equations of heat and mass transfer in capillary-porous bodies. Int. J. Heat Mass Trans., 18:1-14.
35. Mears, D. R., W. J. Roberts, and J.C. Simpkins. 1974. New concepts in greenhouse heating. Amer. Soc. Agri. Eng., St. Joseph, Mich., ASAE Paper No. 74-112.
36. Mears, D. R., W. J. Roberts, and G. A. Taylor. 1975. Controlling moisture levels in trough culture tomato and cucumber production. Trans., ASAE, 18(1):145-148, 151.
37. Nakshabandi, G. A. and H. Kohnke. 1965. Thermal conductivity and diffusivity of soils as related to moisture tension and other physical properties. Agri. Meteorol., 2:271-279.
38. Parker, J. J. 1976. Simulation of a buried warm water pipe system underneath a greenhouse. M.S. thesis, The Ohio State Univ. 66 pp.
39. Parker, J. J., M. Y. Hamdy, R. B. Curry, and W. L. Roller. 1981. Simulation of buried warm water pipes beneath a greenhouse. Trans., ASAE, 24(4):1022-1025, 1029.
40. Philip, J. R. 1955. The concept of diffusion applied to soil water. Proc. Nat. Acad. Sci., India, 24 A, pp. 93-104.
41. Philip, J. R. and D. A. de Vries. 1957. Moisture movement in porous materials under temperature gradients. Trans., Amer. Geophys. Union, 38:222-232.
42. Roller, W. L. and D. L. Elwell. 1981. Greenhouse soil heating for improved production and energy conservation. EPRI EA-2022, Research Project 1110-1. Final Report for Electric Power Research Inst., Palo Alto, Calif.
43. Roller, W. L. and D. L. Elwell. 1980. Waste heat for soil heating in greenhouses. Presented at San Antonio, Texas, June. Amer. Soc. Agri. Eng., St. Joseph, Mich., ASAE Paper No. 80-4032.
44. Rollins, R. L., M. G. Spangler, and D. Kirkham. 1954. Movement of soil moisture under a thermal gradient. National Research Council, Highway Res. Board Proc., 33:492-508.
45. Rykbost, K. A. and L. Boersma. 1974. Crop response to warming soils above their natural temperature. Oregon State Univ., Agri. Exp. Sta.
46. Sepaskhah, A. R., L. Boersma, L. R. Davis, and D. L. Siegel. 1973. Experimental analysis of a subsurface soil warming and irrigation system utilizing waste heat. Presented at ASME Winter Annual Meeting, Detroit, Mich. ASME Paper No. 73-WA/HT-11.
47. Shapiro, H. N. 1975. Simultaneous heat and mass transfer in porous media with application to soil warming with power plant waste heat. Ph.D. dissertation, The Ohio State Univ. 167 pp.
48. Shapiro, H. N. and W. L. Roller. 1975. Feasibility of soil warming with power plant waste heat. Presented at Chicago, December. Amer. Soc. Agri. Eng., St. Joseph, Mich., ASAE Paper No. 75-3542
49. Skaggs, R. W., C. R. Willey, and D. C. Sanders. 1973. Use of waste heat for soil warming in North Carolina. Presented at Chicago, December. Amer. Soc. Agri. Eng., St. Joseph, Mich., ASAE Paper No. 73-3530.
50. Soribe, F. I. 1972. Dynamic simulation of environment and plant growth in an air-supported plastic greenhouse. Ph.D. dissertation, The Ohio State Univ.
51. Soribe, F. I. and R. B. Curry. 1973. Simulation of lettuce growth in an air-supported plastic greenhouse. J. Agri. Eng. Res., 18:133-140.
52. Taylor, S. A. and G. L. Ashcroft. 1972. Physical Edaphology, The Physics of Irrigated and Non-Irrigated Soils. W.H. Freeman and Co., San Francisco.
53. Walker, J. M. 1970. Effects of alternative vs. constant soil temperatures on maize seedling growth. Soil Sci. Soc. Amer. Proc., 34:889-892.
54. Westcott, C. W. and P. J. Wierenga. 1974. Transfer of heat by conduction and vapor movement in a closed soil system. Soil Sci. Soc. Amer. Proc., 38:9-14.

# APPENDIX A
# COMPUTER PROGRAM LISTING

```
      DIMENSION X(68),F(68),AJINV(68,68),W(10000)
      EXTERNAL K1,K2,D1,D2,CALFUN
      COMMON/COM/  TI,TW1,TW2,THW1,THW2,TS,THS,TL,THL,
     CL,M,NP1,NP2,NM,NP1NM,NP2NM,NM2,  N1,ISTART,IEND
C
C     BOUNDARY CONDITIONS
C
      TI = 32.5
      TW1=32.5
      TW2=32.5
      TS=17.5
      TL=0.82*(TI-TS)+TS
      THW1=0.04
      THW2=0.04
      THS=0.15
      THL=0.25
      L=7
      M=9
      NP1=30
      NP2=NP1+L-3
      NM=L*M
      NNMM=NM+1
      NP1NM=NP1+NM
      NP2NM=NP2+NM
      NM2=2*NM
      N=((L-2)*(M-2)-2)*2
      N1=N/2
      N=N+2
      ISTART=L+2
      IEND=NM-L-1
C
C     INITIAL GUESS OF TEMPERATURES AND MOISTURES
C
      J=0
      DO 6001 I=ISTART,IEND
      R=FLOAT(I)/FLOAT(L)
      IF(R.EQ.(FLOAT(IFIX(R)))) GO TO 6001
 6011 NCHECK = (IFIX(R))*L+1
      IF(NCHECK.EQ.I) GO TO 6001
 6021 IF(I.EQ.NP1.OR.I.EQ.NP2) GO TO 6001

 6031 J=J+1
      JN1=J+N1
      READ(5,6041)X(J),X(JN1)
 6041 FORMAT(F10.8,F10.6)
      WRITE(6,6141)I,J,JN1,X(J),X(JN1)
 6141 FORMAT(3I5,2E16.8)
 6001 CONTINUE
      X(N-1)=THW1
      X(N)=THW2
C     SET PARAMETERS AND CALL NONLIN
C
      DSTEP=0.0001
      ACC=0.00000001
      MAXFUN=400
      DMAX=10.
      IPRINT=0
      CALL NONLIN(N,X,F,AJINV,DSTEP,DMAX,ACC,MAXFUN,IPRINT,W)
      IPRINT=1

      CALL NONLIN(N,X,F,AJINV,DSTEP,DMAX,ACC,MAXFUN,IPRINT,W)
      STOP
      END

      SUBROUTINE CALFUN(N,X,F)
      REAL K1,K2,K1TJ,K2TJ
      DIMENSION X(N),F(N),T(1000)
      EXTERNAL K1,K2,D1,D2
      COMMON/COM/  TI,TW1,TW2,THW1,THW2,TS,THS,TL,THL,
     CL,M,NP1,NP2,NM,NP1NM,NP2NM,NM2,  N1,ISTART,IEND
      WRITE(6,757)
```

```
  757 FORMAT(2X,'CALFUN')
       DO 6000 I=1,L
      T(I)=TS
      T(I+NM)=THS
      T(I+NM-L)=TL
 6000 T(I+NM2-L)=THL
      T(NP1)=TW1
      T(NP2)=TW2
      T(NP1NM)=X(N-1)
      T(NP2NM)=X(N)
      J=0
      DO 1000 I=ISTART,IEND
      R=FLOAT(I)/FLOAT(L)
      IF(R.EQ.(FLOAT(IFIX(R)))) GO TO 1000
 1010 NCHECK = (IFIX(R))*L+1

      IF(NCHECK.EQ.I) GO TO 1000
 1020 IF(I.EQ.NP1.OR.I.EQ.NP2) GO TO 1000
 1030 J=J+1
      T(I)=X(J)*(TI-TS)+TS
      T(I+NM)=X(J+N1)
 1000 CONTINUE
      NML1=NM-L+1
      DO 1110 I=1,NML1,L
      T(I)=T(I+2)
      T(I+NM)=T(I+NM+2)
      T(I+L-1)=T(I+L-3)
 1110 T(I+NM+L-1)=T(I+NM+L-3)
      I=0
      DO 1001 J=ISTART,IEND
      R=FLOAT(J)/FLOAT(L)
      IF(R.EQ.(FLOAT(IFIX(R)))) GO TO 1001
 1011 NCHECK=(IFIX(R))*L+1
      IF(NCHECK.EQ.J) GO TO 1001
 1021 IF(J.EQ.NP1.OR.J.EQ.NP2) GO TO 1001
 1031 I=I+1
      K1TJ=K1(T(J),T(J+NM))
      K2TJ=K2(T(J),T(J+NM))
      D1TJ=D1(T(J+NM))
      D2TJ=D2(T(J+NM))
      JPNM=J+NM
      JM1=J-1
      JP1=J+1
      JML=J-L
      JPL=J+L
      JM1PNM=J-1+NM
      JMLPNM=J-L+NM
      JP1PNM=J+1+NM
      JPLPNM=J+L+NM
      FT1  = ((K1TJ+K1(T(JM1),T(JM1PNM)))/2.)*T(JM1)
     C-(2.*K1TJ+(K1(T(JM1),T(JM1PNM))+K1(T(JP1),T(JP1PNM))
     C + K1(T(JML),T(JMLPNM))+K1(T(JPL),T(JPLPNM)))/2.)*T(J    )
     C+((K1(T(JP1),T(JP1PNM))+K1TJ)/2.)*T(JP1    )
     C+((K1(T(JML),T(JMLPNM))+K1TJ)/2.)*T(JML    )
     C+((K1(T(JPL),T(JPLPNM))+K1TJ)/2.)*T(JPL    )
      FTH1= ((K2TJ+K2(T(JM1),T(JM1PNM)))/2.)*T(JM1PNM)
     C-(2.*K2TJ+(K2(T(JM1),T(JM1PNM))+K2(T(JP1),T(JP1PNM))
     C + K2(T(JML),T(JMLPNM))+K2(T(JPL),T(JPLPNM)))/2.)*T(JPNM)
     C+((K2(T(JP1),T(JP1PNM))+K2TJ)/2.)*T(JP1PNM)
     C+((K2(T(JML),T(JMLPNM))+K2TJ)/2.)*T(JMLPNM)
     C+((K2(T(JPL),T(JPLPNM))+K2TJ)/2.)*T(JPLPNM)
      F(I)=FT1+FTH1
      FT2 = ((D1TJ+D1(T(JM1PNM)))/2.)*T(JM1    )
     C-(2.*D1TJ+(D1(T(JM1PNM))+D1(T(JP1PNM))+D1(T(JMLPNM))+D1(T(
     CJPLPNM)))/2.)*T(J    )
     C+((D1(T(JP1PNM))+D1TJ)/2.)*T(JP1    )
     C+((D1(T(JMLPNM))+D1TJ)/2.)*T(JML    )
     C+((D1(T(JPLPNM))+D1TJ)/2.)*T(JPL    )
      FTH2= ((D2TJ+D2(T(JM1PNM)))/2.)*T(JM1PNM)
     C-(2.*D2TJ+(D2(T(JM1PNM))+D2(T(JP1PNM))+D2(T(JMLPNM))+D2(T(
     CJPLPNM)))/2.)*T(JPNM)
     C+((D2(T(JP1PNM))+D2TJ)/2.)*T(JP1PNM)
     C+((D2(T(JMLPNM))+D2TJ)/2.)*T(JMLPNM)
     C+((D2(T(JPLPNM))+D2TJ)/2.)*T(JPLPNM)
      F(I+N1)=FT2+FTH2
```

```
1001 CONTINUE
     DO  1041 JJ=1,2
     IF(JJ.NE.1)GO TO 1043
1042 J=NP1
     I=N-1
     GO TO 1044
1043 J=NP2
     I=N
1044 K1TJ=K1(T(J),T(J+NM))
     K2TJ=K2(T(J),T(J+NM))
     D1TJ=D1(T(J+NM))
     D2TJ=D2(T(J+NM))
     JPNM=J+NM
     JM1=J-1
     JP1=J+1
     JML=J-L
     JPL=J+L
     JM1PNM=J-1+NM
     JMLPNM=J-L+NM
     JP1PNM=J+1+NM
     JPLPNM=J+L+NM
     FT2  = ((D1TJ+D1(T(JM1PNM)))/2.)*T(JM1    )
    C-(2.*D1TJ+(D1(T(JM1PNM))+D1(T(JP1PNM))+D1(T(JMLPNM))+D1(T(
    CJPLPNM)))/2.)*T(J     )
    C+((D1(T(JP1PNM))+D1TJ)/2.)*T(JP1    )
    C+((D1(T(JMLPNM))+D1TJ)/2.)*T(JML    )
    C+((D1(T(JPLPNM))+D1TJ)/2.)*T(JPL    )
     FTH2= ((D2TJ+D2(T(JM1PNM)))/2.)*T(JM1PNM)
    C-(2.*D2TJ+(D2(T(JM1PNM))+D2(T(JP1PNM))+D2(T(JMLPNM))+D2(T(
    CJPLPNM)))/2.)*T(JPNM)
    C+((D2(T(JP1PNM))+D2TJ)/2.)*T(JP1PNM)
    C+((D2(T(JMLPNM))+D2TJ)/2.)*T(JMLPNM)
    C+((D2(T(JPLPNM))+D2TJ)/2.)*T(JPLPNM)

     F(I)=FT2+FTH2
1041 CONTINUE

     RETURN
     END


     REAL FUNCTION K1(TEMP,THETA )
     DTV = 10.**((-0.1/0.25)*(THETA-0.05)-1.95)
     DTL = 10.**((1.75/0.05)*(THETA-0.25)+0.5)
     IF(THETA.LT.0.15)
    CCOND = (0.2/0.15)*THETA+0.5
 501 IF(THETA.GE.0.15.AND.THETA.LT.0.25)
    CCOND = 7.*(THETA-0.15)+0.7
 502 IF(THETA.GE.0.25.AND.THETA.LT.0.28)
    CCOND = (0.4/0.03)*(THETA-0.25)+1.4
 503 IF(THETA.GE.0.28)
    CCOND = (0.2/0.09)*(THETA-0.28)+1.8
 504 K1 = (COND/1000.) + (DTV*(597.+0.433*TEMP)+
    CDTL*TEMP)/(3600.*24.)
     RETURN
     END



     REAL FUNCTION K2(TEMP,THETA)
     IF(THETA.LT.0.06)
    CDTHV = 10.**((-0.7/0.035)*(THETA-0.06)+0.25)
 790 IF(THETA.GE.0.06)
    CDTHV = 10.**((-2.25/0.06)*(THETA-0.06)+0.25)
 792 DTHL = 10.**((3.9/0.21)*(THETA-0.26)+1.9)
     K2 = (DTHV*(597.+0.433*TEMP)+DTHL*TEMP)/(3600.*24.)
     RETURN
     END
```

```
      FUNCTION D1(THETA)
      DTV = 10.**((-0.1/0.25)*(THETA-0.05)-1.95)
      DTL = 10.**((1.75/0.05)*(THETA-0.25)+0.5)
      D1 = (DTV+DTL)/(3600.*24.)
      RETURN
      END


      FUNCTION D2(THETA)
  793 DTHL = 10.**((3.9/0.21)*(THETA-0.26)+1.9)
      IF(THETA.LT.0.06)
     CDTHV = 10.**((-0.7/0.035)*(THETA-0.06)+0.25)
  791 IF(THETA.GE.0.06)
     CDTHV = 10.**((-2.25/0.06)*(THETA-0.06)+0.25)
  799 CONTINUE
      D2 = (DTHV+DTHL)/(3600.*24.)
      RETURN
      END
```

# APPENDIX B

# WASTE HEAT UTILIZATION IN WARMING UP SOILS IN GREENHOUSE

```
***  DEVELPOED BY AHMED E. AHMED AS A PART OF DISSERTATION  ***
*
*      THIS PROGRAM IS TO SOLVE THE COUPLED HEAT & MOISTURE TRANSFER IN
*     SOIL WITH SUBSURFACE HEATING.
*     THE DEVELOPED MODEL USES THE PHILLIP & DEVRIES'S APPROACH IN THE
*     APPLICATION OF SOIL SUBSURFACE HEATING BY BURIED PIPE NET WORK
*
*      THE TEMPERATURE AT THE 10 CM DEEP IS USED AS IS TO REPRESENT THE
*      UPPER BOUNDARY CONDITION.
*
*      COMPUTER VARIABLES - NOMENCLATURE.
*
*   SBP : SPACING BETWEEN PIPES, CM.
*   DD : DOMAIN DEPTH , CM.
*   PD : PIPE DEPTH (MEASURED FROM THE WATER TABLE).
*   NHP: NUMBER OF HORIZONTAL POINTS.
*   NVP: NUMBER OF VERTICAL POINTS.
*   NP : POSITION OF THE HEATING PIPE COUNTING FROM DOWN UP.
*   DX : DISTANCE BETWEEN NODES,HORIZONTAL = VERTICAL IN CM.
*   TS : SURFACE OR TOP DOMAIN TEMPERATURE, DEG C.
*   TB : BOTTOM TEMPERATURE,DEG C.
*   WS : SURFACE OR TOP DOMAIN MOISTURE CONTENT,(VOLUMETRIC).
*   WB : BOTTOM MOISTURE CONTENT (VOLUMETRIC).
*   LH : HEAT OF VAPORIZATION.
*   TI : INITIAL SOIL TEMPERATURE, DEG C.
*   WI : INITIAL SOIL WATER CONTENT,(VOLUMETRIC).
*   PT : PIPE TEMPERATURE, DEG C.
*   TF : INTEGRATOR OUTPUT FOR TEMPERATURE.
*   WF : INTEGRATOR OUTPUT FOR WATER CONTENT
*   WPO : MOISTURE PROFILE ABOVE AND BELOW PIPES.
*   WPB : MOISTURE PROFILE MIDWAY BETWEEN PIPES.
*   T10 : TIME DEPENDENT TEMPERATURE AT 10 CM DEEP,(TEMP10).
*   TMD30 : MEASURED TEMPERATURE AT 30 CM DEEP MIDWAY BETWEEN PIPES.
*   T(I,J) : NODE TEMPERATURE , DEG C
*   W(I,J) : NODE WATER CONTENT , VOLUMETRIC
*   TDOT(I,J) : NODE RATE OF CHANGE OF TEMPERATURE
*   WDOT(I,J) : NODE RATE OF CHANGE OF WATER CONTENT
*
*    THE PROGRAM SOLVES FOR (NHP X NVP) MOISTURE UNKNOWNS , AND LESS BY
*    ONE TEMPERATURE UNKNOWNS.( PIPE TEMPERATURE IS ALWAYS KNOWN ).
*
**************************************************************************
*                                                                        *
*    THIS RUN IS FOR THE SAND TEST PLOT AT THE 40 DEG C HEATING LEVEL    *
*                                                                        *
**************************************************************************

/      DIMENSION T(4,7) , TDOT(4,7)
/      DIMENSION W(4,7) , WDOT(4,7)
/      DIMENSION DL(4,7) , DV(4,7) , DT(4,7)
/      DIMENSION THK(4,7) , HK(4,7) , C(4,7)
/      DIMENSION WPO(7) , WPB(7)
*
*      GENERATION OF FUNCTIONS
*   ALL THE FOLLOWING FUNCTIONS ARE MOISTURE-DEPENDENT.
*
*   HDK GENERATES THE HYDRAULIC CONDUCTIVITY (HK, CM/HR.)
*
 FUNCTION HDK=0.0,.000001,.05,.00001,.1,.0217,.125,.1000,.15,.170,    ...
       .2,.200,.25,.24,.3,.6,.35,2.01
*
*   VAPDIF GENERATES THE ISOTHERMAL VAPOR DIFFUSIVITY (DV,SQ CM/DAY)
*
 FUNCTION VAPDIF=0.0,0.0,.01,3.142,.02,9.148,.03,1.663,.04,1.61,       ...
       .05,1.559,.06,1.507,.07,1.455,.08,1.403,.09,1.3514,.1,1.299,    ...
       .2,.779,.25,.519,.3,.2599,.35,0.0
*   ISTHMD GENERATES THE ISO-THERMAL MOISTURE DIFFUSIVITY (DL,SQ CM/DAY)
*
 FUNCTION ISTHMD=0.0,0.0,0.01,3.142,.02,9.148,.03,1.663,.04,1.61,      ...
       .05,7.0,.056,16.0,.111,110.0,.15,418.0,.16,530.0,.17,640.0,     ...
       .18,730.0,.19,700.0,.2,580.0,.219,530.0,.2375,610.0,.25,730.0,  ...
       .3,2350.0,.3375,6300.0,.35,7200.0
*
*   THMD GENERATES THE THERMAL MOISTURE DIFFUSIVITY (DT,SQ CM/DAY DEG C)
*
 FUNCTION THMD=0.0,.01,.02,.01,.03,.024,.05,.0245,.075,.05,.1,.32,    ...
       .15,1.65,.2,3.25,.25,7.6,.3,15.0,.325,28.5,.35,28.5
*
*   THKD GENERATES THE THERMAL CONDUCTIVITY (THK,MCAL/SEC CM DEG C)
*
 FUNCTION THKD=0.0,1.15,.0125,3.9,.025,4.5,.05,4.9,.1,5.5,.15,6.1,    ...
       .2.6.6,.25,7.0,.3,7.25,.35,7.7
```

```
 FUNCTION PIPTEM=0.0,36.3,2.,36.2,4.,36.0,6.,35.9,8.,35.8,10.,35.6,   ...
       12.,35.7,14.,35.8,16.,35.9,18.,36.1,20.,36.1,22.,35.9,24.,35.9,...
       26.,35.9,28.,35.7,30.,35.7,32.,35.7,34.,35.6,36.,35.5,38.,35.7,...
       40.,36.0,42.,36.2,44.,36.3,46.,36.3,48.,36.2,50.,36.1,52.,36.0,...
       54.,35.9,56.,35.7,58.,35.7,60.,35.7,62.,35.8,64.,36.1,66.,36.1,...
       68.,36.3,70.,36.2,72.,36.1,74.,35.9,76.,35.9,78.,35.8,80.,35.8,...
       82.,35.7,84.,35.8,86.,35.9,88.,36.2,90.,36.4,92.,36.6,94.,36.6,...
       96.,36.4
*
 FUNCTION TEMP10=0.0,30.9,2.,30.3,4.,29.8,6.,29.5,8.,29.4,10.,30.6,   ...
       12.,31.7,14.,31.9,16.,31.9,18.,31.3,20.,30.7,22.,30.3,24.,30.1,...
       26.,29.8,28.,29.7,30.,29.6,32.,29.4,34.,30.5,36.,32.0,38.,33.7,...
       40.,34.2,42.,34.1,44.,32.8,46.,31.6,48.,30.8,50.,30.3,52.,30.0,...
       54.,29.7,56.,29.6,58.,30.8,60.,31.7,62.,32.7,64.,32.6,66.,32.3,...
       68.,31.4,70.,30.8,72.,30.3,74.,30.0,76.,29.7,78.,29.4,80.,29.4,...
       82.,30.6,84.,32.1,86.,33.7,88.,34.5,90.,34.3,92.,33.0,94.,31.8,...
       96.,31.0
*
 FUNCTION TMD30=0.0,34.6,2.,34.4,4.,34.1,6.,33.9,8.,33.8,10.,33.7,    ...
       12.,33.7,14.,33.9,16.,34.1,18.,34.1,20.,34.1,22.,34.0,24.,33.9,...
       26.,33.8,28.,33.7,30.,33.6,32.,33.6,34.,33.6,36.,33.6,38.,33.9,...
       40.,34.2,42.,34.4,44.,34.6,46.,34.6,48.,34.5,50.,34.3,52.,34.1,...
       54.,33.9,56.,33.7,58.,33.7,60.,33.8,62.,34.0,64.,34.2,66.,34.2,...
       68.,34.2,70.,34.2,72.,34.1,74.,33.9,76.,33.8,78.,33.8,80.,33.7,...
       82.,33.6,84.,33.7,86.,34.0,88.,34.3,90.,34.6,92.,34.7,94.,34.7,...
       96.,34.6
*
*
      FIXED I,J,K,L,M,N,NP,NHP,NVP,NP1,NP2,NVP1,LM,MM,NN,KK
*
PARAM SBP=30. , DD=40. , PD=20. , DX=5.
PARAM TB=33.25 , W10=0.045 , WB=0.35
PARAM LH=597.0 , C1=0.32
*
INITIAL
*
*    TABLE IS A ONE DIMENSIONAL ARRAY TO BE USED AS INITIAL CONDITION
*    IN THE INTEGRATION PROCESS.
*
*      1). MOISTURE INITIAL CONDITION
*
TABLE WI(1-2)=2*.2892,WI(3-4)=2*.3325,WI(5-6)=2*.2571,WI(7-8)=2*.3160
TABLE WI(9-10)=2*.2350,WI(11-12)=2*.2337,WI(13-14)=2*.2129
TABLE WI(15-16)=2*.1527,WI(17-18)=2*.1227,WI(19-20)=2*.0950
TABLE WI(21-22)=2*.0781,WI(23-24)=2*.0712,WI(25-26)=2*.0557
TABLE WI(27-28)=2*.0505
*
*     2). TEMPERATURE INITIAL CONDITION
*
TABLE TI(1)=32.88,TI(2)=32.85,TI(3)=32.82,TI(4)=32.80,TI(5)=33.32
TABLE TI(6)=33.23,TI(7)=33.11,TI(8)=33.07,TI(9)=33.97,TI(10)=33.61
TABLE TI(11)=33.34,TI(12)=33.25,TI(13)=35.37,TI(14)=33.39
TABLE TI(15)=33.25,TI(16)=33.70,TI(17)=33.33,TI(18)=33.05, TI(19)=32.95
TABLE TI(20)=32.73,TI(21)=32.62,TI(22)=32.50,TI(23)=32.45,TI(24)=31.91
TABLE TI(25)=31.88,TI(26)=31.84,TI(27)=31.82
*
*    EVALUATION OF SURFACE PARAMETER
*
       WS=W10
       HKS = AFGEN(HDK,WS)
       THKS=3.6*AFGEN(THKD,WS)
       DLS=1./24.*NLFGEN(ISTHMD,WS)
       DTS=1./24.*NLFGEN(THMD,WS)
       DVS=1./24.*NLFGEN(VAPDIF,WS)

*    EVALUATION OF BOTTOM PARAMETER
*
       HKB = AFGEN(HDK,WB)
       THKB=3.6*AFGEN(THKD,WB)
       DLB=1./24.*NLFGEN(ISTHMD,WB)
       DTB=1./24.*NLFGEN(THMD,WB)
       DVB=0.0
*
*    CALCULATING THE NUMBER OF VERTICAL AND HORIZONTAL NODES
*    AND THE POSITION OF THE PIPE
*
       NVP=(DD/DX)-1
       NHP=(SBP/2)/DX+1
       NP=PD/DX
*
NOSORT
*
*    DOMAIN INITIALIZATION
*      INITIAL TEMPERATURE
*
       DO 10 I=1,NHP
    10 READ (5,300) (T(I,J),J=1,NVP)
   300 FORMAT (7F6.3)
```

```
*      INITIAL MOISTURE CONTENT
*
*    READ IN THE MOISTURE PROFILE ON THE PIPES
*
       READ (5,350) (WPO(J),J=1,NVP)
       DO 11 I=1,2
       DO 11 J=1,NVP
    11 W(I,J)=WPO(J)
*
*    READ IN THE MOISTURE PROFILE BETWEEN PIPES
*
       READ (5,350) (WPB(J),J=1,NVP)
       DO 12 I=3,NHP
       DO 12 J=1,NVP
    12 W(I,J)=WPB(J)
   350 FORMAT (7F6.5)
*
       DXSQ = DX**2
*
SORT
DYNAMIC
NOSORT
*
*   EVALUATION OF THE TRANSPORT COEFFICIENTS AT THE INITIAL TEMPERATURE
*    AND MOISTURE CONTENT CONDITIONS.
*
       IF(TIME.EQ.0.) GO TO 1
*
*   UPDATING THE NODES MOISTURE CONTENT
*
       LM=0
       DO 15 M=1,NVP
       DO 15 L=1,NHP
       LM=LM+1
    15 W(L,M)=WF(LM)
*
*   UPDATING THE NODES TEMPERATURE AND BYPASSING THE NODE AT THE PIPE
*
       LM=0
       NP1=NP-1
       DO 16 M=1,NP1
       DO 16 L=1,NHP
       LM=LM+1
    16 T(L,M)=TF(LM)
       LM=LM
       M=NP
       DO 17 L=2,NHP
       LM=LM+1
    17 T(L,M)=TF(LM)
       LM=LM
       NP2=NP+1
       M=NP2
       DO 18 M=NP2,NVP
       DO 18 L=1,NHP
       LM=LM+1
    18 T(L,M)=TF(LM)
*
*    UPDATING THE TRANSPORT COEFFICIENTS
*
     1 DO 20 M=1,NVP
       DO 20 L=1,NHP
       C(L,M)= C1+W(L,M)
       HK(L,M)=AFGEN(HDK,W(L,M))
       THK(L,M)=3.6*AFGEN(THKD,W(L,M))
       DL(L,M)=1./24.*NLFGEN(ISTHMD,W(L,M))
       DT(L,M)=1./24.*NLFGEN(THMD,W(L,M))
    20 DV(L,M)=1./24.*NLFGEN(VAPDIF,W(L,M))
*
*      ASSIGNE PIPE TEMPERATURE
       PT=AFGEN(PIPTEM,TIME)
       T(1,NP)= PT
       TBP30=NLFGEN(TMD30,TIME)
       T10=NLFGEN(TEMP10,TIME)
       TS=T10
*
*
*    DEVELOPING OF THE NODE TEMPERATURE AND MOISTURE EQUATIONS
*
*
*    NODE (1,1) :
*
       TD=THK(1,1)*(2.*(T(2,1)-T(1,1))+T(1,2)+TB-2.*T(1,1))
       TD=TD+(T(1,2)-TB)*(THK(1,2)-THKB)/4.
       TD=TD-LH*(DV(1,1)*(2.*(W(2,1)-W(1,1))+W(1,2)+WB-2.*W(1,1)))
       TD=TD-LH*((DV(1,2)-DVB)*(W(1,2)-WB))/ 4.
       TDOT(1,1)=TD/(DXSQ*C(1,1))
       WD=DL(1,1)*(2.*(W(2,1)-W(1,1))+W(1,2)+WB-2.*W(1,1))
       WD=WD+(W(1,2)-WB)*(DL(1,2)-DLB) /4.
       WD=WD+DT(1,1)*(2.*(T(2,1)-T(1,1))+T(1,2)+TB-2.*T(1,1))
       WD=(WD+(DT(1,2)-DTB)*(T(1,2)-TB)/4.)/DXSQ
       WDOT(1,1)=WD+(HK(1,2)-HKB)/(2.*DX)
```

```
*    BOTTOM NODES (2 -(NHP-1) , 1) :
*
       N=NHP-1
       DO 30 I=2,N
       TD=THK(I,1)*(T(I+1,1)+T(I-1,1)+T(I,2)+TB-4.*T(I,1))
       TD=TD+(THK(I+1,1)-THK(I-1,1))*(T(I+1,1)-T(I-1,1))/4.
       TD=TD+(THK(I,2)-THKB)*(T(I,2)-TB)/4.
       TD=TD-LH*(DV(I,1)*(W(I+1,1)+W(I-1,1)+W(I,2)+WB-4.*W(I,1)))
       TD=TD-LH*(DV(I+1,1)-DV(I-1,1))*(W(I+1,1)-W(I-1,1))/ 4.
       TD=TD-LH*(DV(I,2)-DVB)*(W(I,2)-WB)/ 4.
       TDOT(I,1)=TD/(DXSQ*C(I,1))
       WD=DL(I,1)*(W(I+1,1)+W(I-1,1)+W(I,2)+WB-4.*W(I,1))
       WD=WD+(DL(I+1,1)-DL(I-1,1))*(W(I+1,1)-W(I-1,1))/4
       WD=WD+(DL(I,2)-DLB)*(W(I,2)-WB)/4.
       WD=WD+DT(I,1)*(T(I+1,1)+T(I-1,1)+T(I,2)+TB-4.*T(I,1))
       WD=WD+(DT(I+1,1)-DT(I-1,1))*(T(I+1,1)-T(I-1,1))/4.
       WD=(WD+(DT(I,2)-DTB)*(T(I,2)-TB)/4.)/DXSQ
   30  WDOT(I,1)=WD+(HK(I,2)-HKB)/(2.*DX)
*
*    NODE (NHP,1) :
*
       K=NHP
       TD=THK(K,1)*(2.*(T(N,1)-T(K,1))+T(K,2)+TB-2.*T(K,1))
       TD=TD+(T(K,2)-TB)*(THK(K,2)-THKB)/4.
       TD=TD-LH*(DV(K,1)*(2.*(W(N,1)-W(K,1))+W(K,2)+WB-2.*W(K,1)))
       TD=TD-LH*(DV(K,2)-DVB)*(W(K,2)-WB)/  4.
       TDOT(K,1)=TD/(DXSQ*C(K,1))
       WD=DL(K,1)*(2.*(W(N,1)-W(K,1))+W(K,2)+WB-2.*W(K,1))
       WD=WD+(W(K,2)-WB)*(DL(K,2)-DLB)/4.
       WD=WD+DT(K,1)*(2.*(T(N,1)-T(K,1))+T(K,2)+TB-2.*T(K,1))
       WD=(WD+(DT(K,2)-DTB)*(T(K,2)-TB)/4.)/DXSQ
       WDOT(K,1)=WD+(HK(K,2)-HKB)/(2.*DX)
*
*    DOMAIN LEFT SIDE, FROM J=2 TO THE NODE BEFOR THE PIPE.
*    TEMPERATURE EQUATIONS
*
       NP1=NP-1
       DO 40 J=2,NP1
       TD=THK(1,J)*(2*(T(2,J)-T(1,J))+T(1,J+1)+T(1,J-1)-2.*T(1,J))
       TD=TD+(T(1,J+1)-T(1,J-1))*(THK(1,J+1)-THK(1,J-1))/4.
       TD=TD-LH*DV(1,J)*(2.*(W(2,J)-W(1,J))+W(1,J+1)+W(1,J-1)-2.*W(1,J))
       TD=TD-LH*((DV(1,J+1)-DV(1,J-1))*(W(1,J+1)-W(1,J-1)))/ 4.
   40  TDOT(1,J) = TD/(DXSQ*C(1,J))

*    DOMAIN LEFT SIDE TEMPERATURE EQUATIONS-AFTER THE PIPE
*
       NP2=NP+1
       NVP1=NVP-1
       DO 50 J=NP2,NVP1
       TD=THK(1,J)*(2.*(T(2,J)-T(1,J))+T(1,J+1)+T(1,J-1)-2.*T(1,J))
       TD=TD+(T(1,J+1)-T(1,J-1))*(THK(1,J+1)-THK(1,J-1))/4.
       TD=TD-LH*DV(1,J)*(2.*(W(2,J)-W(1,J))+W(1,J+1)+W(1,J-1)-2.*W(1,J))
       TD=TD-LH*((DV(1,J+1)-DV(1,J-1))*(W(1,J+1)-W(1,J-1)))/ 4.
   50  TDOT(1,J)=TD/(DXSQ*C(1,J))
*
*    DOMAIN LEFT SIDE MOISTURE EQUATIONS FROM J=2 TO NVP1
*
       DO 60 J=2,NVP1
       WD=DL(1,J)*(2.*(W(2,J)-W(1,J))+W(1,J+1)+W(1,J-1)-2.*W(1,J))
       WD=WD+(W(1,J+1)-W(1,J-1))*(DL(1,J+1)-DL(1,J-1))/4.
       WD=WD+DT(1,J)*(2.*(T(2,J)-T(1,J))+T(1,J+1)+T(1,J-1)-2.*T(1,J))
       WD=(WD+(DT(1,J+1)-DT(1,J-1))*(T(1,J+1)-T(1,J-1))/4.)/DXSQ
   60  WDOT(1,J)=WD+(HK(1,J+1)-HK(1,J-1))/(2.*DX)
*
*    UP LEFT CORNER NODE (1,NVP):
*
       M=NVP
       MM=M-1
       TD=THK(1,M)*(2.*(T(2,M)-T(1,M))+TS+T(1,MM)-2.*T(1,M))
       TD=TD+(TS-T(1,MM))*(THKS-THK(1,MM))/4.
       TD=TD-LH*DV(1,M)*(2.*(W(2,M)-W(1,M))+WS+W(1,MM)-2.*W(1,M))
       TD=TD-LH*(DVS-DV(1,MM))*(WS-W(1,MM))/ 4.
       TDOT(1,M)=TD/(DXSQ*C(1,M))
       WD=DL(1,M)*(2.*(W(2,M)-W(1,M))+WS+W(1,MM)-2.*W(1,M))
       WD=WD+(WS-W(1,MM))*(DLS-DL(1,MM))/4.
       WD=WD+DT(1,M)*(2.*(T(2,M)-T(1,M))+TS+T(1,MM)-2.*T(1,M))
       WD=(WD+(DTS-DT(1,MM))*(TS-T(1,MM))/4.)/DXSQ
       WDOT(1,M)=WD+(HKS-HK(1,MM))/(2.*DX)
*
*    TOP NODES (2 - (NHP-1) ,NVP) :
*
       N=NHP-1
       J=NVP
       DO 70 I=2,N
       TD=THK(I,J)*(T(I+1,J)+T(I-1,J)+TS+T(I,J-1)-4.*T(I,J))
       TD=TD+(THK(I+1,J)-THK(I-1,J))*(T(I+1,J)-T(I-1,J))/4.
       TD=TD+(THKS-THK(I,J-1))*(TS-T(I,J-1))/4.
       TD=TD-LH*DV(I,J)*(W(I+1,J)+W(I-1,J)+WS+W(I,J-1)-4.*W(I,J))
```

```
      TD=TD-LH*(DV(I+1,J)-DV(I-1,J))*(W(I+1,J)-W(I-1,J))/ 4.
      TD=TD-LH*(DVS-DV(I,J-1))*(WS-W(I,J-1))/ 4.
      TDOT(I,J)=TD/(DXSQ*C(I,J))
      WD=DL(I,J)*(W(I+1,J)+W(I-1,J)+WS+W(I,J-1)-4.*W(I,J))
      WD=WD+(DL(I+1,J)-DL(I-1,J))*(W(I+1,J)-W(I-1,J))/4.
      WD=WD+(DLS-DL(I,J-1))*(WS-W(I,J-1))/4.
      WD=WD+DT(I,J)*(T(I+1,J)+T(I-1,J)+TS+T(I,J-1)-4.*T(I,J))
      WD=WD+(DT(I+1,J)-DT(I-1,J))*(T(I+1,J)-T(I-1,J))/4.
      WD=(WD+(DTS-DT(I,J-1))*(TS-T(I,J-1))/4.)/DXSQ
   70 WDOT(I,J)=WD+(HKS-HK(I,J-1))/(2.*DX)
*
*    UP RIGHT CORNER NODE  (NHP,NVP) :
*
      L=NHP
      M=NHP-1
      N=NVP
      TD=THK(L,N)*(2.*(T(M,N)-T(L,N))+TS+T(L,N-1)-2.*T(L,N))
      TD=TD+(TS-T(L,N-1))*(THKS-THK(L,N-1))/4.
      TD=TD-LH*DV(L,N)*(2.*(W(M,N)-W(L,N))+WS+W(L,N-1)-2.*W(L,N))
      TD=TD-LH*(DVS-DV(L,N-1))*(WS-W(L,N-1))/ 4.
      TDOT(L,N)=TD/(DXSQ*C(L,N))
      WD=DL(L,N)*(2.*(W(M,N)-W(L,N))+WS+W(L,N-1)-2.*W(L,N))
      WD=WD+(WS-W(L,N-1))*(DLS-DL(L,N-1))/4.
      WD=WD+DT(L,N)*(2.*(T(M,N)-T(L,N))+TS+T(L,N-1)-2.*T(L,N))
      WD=(WD+(DTS-DT(L,N-1))*(TS-T(L,N-1))/4.)/DXSQ
      WDOT(L,N)=WD+(HKS-HK(L,N-1))/(2.*DX)
*
*    DOMAIN RIGHT SIDE NODE EQUATIONS :
*
      N=NHP
      NN=NHP-1
      NVP1=NVP-1
      DO 80 J=2,NVP1
      TD=THK(N,J)*(2.*(T(NN,J)-T(N,J))+T(N,J+1)+T(N,J-1)-2.*T(N,J))
      TD=TD+(T(N,J+1)-T(N,J-1))*(THK(N,J+1)-THK(N,J-1))/4.
      TD=TD-LH*DV(N,J)*(2*(W(NN,J)-W(N,J))+W(N,J+1)+W(N,J-1)-2*W(N,J))
      TD=TD-LH*((DV(N,J+1)-DV(N,J-1))*(W(N,J+1)-W(N,J-1)))/ 4.
      TDOT(N,J)=TD/(DXSQ*C(N,J))
      WD=DL(N,J)*(2.*(W(NN,J)-W(N,J))+W(N,J+1)+W(N,J-1)-2.*W(N,J))
      WD=WD+(W(N,J+1)-W(N,J-1))*(DL(N,J+1)-DL(N,J-1))/4.
      WD=WD+DT(N,J)*(2.*(T(NN,J)-T(N,J))+T(N,J+1)+T(N,J-1)-2.*T(N,J))
      WD=(WD+(DT(N,J+1)-DT(N,J-1))*(T(N,J+1)-T(N,J-1))/4.)/DXSQ
   80 WDOT(N,J)=WD+(HK(N,J+1)-HK(N,J-1))/(2.*DX)
*
*    INTERIOR NODES - TEMPERATURE & MOISTURE EQUATIONS
*
      N=N-1
      DO 90 I=2,N
      DO 90 J=2,NVP1
      TD=THK(I,J)*(T(I+1,J)+T(I-1,J)+T(I,J+1)+T(I,J-1)-4.*T(I,J))
      TD=TD+(THK(I+1,J)-THK(I-1,J))*(T(I+1,J)-T(I-1,J))/4.
      TD=TD+(THK(I,J+1)-THK(I,J-1))*(T(I,J+1)-T(I,J-1))/4.
      TD=TD-LH*DV(I,J)*(W(I+1,J)+W(I-1,J)+W(I,J+1)+W(I,J-1)-4.*W(I,J))
      TD=TD-LH*(DV(I+1,J)-DV(I-1,J))*(W(I+1,J)-W(I-1,J))/ 4.
      TD=TD-LH*(DV(I,J+1)-DV(I,J-1))*(W(I,J+1)-W(I,J-1))/ 4.
      TDOT(I,J)=TD/(DXSQ*C(I,J))
      WD=DL(I,J)*(W(I+1,J)+W(I-1,J)+W(I,J+1)+W(I,J-1)-4.*W(I,J))
      WD=WD+(DL(I+1,J)-DL(I-1,J))*(W(I+1,J)-W(I-1,J))/4.
      WD=WD+(DL(I,J+1)-DL(I,J-1))*(W(I,J+1)-W(I,J-1))/4.
      WD=WD+DT(I,J)*(T(I+1,J)+T(I-1,J)+T(I,J+1)+T(I,J-1)-4.*T(I,J))
      WD=WD+(DT(I+1,J)-DT(I-1,J))*(T(I+1,J)-T(I-1,J))/4.
      WD=(WD+(DT(I,J+1)-DT(I,J-1))*(T(I,J+1)-T(I,J-1))/4.)/DXSQ
   90 WDOT(I,J)=WD+(HK(I,J+1)-HK(I,J-1))/(2.*DX)
*
*   REPLACING THE SUBSCRIPTED TWO DIMENSION  DIFFERENTIAL EQUATIONS IN
*    ONE DIMENSION ARRAY IN PREPERATION FOR INTEGRATION.
*
      KK=0
      DO 100 L=1,NVP
      DO 100 J=1,NHP
      KK=KK+1
  100 WADTL(KK)=WDOT(J,L)
      KK=0
      NP1=NP-1
      DO 101 L=1,NP1
      DO 101 J=1,NHP
      KK=KK+1
  101 TDTL(KK)=TDOT(J,L)
      L=NP
      KK=KK
      DO 102 J=2,NHP
      KK=KK+1
  102 TDTL(KK)=TDOT(J,L)
      NP2=NP+1
      KK=KK
      DO 103 L=NP2,NVP
      DO 103 J=1,NHP
      KK=KK+1
  103 TDTL(KK)=TDOT(J,L)
```

```
SORT
*
*       INTEGRATION OF THE DIFFERENTIAL EQUATIONS
*
        TF=INTGRL(TI,TDTL,27)
        WF=INTGRL(WI,WADTL,28)
*
TIMER DELT=0.25 , OUTDEL=2.0 , FINTIM=96.0
OUTPUT TF(15) , TBP30 , T10 ,PT
LABEL TEMPERATURE VARIATION WITH TIME
OUTPUT TF(1-27)
LABEL TEMPERATURE DISTRIBUTION OF THE DIFFERENT NODES
OUTPUT WF(1-28)
LABEL MOISTURE DISTRIBUTION OF THE DIFFERENT NODES
        END
INPUT
32.88 33.32 33.97 36.30 33.70 32.73 31.91
32.85 33.23 33.61 35.37 33.33 32.62 31.88
32.82 33.11 33.34 33.39 33.05 32.50 31.84
32.80 33.07 33.25 33.25 32.95 32.45 31.82
.2892 .2571 .2350 .2129 .1227 .0781 .0557
.3325 .3160 .2337 .1527 .0950 .0712 .0505
ENDINPUT
STOP
ENDJOB
```

```
*
*************************************************************************
*************************************************************************
*                                                                       *
*  CHANGES TO BE ADDED WHEN THE PROGRAM IS USED FOR SILT-LOAM SOIL      *
*                                                                       *
*  1. DELET HK FROM THE DIMENSION STATMENT.                             *
*  2. REPLACE THE TRANSPORT COEFFICIENT FUNCTIONS BY THE FOLLOWING:     *
*                                                                       *
 FUNCTION VAPDIF=0.012,.01,0.025,4.50,0.05,1.35,0.075,0.14,0.10,.027,...
      0.118,0.01
 FUNCTION ISTHMD=.012,.01,.025,4.50,.0375,5.0,.05,1.35,.075,.14,      ...
      .0875,.07,.10,.073,.125,.235,.15,1.45,.175,10.0,.20,13.5,       ...
      .225,100.0,.25,180.0,.275,320.0,.30,460.0,.325,700.0,.35,1000.,....
      .375,1650.0,.40,2700.0,.425,4400.0,.45,8800.0
 FUNCTION THMD=.025,.01,.05,.025,.075,.0315,.10,.031,.125,.03,.15,.03...
      ,.175,.028,.2,.028,.225,.026,.25,.028,.275,.035,.30,.085,       ...
      .325,.22,.35,.45,.375,.84,.40,1.60,.425,3.40,.45,7.0
 FUNCTION THKD=0.0245,0.475,0.06125,0.675,0.1011,0.900,0.1225,1.35,  ...
      0.1439,1.80,0.1838,2.25,0.245,3.00,0.4165,4.175,0.5,4.175
*                                                                       *
*  3. REPLACE THE VALUE OF C1 ON THE PARAMETER CARD BY C1=0.246         *
*  4. REPLACE THE VERY LAST CARD IN THE DO LOOP # 20 BY THE FOLLOWING:  *
*                                                                       *
      IF((W(L,M).GT.0.012).AND.(W(L,M).LE.0.118)) GO TO 19
      DV(L,M)=0.0
      GO TO 20
   19 DV(L,M)=1./24.*NLFGEN(VAPDIF,W(L,M))
   20 CONTINUE
*                                                                       *
*  5. TAKE OUT THE EFFECT OF GRAVITY FROM EACH MOISTURE EQUATION.       *
*     THIS TERM IS WRITTEN AT THE END OF EACH MOISTURE EQUATION.        *
*************************************************************************
*************************************************************************
```

This page intentionally blank.

This page intentionally blank.

This page intentionally blank.

OSU

The Ohio State University

Ohio Agricultural Research and Development Center